Graduate School ETD Form 9
(Revised 12/07)

PURDUE UNIVERSITY
GRADUATE SCHOOL
Thesis/Dissertation Acceptance

This is to certify that the thesis/dissertation prepared

By Ethan Charles Blocher-Smith

Entitled Investigations of Lipid Metabolism in Yarrowia lipolytica

For the degree of Master of Science

Is approved by the final examining committee:

Robert Minto
Chair

Eric Long

Lisa Jones

To the best of my knowledge and as understood by the student in the *Research Integrity and Copyright Disclaimer (Graduate School Form 20)*, this thesis/dissertation adheres to the provisions of Purdue University's "Policy on Integrity in Research" and the use of copyrighted material.

Approved by Major Professor(s): Robert Minto

Approved by: Eric Long 10/22/2013
Head of the Graduate Program Date

INVESTIGATIONS OF LIPID METABOLISM IN YARROWIA LIPOLYTICA

A Thesis
Submitted to the Faculty
of
Purdue University
by
Ethan Charles Blocher-Smith

In Partial Fulfillment of the
Requirements for the Degree
of
Master of Science

December 2013
Purdue University
Indianapolis, Indiana

For Dr. William H. Bordeaux, the man who
ignited my passion for Chemistry

Solus Deo Gloria, qui tribuit mihi sapientiam Deo,
Enim vidi Eo et audivi Eo vocem.
Veni. Vidi. Didici.
In nomine Christi, laboro.

ACKNOWLEDGMENTS

This thesis would not be possible without the oversight of my mentor, Dr. Robert Minto. His intelligence and keen wit have served our research well. I owe many edits and superior revisions to my other thesis advisors, Dr. Eric Long and Dr. Lisa Jones. My presentations and presenting skills have been honed by the probing questions of Dr. Brenda Blacklock. And much of the skill I now have in the lab I owe to the insightful discussions, assistance, and patience of my labmates, Mike Shepard, Anthony Ransdell, Selene Hernandez-Buquer, and Alicen Teitgen, with special emphasis on Mike's useful commentary and Anthony's tricks of the trade. I would also like to acknowledge Xiaoyun Deng of Miami University for her aid in acquiring sequence results.

TABLE OF CONTENTS

Page

Page

Page

LIST OF TABLES

LIST OF FIGURES

Figure Page

Figure Page

LIST OF ABBREVIATIONS

aa	amino acid
ACP	acyl carrier protein
AHAS	acetohydroxyacid synthase
Amp	ampicillin
bp	base pair(s)
Chl	chloramphenicol
CM	complete minimal media
CME	chlorimuron ethyl
CoA	Coenzyme A
Cre	Cre recombinase
dex	dextrose
DNA	deoxyribonucleic acid
dNTPs	deoxyribonucleotides
EDTA	ethylenediaminetetraacetic acid
Epa2161T	*Echinacea purpurea* 2161 gene corrected to the consensus *E. purpurea* transcriptomic data
Epa955R2	*Echinacea purpurea* 955 gene corrected to the consensus *E. purpurea* RACE data, strain #2
Epa955R3	*Echinacea purpurea* 955 gene corrected to the consensus *E. purpurea* RACE data, strain #3
Epa955T	*Echinacea purpurea* 955 gene corrected to the consensus *E. purpurea* transcriptomic data
FA	fatty acid
FAME	fatty acid methyl ester

FFA	free fatty acid
G-3-P	glycerol-3-phosphate
GC-MS	gas chromatography-mass spectroscopy
His	histidine
Hyg	hygromycin
Ile	isoleucine
Kan	kanamycin
kb	kilobase
KO	knockout
L	leucine
LCFA	long-chain fatty acids
LB	Luria-Bertani broth
Leu	leucine
MCFA	medium-chain fatty acids
MUFA	monounsaturated fatty acid
$NADP^+$	nicotinamide adenine dinucleotide phosphate, oxidized
NADPH	nicotinamide adenine dinucleotide phosphate, reduced
NEB	New England Biolabs
nt	nucleotide
P	proline
PCI	25:24:1 phenol:chloroform:isoamyl alcohol
PCR	polymerase chain reaction
PUFA	polyunsaturated fatty acid
RACE	rapid amplification of cDNA ends
RNA	ribonucleic acid
SCFA	short-chain fatty acid
SDM	site-directed mutagenesis
SE	sterol esters
SNP	single nucleotide polymorphism
TAG	triacylglycerol

TE	Tris/EDTA buffer
UTR	untranslated region
Val	valine
VLCFA	very long-chain fatty acids
W	tryptophan
YNB	yeast nitrogenous base
YPD	yeast extract/peptone/dextrose media

ABSTRACT

Blocher-Smith, Ethan Charles. M.S., Purdue University, December 2013. Investigations of Lipid Metabolism in *Yarrowia lipolytica.* Major Professor: Dr. Robert E. Minto

An investigation of the lipid metabolism pathway in the yeast *Yarrowia lipolytica* was conducted. *Yarrowia* is an oleaginous ascomycete that is capable of growing on many different substrates, which derives its name from its high efficiency of growth on lipids. Once the exogenous lipids are converted into free fatty acids and internalized by the yeast, the primary mode of degradation is through β -oxidation mediated by the peroxisomal oxidases, or *POX* genes. These enzymes catalyze the formation of a trans double bond, producing the trans-2-enoyl product. Our study looked at the comparison of the *Y. lipolytica* prototrophic strain against a knockout of the Pox2 gene on the uptake, incorporation, and degradation of relevant fatty acids. To construct this gene knockout, a novel gene deletion method using a combination of Cre recombinase and the AHAS* gene was synthesized, developed, and tested successfully. This knockout system allows for serial deletion of genes with the use of only one resistance marker, with excision of the marker after selection.

CHAPTER 1. INTRODUCTION

Yarrowia lipolytica is an oleaginous ascomycetaneous yeast capable of producing as much as 50% lipid by mass in the wild type strain. It derives the designation "*lipolytica*" from its inherent capability of growing on lipids as its sole carbon source. While capable of growth on many nonstandard feedstocks, such as glycerol, soap wastes, or amino acids, the yeast rapidly accumulates lipids as TAGs (triacylglycerols) in specialized organelles called lipid bodies when cultured on media with a nutrient restriction. While many dietary restrictions are capable of producing this result, such as low magnesium, sulfur, or oxygen concentrations, increased TAG accumulation is most conveniently accomplished through restriction of nitrogen content.

Once lipids are synthesized *de novo* or taken up from the media they will take one of three metabolic paths. Some lipids, especially short chain fatty acids, will be degraded to acetyl-CoA for sustaining energy needs. Other lipids will be modified for signaling or metabolic needs through elongation, desaturation, hydroxylation, or appropriate conjugation to a polar headgroup, such as phosphocholine. Lastly, the remaining lipids and some of the altered lipids will be retained as either TAGs or stearoyl esters within lipid bodies.

This study examined each of these three lipid metabolic paths and the roles they play in lipid degradation and storage. A molecular biology technique for repetitive gene knockouts based upon homologous recombination was established, using a single excisable resistance cassette and iterative growth. Additionally, investigations of the role of the peroxisomal oxidase genes aimed to find any differences in activity based on cis/trans isomerism, degree of unsaturation, and the location of the double bonds.

1.1 Overview of Fatty Acids

1.1.1 What are Fatty Acids?

Fatty acids (FAs) and fatty acid derivatives are key components in cell structure, signaling, and energy storage (1). These derivatives, such as sphingolipids or phospholipids, form the membrane bilayer of the cell and TAG products like specialized organelles (2). Fat stores of TAGs in specialized lipocytes or lipid bodies allow for easy accumulation and mobilization of excess energy (3). Fatty acids may be used for protein modifications through acylation (4), modified to produce hormones like eicosanoids (5) or signaling compounds like platelet-activating factor (6), and utilized to both stimulate and study regulatory enzymes (7).

FAs consist of an acyl tail of variable length capped with a carboxylic acid. Many different varieties of FAs exist, typically ranging between four and twenty-eight carbons (8) in length but observed as long as 34 carbons in plant cuticular waxes (9). Unmodified FAs have acyl chains of only methylene groups that are saturated with hydrogens and are known as *saturated* FAs. Chemical modification of fatty acids for storage or use may introduce many other functional groups, such as halogen substituents, hydroxyl groups, alkenes, alkynes, epoxides, and many more. Modifications like epoxides or multiple bonds result in an *unsaturated* FA, since the acyl chain is no longer saturated with the maximum number of hydrogens.

In yeasts, the *de novo* synthesis of FA occurs within the cytosol. As in most eukaryotes, the biosynthesis is carried out by a multifunctional fatty acid synthase complex which uses acetyl-CoA and malonyl-CoA to generate saturated fatty acids with chain lengths of typically 16-18 carbons (10). Modifications of this synthesis, both through elongation and β-oxidation, will result in the varied chain lengths previously described. In addition, for ease of discussion fatty acids are subdivided into groups via chain length, irrespective of their additional functionalities (Table 1).

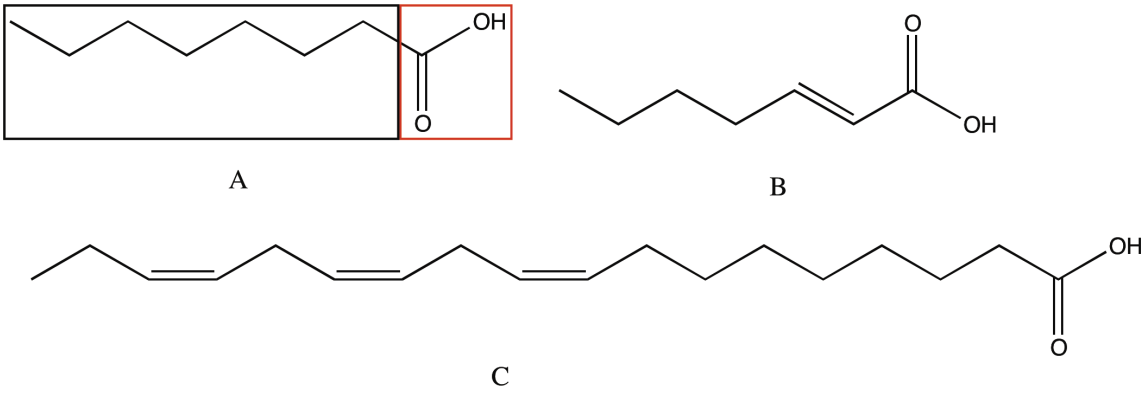

Figure 1: Structure of fatty acids. Caprylic, or octanoic, acid (A) is a saturated fatty acid. The carboxylic acid is marked in red, with the hydrocarbon tail marked in black. (E)-hept-2-enoic acid (B) is a monounsaturated trans fatty acid. The last lipid, α-linolenic acid (C) is a polyunsaturated FA, or PUFA.

Classification	Chain length
Short-Chain Fatty Acid (SCFA)	≤11 carbons
Medium-Chain Fatty Acid (MCFA)	12-15 carbons
Long-Chain Fatty Acid (LCFA)	16-18 carbons
Very Long-Chain Fatty Acid (VLCFA)	≥19 carbons

Table 1: Fatty acid chain length classification. Most common FAs in this study are LCFAs.

1.1.2 Fatty Acid Nomenclature

Fatty acids are identified via three core systems: 1) trivial names; 2) IUPAC names; and 3) lipid shorthand notations. While trivial names clearly designate the compound, such as oleic acid, they provide no description as to its structure. Conversely, IUPAC names are complete in their description, but awkward and unnecessarily long. To maximize information without data loss, many shorthand forms for lipids exist, of which this work will use (Δ) notation. Linoleic acid, properly known as (9*Z*,12*Z*)-octadec-9,12-dienoic acid, may be easily abbreviated as $18{:}2^{\Delta 9,12}$. In this notation, represented here as $A{:}B^{\Delta C}$, 'A' represents the length of the carbon chain in the FA. 'B' gives the number of double bonds present in the chain, and 'C' gives the positions of those double bonds and any other alterations in the acyl chain. This notation is highly useful with PUFAs, allowing the condensation of both stereochemistry and positioning into an easily

deciphered form. This notation assumes that, unless noted, all double bonds are in the cis-configuration. Any trans-double bonds are designated with the letter 't' appended after their position identifier. Similarly, triple bonds do not contribute to the count of double bonds and are designated by the appending of the letter 'a' after their identifier.

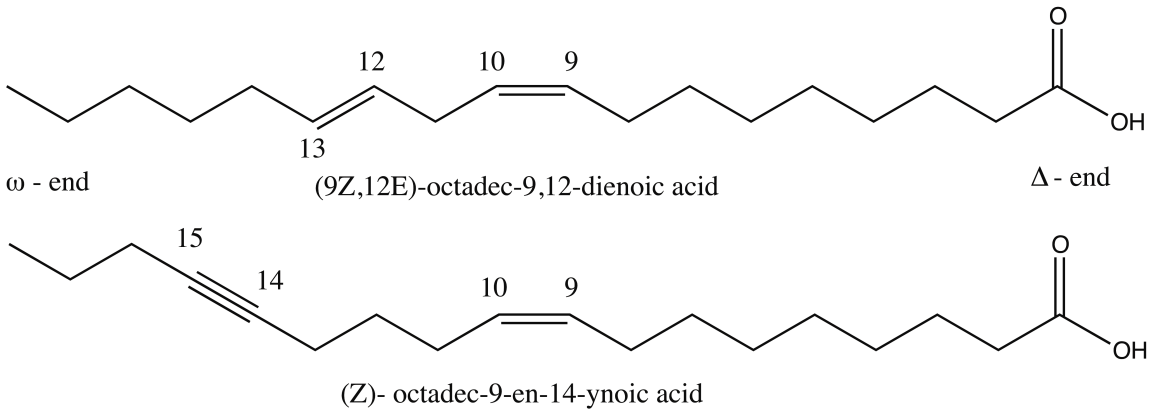

Figure 2: Fatty acid shorthand nomenclature. The Δ designation gives the position of the feature relative to the carboxy terminus. The top and bottom structures may be named as $18{:}2^{\Delta 9,12t}$ and $18{:}1^{\Delta 9,14a}$, respectively. An alternative nomenclature numbers from the opposite ω end, giving rise to common terms like ω-6 FA indicating an FA with a double bond at C6 from the ω end.

1.1.3 Fatty Acid Desaturases

1.1.3.1 Background on the Desaturase Family

Fatty acid desaturases perform oxidative dehydrogenation of acyl chains. Prototypically, this enzyme family abstracts a hydrogen atom from two adjacent methylene groups to form a double bond. While naturally occurring double bonds are almost entirely in the *cis* configuration, a small percentage of the double bonds produced by other biochemical paths exist as the *trans* isomers (11). To perform their functions, this family requires two electrons, two protons (H^+), and molecular oxygen for each double bond formed. Activated oxygen cleaves the stable C-H bonds with the electrons providing the reducing equivalents. Once complete, the oxygen is reduced to water and the double bond has been installed (12).

This family of enzymes is present in both eukaryotes and prokaryotes, providing essential functions in regulating membrane fluidity through the variable desaturation of its constituent lipids. Desaturases are also central to the production of highly unsaturated

products for use in hormones, regulatory compounds, and compounds involved in anti-inflammatory responses (1,13,14). Desaturases are capable of accepting a range of distinctively conjugated acyl substrates, contributing to their prevalence as specialized and compartmentalized processes regulating cellular lipid metabolism. Four classes of substrates have been characterized: acyl-CoAs, acyl-ACPs, complex acyl-lipids, and sphingolipids (15). Desaturases are also specialized as to the location of the installed double bond, showing predominant regioselectivities such as Δ6, Δ9, Δ12, or Δ15. Certain diverged desaturases are even capable of forming alkyne bonds or hydroxylated products, through the desaturation of an alkene to form the carbon-carbon triple bonded product or alcohols. These subclasses are known as the acetylenases and hydroxylases, respectively (16-18).

1.1.3.2 Diverged Desaturases – Acetylenases

To date, all acetylenase enzymes characterized are membrane-bound desaturases which present the same characteristic motifs and hydrophobic regions as seen in other desaturases (19,20), including three His box motifs believed to be essential to catalysis (21). Acetylenases have high sequence homology to FAD2, a gene first characterized in *Arabidopsis thaliana* by Okuley et al. (13) that converts oleic acid to linoleic acid (shown in Figure 3). Studies by Reed et al. in 2003 showed a stepwise mechanism for the action of the Δ12-acetylenase Crep1 from *Crepis alpina* which was analogous to the well established action of FAD2 Δ12-desaturases (22). Additionally, beyond the ability of the characterized CfACET gene from *Cantharellus formosus* to act as a Δ12-acetylenase, an additional Δ14 desaturation step has also been observed (16). It is hypothesized that this function is in fact the result of action by endogenous Δ12 desaturase activity, which, due to the foreshortening of the C12-C13 distance by the alkyne bond, is capable of reaching C14-C15 to perform the desaturation step.

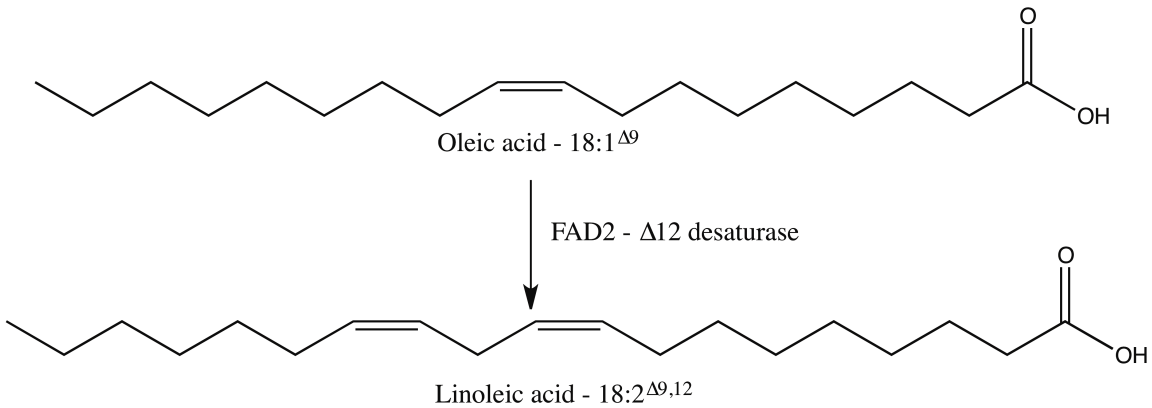

Figure 3: FAD2 function. The FAD2 abstracts the pro-*R* hydrogen at C12 first, then rapidly abstracts the pro-*R* hydrogen from C13, resulting in the double bond formation.

1.1.3.3 Previous Investigations – Epa955 & Epa2161

Recent thesis work presented by Anthony Ransdell from our lab looked at the function of two genes isolated from Echinacea purpurea. E. purpurea has been shown to produce a number of acetylene-containing natural products, implying the presence of at least one Δ12-acetylenase. A BLAST screen of the E. purpurea transcriptome versus known acetylenases and desaturases resulted in the discovery of two genes of note. Epa955 and Epa2161 showed up as the top two hits, and both showed high sequence homology to well-characterized acetylenases as well as the presence of the three His box motifs and hydrophobic regions seen previously. Both genes were cloned from Echinacea and inserted into plasmids for use in the yeasts Saccharomyces cerevisiae and Y. lipolytica. To observe the function of the heterologous genes in Yarrowia, codon optimization was required. Careful analysis of the metabolic products from expression cultures clearly indicated that both genes possessed the Δ12-acetylenase function, converting linoleic acid to crepenynate (18:1Δ9,12a) in the crepenynic acid pathway (Figure 4). The study clearly showed significant production of 18:1Δ9,12a both with and without supplementation of its immediate precursor linoleic acid. Supplementation of the strain transformed with active Epa955 and Epa2161 plasmids with crepenynate showed significant production of dehydrocrepenynate, strongly implying that the genes also

possess a Δ14-desaturase activity. However, the strains of Yarrowia in use contained the native FAD2 Δ12-desaturase, limiting definitive characterization of the enzymes (23).

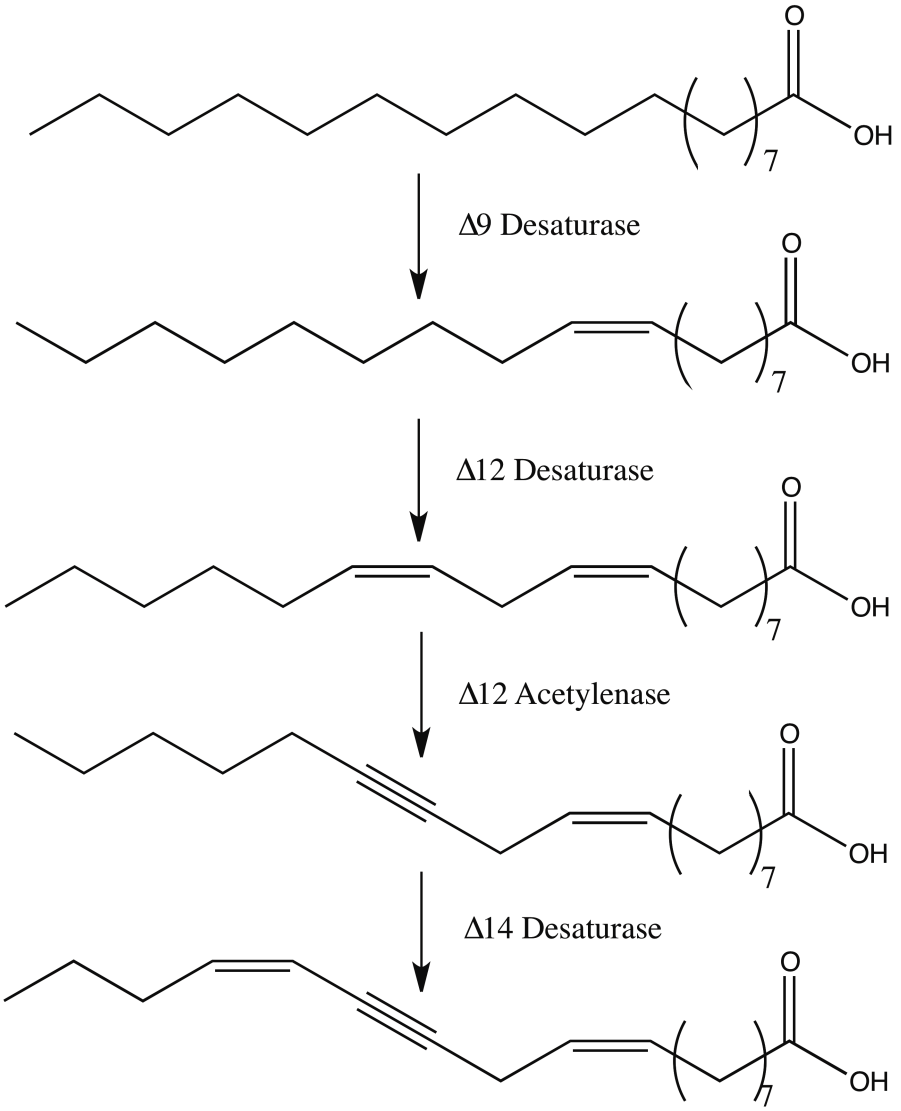

Figure 4: The crepenynate pathway through dehydrocrepenynate, as originally proposed by Bu'Lock (24)

1.2 *Yarrowia lipolytica*

Yarrowia lipolytica is an ascomycete yeast which shows distinct dimorphism with a sexual stage (25). The genus *Yarrowia* is monotypic, thus the genus and species titles are unique and will be used interchangeably. Previously designated *Candida lipolytica,* the yeast draws its species name from the wide variety of lipid products on which it can grow. *Y. lipolytica* utilizes a wide range of carbon sources, including carbohydrates such as

fructose, mannose, or sorbose, lipids ranging from FFAs to TAGs, alcohols, glycerol (26), and even aromatic/organic pollutant compounds (27). *Y. lipolytica* is capable of accumulating up to 50% of its dry weight as lipids in the prototrophic strain, leading to its classification as an oleaginous yeast (28). While more recent studies have looked at atypical uses, such as bioremediation, industrial research has focused on 3 core goals: 1) production of rare or useful lipids (5); 2) manipulation of the lipid content profile to mimic biologically or economically relevant forms (29); and 3) increased accumulation of lipids for use in biodiesel production (30,31).

Previous studies have resulted in high efficiency production of specialized compounds like polyhydroxyalkanoates (PHAs), polymers of 3-hydroxyacids that form a biodegradable and renewable synthetic alternative to petroleum-based plastics (32). The peach-like perfume component γ -decalactone may be produced in *Y. lipolytica* from methyl ricinoleate (33,34), and many of the Kreb's cycle intermediates may be excreted into the media (35). Other studies have considered the viability of modified *Yarrowia* strains as a source of cocoa butter substitutes (29). Still others have engineered strains capable of lipid accumulation as high as 80% of the dry weight (36). Of the three goals, this project seeks to further capabilities in biodiesel production through increased understanding of the activities of lipid degradation mechanisms against a range of FA, MUFA, and PUFA compounds.

1.2.1 Lipid Sources

Yarrowia produces, accumulates, and degrades a wide range of lipids. These lipids are initially produced through one of two methods: *de novo* synthesis of new lipids from acetyl- and malonyl-CoA, or accumulation of exogenously fed lipids.

1.2.1.1 *De novo* Lipid Synthesis

Unless grown on a lipid substrate, *de novo* lipid synthesis accounts for the vast majority of lipids produced in *Yarrowia*. Acetyl-CoA and malonyl-CoA are transferred to ACP, condensed to form the initial 3-ketobutanoyl-ACP product with the release of CO_2 and one ACP. The acyl conjugate is then reduced to the alcohol, dehydrated to form a

trans double bond, and lastly hydrogenated to form the butanoyl-ACP product in the first FA synthesis cycle. This cycle is then repeated, incrementing the chain by 2 carbons until the desired final length is achieved. The product FAs, heavily skewed in favor of 16:0 and 18:0 (11), are then either degraded or modified/stored. This process is illustrated in Figure 5. *Yarrowia* possesses a number of qualities uncommon to most yeast species that encourage the production of lipid products. Comparative analysis of oleaginous versus non-oleaginous yeast and fungi by Vorapreeda et al. in 2012 (37) revealed alternative routes to produce acetyl-CoA. The oleaginous strains studied, *Y. lipolytica* and three others, showed the capability to degrade fatty acids through mitochondrial β-oxidation, an ability analogous to peroxisomal β-oxidation but that was not observed in the non-oleaginous species. In addition, the oleaginous strains could degrade leucine as well as lysine to acetyl-CoA. While the non-oleaginous species could degrade lysine to glutaryl-CoA, only this oleaginous species has been shown to possess the enzymes necessary to modify glutaryl-CoA into acetyl-CoA. These alternative pathways integrate otherwise isolated metabolic paths to funnel into acetyl-CoA, which can be funneled into lipid production (37).

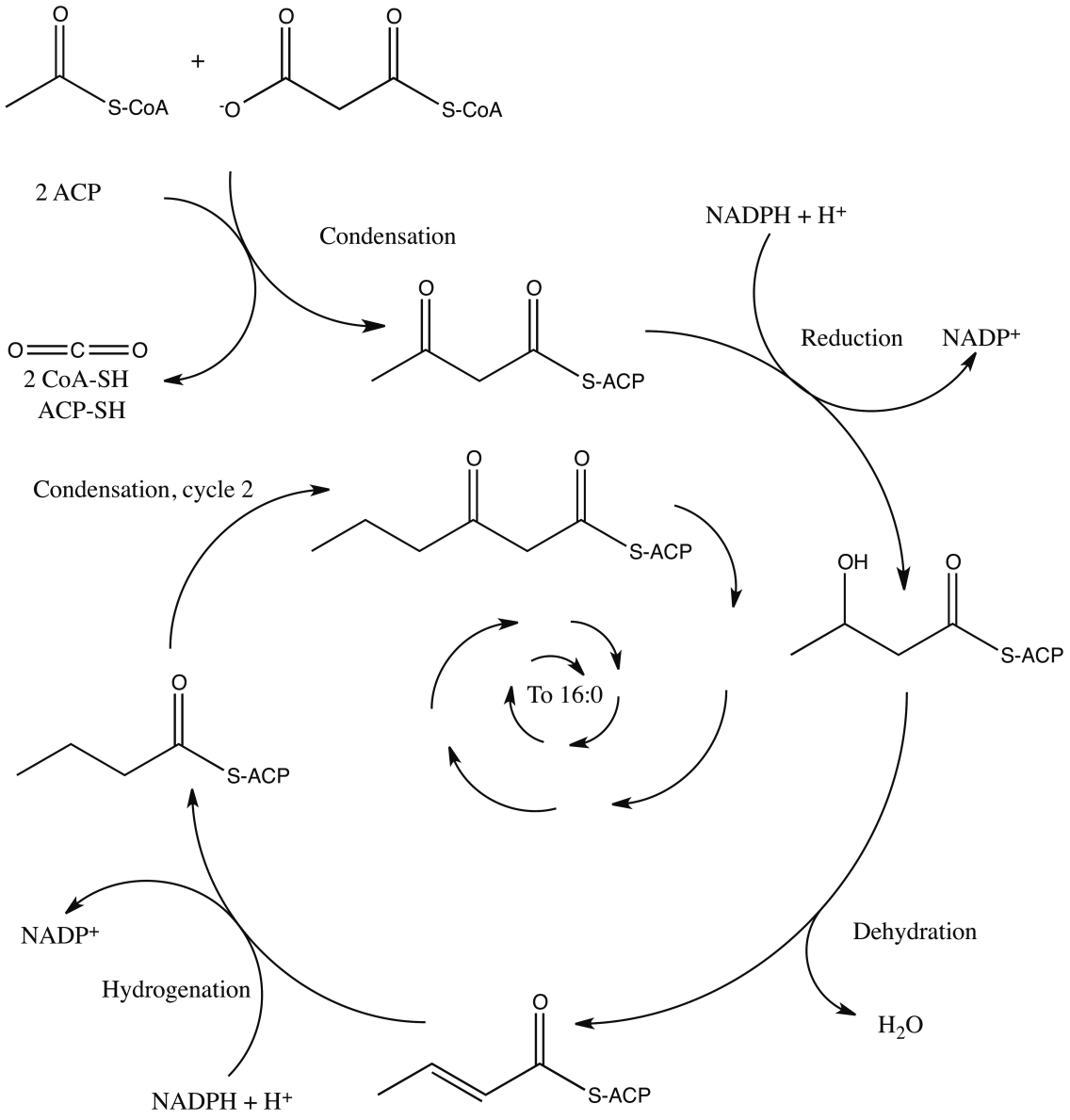

Figure 5: *De novo* lipid synthesis. While other capabilities deviate notably, especially the specialized ways oleaginous organisms produce acetyl-CoA from nonstandard sources, the core *de novo* anabolic pathway is the same as in *S. cerevisiae*.

1.2.1.2 Extracellular Lipid Degradation and Uptake

While *de novo* FA synthesis accounts for much of the lipid content, *Yarrowia* is especially efficient in accumulating exogenously fed extracellular lipids. To prepare the lipids, a wide range of lipases are actively secreted into the media, which hydrolyze the ester linkages in TAGs and other lipid derivatives to produce free fatty acids (35).

Yarrowia makes and excretes such a high level of useful lipases that strains have been engineered to industrially produce these enzymes (35,38,39). Its species name *lipolytica* is entirely due to this mechanism, since without the range of lipases to degrade the lipids into FFA, the exogenously fed lipids could not be transported or utilized. These newly freed FFAs are then taken up through active transport mechanisms into the cytosol of the cell, where they may be degraded or modified/stored.

1.2.2 Lipid Alteration and Storage

Yarrowia contains highly active Δ9 and Δ12 FA desaturases, both of which have activities clearly shown in the yeast's major products. When the overall lipid profile from the wild type *Y. lipolytica* strain is analyzed after growth in a standard medium such as YNB, 85-90% of the total lipid content is comprised of five fatty acids: 16:0, $16:1^{\Delta 9}$, 18:0, $18:1^{\Delta 9}$, and $18:2^{\Delta 9,12}$ (31). This behavior is maintained in minimal media with a low C/N ratio, such as with growth in high concentrations of glucose (40,41). Since 16:0 and 18:0 are the dominant products from FA synthesis, it is unsurprising that they and their direct desaturation products comprise the majority of stored lipid. Once the lipid acyl chain has been altered as necessary through desaturation or other modification processes, the products are processed into their final storage forms through one of two paths, as shown in Figure 6.

Once the synthesis is complete, the final SE and TAG are accumulated in the lipid body, or bodies. Depending on the growth conditions, *Yarrowia* may produce one or several large lipid bodies, or many small ones. Total lipid content in the lipid body is between 80-90% TAG by weight, with the remainder being SE and trace amounts of FFA (42,43). The lipid body is enclosed in a phospholipid monolayer, studded with proteins needed to remobilize the neutral lipids and degrade them back to FFAs to enable β-oxidation (3,44). This process is illustrated in Figure 7.

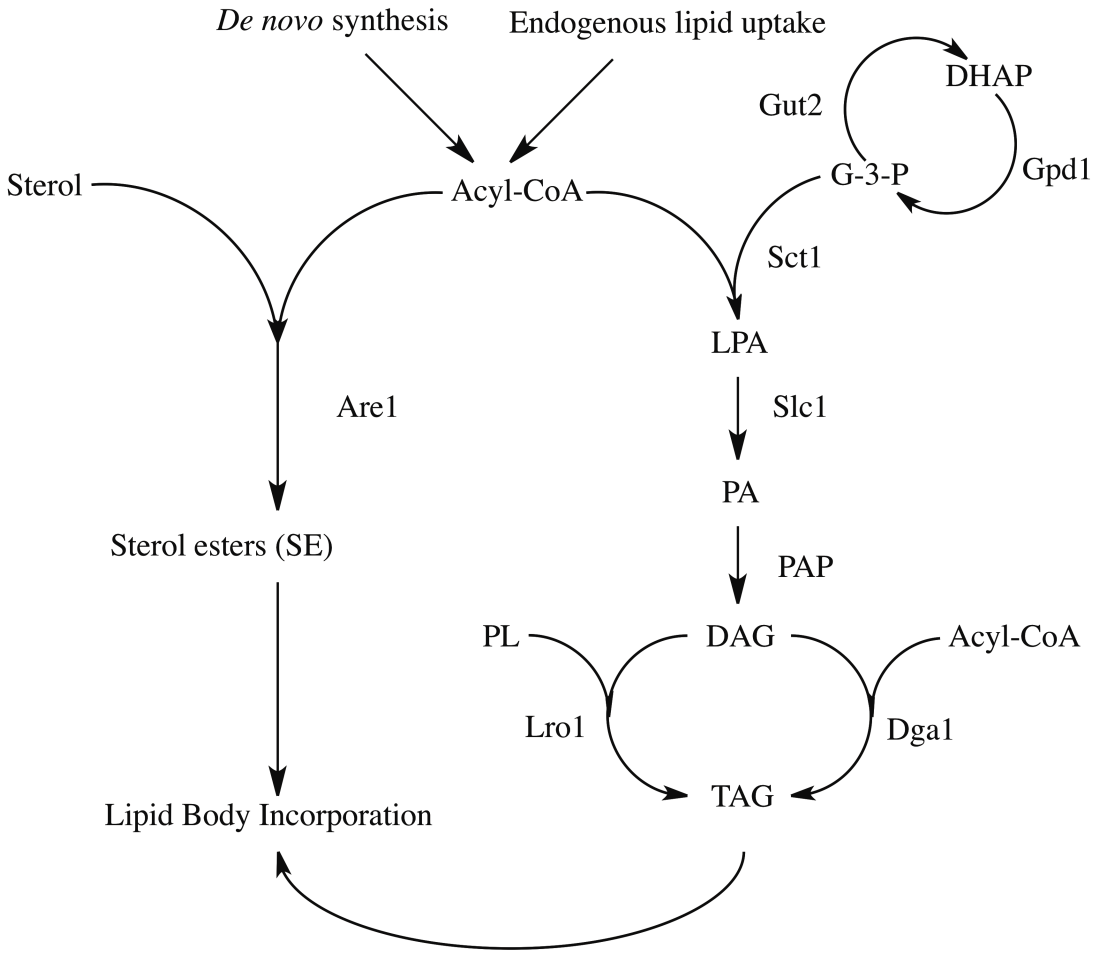

Figure 6: SE and TAG synthesis. The synthesis of the SE is achieved through an acyltransferase, producing the neutral lipid. To form the TAG products, DHAP is converted into glycerol-3-phosphate. The resulting G-3-P is condensed at the *sn*-1 position with the acyl-CoA to form the phosphorylated monoacylglycerol. A second acyl-CoA is then esterified onto the glycerol backbone, and the glycerol is dephosphorylated, forming the DAG. Finally, the last acyl chain is installed through several acytransferase paths, forming the TAG (31). Genes shown: Gut2, G-3-P dehydrogenase; Gpd1, G-3-P dehydrogenase, forms G-3-P from DHAP; Sct1, G-3-P acyltransferase; Slc1, 1-acyl G-3-P acyltransferase; PAP, PA phosphohydrolase; Dga1, diacylglycerol acyltransferase; Lro1, a lecithin cholesterol acyltransferase-like gene; Are1, Acyl-CoA:sterol acyltransferase

Total lipid content and citric acid produced is enhanced when necessary nutrition is limited. Because of this, growth is typically performed in media with a high C/N ratio that enhances the conversion of carbohydrates into lipids (45). By providing an excess of the carbon source and harvesting cells prior to its exhaustion as a foodstock, analysis of cultures can identify conditions with the maximal lipid content and without alteration of its cellularly regulated lipid ratios.

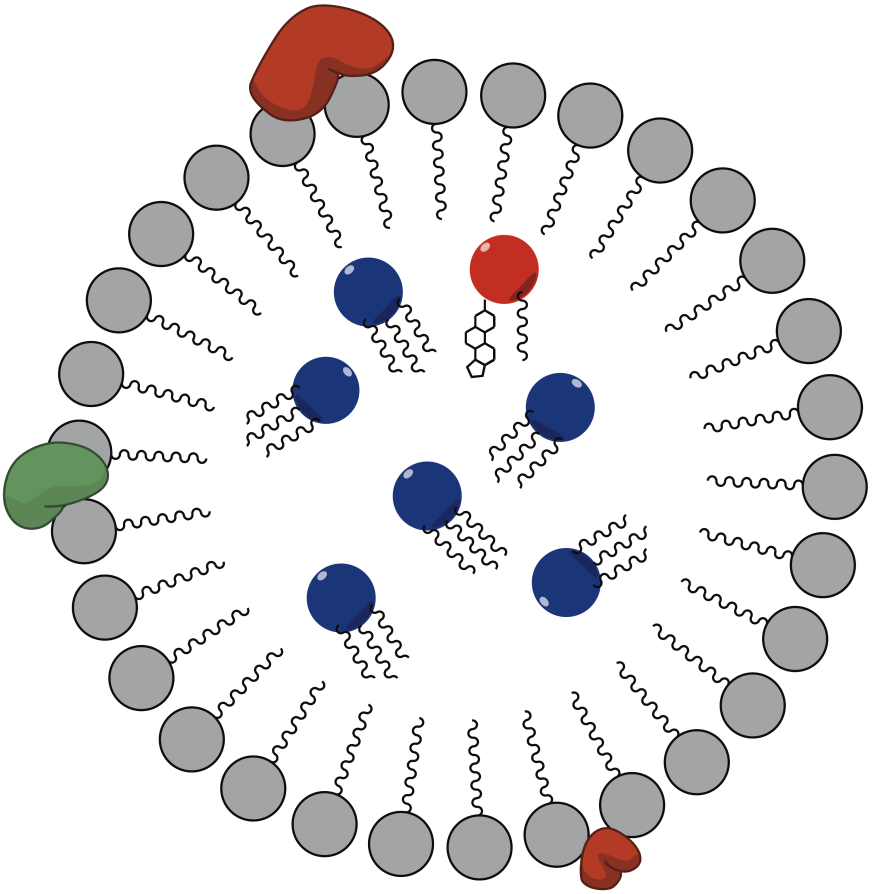

Figure 7: The lipid body. The outer phospholipid monolayer is studded with useful proteins for mobilization (in green and orange), while the inner core consists of the TAGs (in blue) and the SEs (in red).

1.2.3 Lipid Degradation

Yarrowia will degrade lipids either for energy or to produce more of a desired regulatory/storage product. Mobilization of the stored lipids happens during the exponential growth phase for membrane lipid synthesis, during the stationary phase upon nutrient depletion, and once exiting starvation and entering the vegetative state (31). Lipid stored as TAGs and SE are hydrolyzed to form FFA that is shunted off for synthetic purposes or proceeds through β-oxidation to form acetyl-CoA (46). Unlike in mammals, yeast β-oxidation occurs entirely in the peroxisome without any involvement of the mitochondria, although *Yarrowia* does contain most of the enzymes needed for mitochondrial β-oxidation (41). While the hydration and oxidation steps are performed by one multifunctional enzyme complex (*MFE1*) and there is only one peroxisomal

thiolase, *Yarrowia* possesses a range of six different peroxisomal oxidases, or *POX* genes (31). This suite of genes, designated as *POX1, POX2, POX3, POX4, POX5* and *POX6* (previously named Pox2like for its discovery via sequence homology), work together in

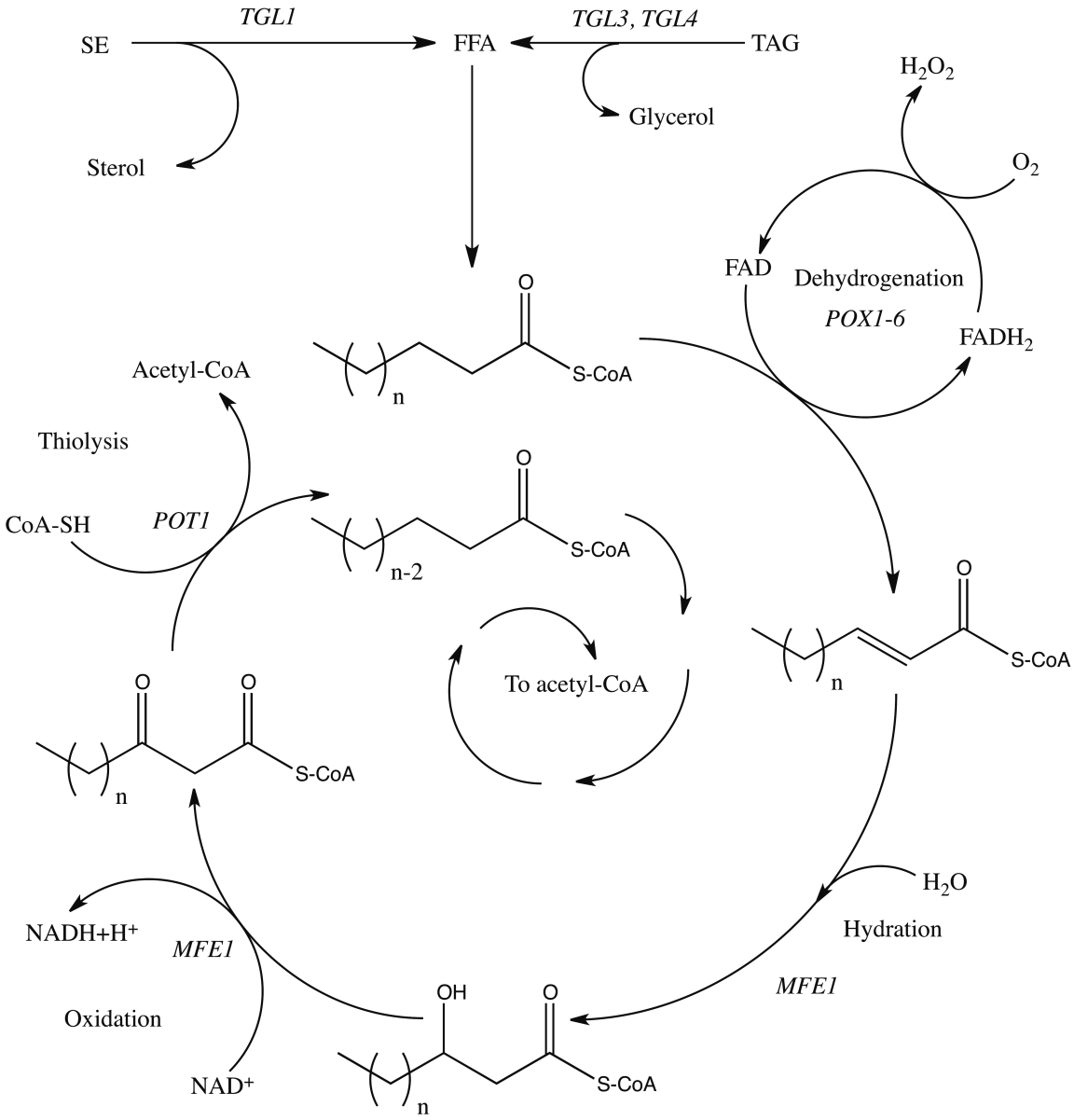

Figure 8: Peroxisomal β-oxidation. Note that as the acyl chain shortens, the involvement of Pox isozymes will change due to chain-length specificity.

concert to perform β-oxidation. The *POX* genes are translated as separate polypeptides in the cytosol, but will self-assemble into heteropentameric complexes prior to their import into the peroxisomes (47). Of two of the Pox genes products, POX2 and POX3, at least one must be present to achieve functional assembly and targeting the complex to the

peroxisome. If both of these genes are knocked out, the complex will not form and the polypeptides will remain separate and in the cytosol; Pox monomers are incapable of penetrating the peroxisome (47). Each POX has a differing specificity, with well-defined substrates found for 4 of the 6 genes. POX1 and POX6 both have specific activity against dicarboxylic acids, POX3 is a short chain oxidase for FA chains C_3-C_{10} (48,49), and POX2 is a medium chain oxidase acting on C_8-C_{14} acyl groups (50). POX4 and POX5 have a general nonspecific binding across saturated FAs between C_4 and C_{16} (51,52); however, a recent study looking at the viability of PHA production demonstrated a high activity of POX5 against the odd chain LCFA $17{:}1^{\Delta 10}$ (32).

Unlike peroxisomal β-oxidation in other higher organisms, the peroxisomes in *Yarrowia* will degrade lipids all the way to acetyl-CoA (Figure 8). In the case of odd-chain fatty acids, the degradation will be the same but the final product will be propionyl-CoA. Unsaturated lipids are either isomerized to form the *trans*-2-alkene or the double bond location is isomerized if necessary to allow the progression of normal β-oxidation (41).

CHAPTER 2. KNOCKOUT CONSTRUCTS AND CRE-AHAS*

Core to the completion of the studies detailed in this thesis is the production of engineered gene knockout strains of *Y. lipolytica*. Successful implementation of this technology requires a system for rapid and consistent gene knock-outs and knock-ins with clear, testable markers to select and identify transformants and integration sites. The limitations presented by *Y. lipolytica* arise from a system that can be screened with few effective antibiotics and few standard resistance markers available. Lastly, this transformation system must provide an easy and testable way to be removed and/or reused effectively.

This chapter details the development of pCre-AHAS* and the biotechnologies in use, production of the final plasmid and genetic constructs, and initial testing of the system on the FAD2 gene. Special emphasis is placed on the design factors, intended to highlight the reasoning behind key decisions. While similar in some aspects to the classical method of using *LEU2* and *URA3* knockouts (53), our method, an extension of the work by Fickers et al. (54), allows for high specificity and selectivity through all steps of both construction and use.

2.1 Background

2.1.1 Why Does *Yarrowia lipolytica* Require a Custom Knockout Strategy?

Besides the obvious requirement for organism-specific initiators and terminators for any genes, *Y. lipolytica* has a high codon usage bias, requiring the codon optimization of relevant genes. In addition, *Yarrowia* is resistant to the majority of the commonly used antibiotics, eliminating a wide range of typical markers (55,56). Of these, only hygromycin B (hyg^B, shown hereafter as hyg) is highly effective (57), along with the much less common bleomycin/phleomycin group. While mutants with blockages in required metabolic processes have provided a few paths to gene manipulation, our eventual intention of multiple gene knockout products would require the use of many markers. Even though success has been seen with the use of the classical one gene-one marker knockout approach, the production of useful heavily modified strains, such as that reported by Dulermo and Nicaud (36) would require 8 markers, far more than exist. To circumvent this difficulty, a knockout system must optimally reuse one resistance cassette, with removal after each confirmed knockout. This criteria is met by the use of the Cre-AHAS* system, which operates with high specificity and an excision rate of over 98% in the seminal study (54).

2.1.2 Genetic Technologies in Use

2.1.2.1 Cre Recombinase

Cre recombinase is a topoisomerase derived from the P1 bacteriophage. It catalyzes the site-specific recombination of DNA between *loxP* sites, with the result dependent on the site orientation (58). The *loxP* recognition site is a 34-bp sequence with two 13-bp inverted repeats flanking an 8-bp spacer region that confers directionality (59). Three distinct configurations exist (Figure 9), but for our purposes we will use the orientation leading to deletion exclusively (60,61). Once the DNA segment is deleted, the product will still contain one active *loxP* site, which could cause problems upon a secondary transformation. To prevent this difficulty, two modified *loxP* sequences dubbed *loxLE*

and *loxRE* (so named as the left and right elements) will be used. These mutants are designed so that upon the catalytic action by Cre recombinase, the product *loxP* site formed is unrecognized by the recombinase and is thus inactive (62).

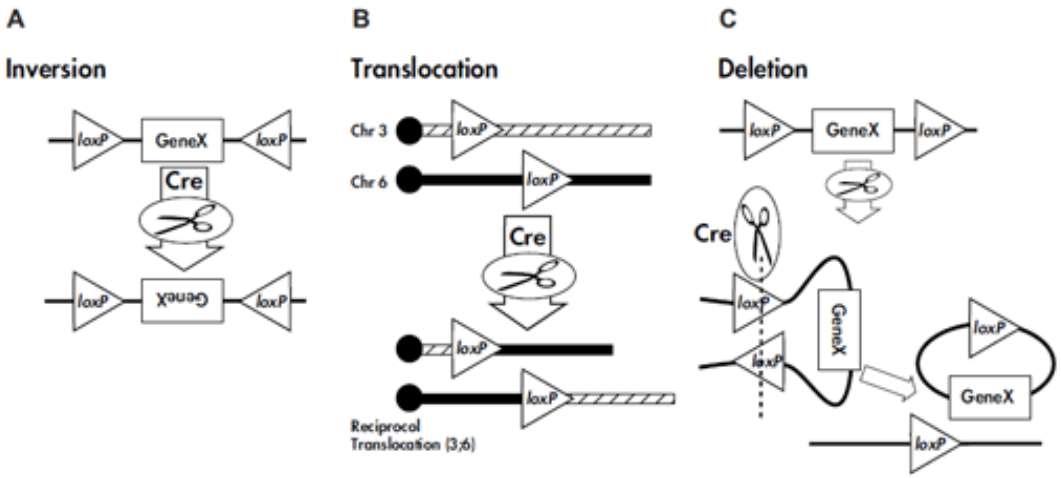

Figure 9. The functions of Cre recombinase. Most studies use Cre recombinase for genetic deletions. However, arrangement A allows for gene inversion and option B translocation, can in fact join together two segments of DNA into one cohesive strand. Figure courtesy of The Jackson Laboratory, Bar Harbor, Maine. All rights reserved (60).

By flanking our resistance cassette with the *loxLE* and *loxRE* sites, transformation with a plasmid to produce Cre recombinase will excise the desired sequence with no effect on the remaining genome beyond the short *loxLR* scar. However, without loss of this *Cre*-containing plasmid and an easy way to confirm its loss, iterative transformation will be impossible as the recombinase will excise the resistance prior to selection. To compensate for this, we have utilized an independent chlorimuron ethyl (CME)-resistant AHAS marker for the *Cre*-bearing plasmid.

2.1.2.2 CME and the *AHAS* gene

CME, or chlorimuron ethyl, is a sulfonylurea herbicide used on a number of plants for weed control. CME and its class of herbicides are of special interest, as they provide no harm to humans or animals, demonstrating little toxicity in birds with an acute toxicity of 2,510 mg/kg, and low toxicity to fish and invertebrates (63). While initial studies demonstrated no oncogenicity, teratogenicity, or mutagenicity (63), further research has led to its classification as a possible human carcinogen by DuPont (64). However, the previous results are upheld along with no carcinogenicity seen in tested mammals, thus the only reported threat to humans is skin and/or eye irritation.

CME inhibits the action of the acetohydroxyacid synthase (AHAS), thus arresting branched-chain amino acid synthesis (65). AHAS, also known as acetolactate synthase, is a transketolase which condenses two molecules of pyruvate to form carbon dioxide and acetolactate, the key first reaction in the synthesis of valine and leucine. AHAS also can convert α-ketobutyrate to α-aceto-α-hydroxybutyrate, a key step in the production of isoleucine from threonine. Without the ability to synthesize these key amino acids, the organism in question can not survive in minimal media that does not contain Val, Leu, and Ile (66). AHAS is present in bacteria, fungi, algae, and plants, and has been shown to be present in *Yarrowia* (67). Interestingly, several point mutations in the *AHAS* gene, including P197L and W497L, confer strong resistance to sulfonylurea herbicides (68). After verifying the activity of CME against our *Yarrowia* strain, the presence of this AHAS W497L mutant (designated AHAS*) on the Cre recombinase plasmid will allow selection of transformants via both CME and hyg. As the Cre recombinase works, the resistance to hygromycin will be deleted, allowing for selection through replica plating to identify colonies that grow in CME and not with hyg. Subsequent periods of growth in

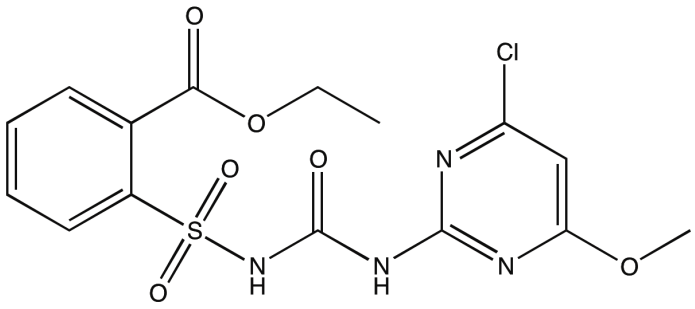

Figure 10: The structure of chlorimuron ethyl. While subclassified in a number of specialized categories, it derives the sulfonylurea title from its characteristic linker of the two aromatic groups.

nonselective media will allow for the eventual loss of pCre-AHAS*, reinstating susceptibility to CME once more. While all of the genes and transcriptional sequences existed separately, their assembly to a single functional construct was performed using a high-efficiency BP/LR Clonase reaction for easy integration.

2.1.2.3 BP/LR Clonase Reactions

Gateway® Technology (Invitrogen) is driven by the BP and LR Clonase reactions, catalyzed by enzymes derived from the lambda bacteriophage (69). Use of this system allows high efficiency transfer of a genetic sequence tagged with the transfer sites while maintaining orientation. The BP and LR reactions are so named due to the recognition sites which are targeted, namely *att*B, *att*P, and so on. These sites consist of 15-bp core regions that are homologous in all of the sites, flanked by selective targeting sequences. In the original lambda phage, the phage DNA, flanked by *att*P sites, is switched via the BP Clonase reaction with a segment of DNA in the bacteria it infects, flanked by *att*B sites. This allows the insertion of the phage DNA into the bacterium through the

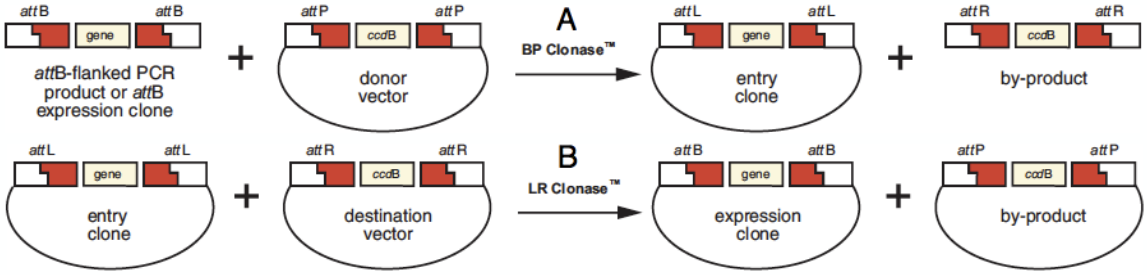

Figure 11. The Gateway® technology Clonase reactions. These two reactions constitute a two-step process, allowing for the use of any plasmid as the donor or destination vector, so long as it contains the appropriate Gateway sequence. The final expression clone from reaction B will have inactive *att*B sites. Image courtesy of Life Technologies (70).

lysogenic pathway, where it remains dormant. Once ready for excision from the bacterium through the lytic pathway, the phage DNA, now flanked by the *att*L sites produced through the insertion, will react with the *att*R sites and swap back the DNA through the LR Clonase reaction, reforming the *att*B and *att*P sites. In each case, the reaction occurs with homologous crossover at the core 15-bp sites, and the exchange of the DNA strand and half of each targeting sequence. This process is conservative,

directional, and able to be performed on DNA in any configuration (supercoiled, linear, etc.), albeit with differences in efficiency (71).

The proprietary patented version of this system from Invitrogen has a number of alterations from the original, including modifications to remove stop codons, to accommodate all reading frames, and to prevent secondary structure formation in the single stranded form at the *att*B sites. Additionally, the sites have been modified to ensure directionality; each *att*B site will react with only one of the *att*P sites, and vice versa. The donor vector and Gateway for use in the destination vector have both *ccd*B (discussed in the next section) and the Cm^R gene, conferring resistance to chloramphenicol (abbreviated Chl). Lastly, the final LR Clonase reaction produces inactive sites, guaranteeing irreversibility and guarding against any potential issues *in vivo* (70).

For our purposes, the desired gene (in this case, AHAS*) was synthesized as an *att*B-flanked PCR product and reacted with the provided donor vector, producing an entry clone. An appropriate Gateway sequence is inserted into the desired final plasmid, producing the destination vector. Finally, the entry clone and destination vector are reacted to produce the desired expression clone, which is ready for use.

2.1.2.4 Transformant Selection via *ccd*B

The *ccd*B gene, originally found in *Escherichia coli,* encodes CcdB, an F plasmid protein product that binds DNA gyrase. Once bound, the gyrase is inactivated, promoting the breakage of DNA and resulting in cell death. While this complex may be separated by another F plasmid protein, CcdA, the rapid demise of any *E. coli* strains containing the *ccd*B gene can be used as a transformation selection mechanism (72). Consider a situation as is shown in Figure 11A, where the entry clone is produced. After the BP Clonase reaction a total of four different products will be present: the unreacted PCR sequence, the unreacted donor vector, the reacted entry clone, and the byproduct strand. Of these, two contain the *ccd*B gene, resulting in cell death upon transformation. To select between the remaining two options, the donor vector plasmid contains the kanamycin resistance gene. Thus, even with transformation of the reaction mixture

directly into *E. coli* cells, growth on Kan-containing plates will result in growth of only cells containing the entry clone. Similarly, the destination vector contains the Chl resistance and a second resistance gene, which in our case codes for ampicillin resistance. After performing the LR Clonase reaction, transforming into *E. coli,* and growing on plates with Amp, all surviving product colonies should only contain the final expression clone (70). The published efficiency of this system is ≥99%.

2.1.3 Design Summary

The initial gene knockout was performed using a designed knockout construct (Figure 12). Using 1-kb untranslated regions (UTRs) on either side to target the appropriate gene,

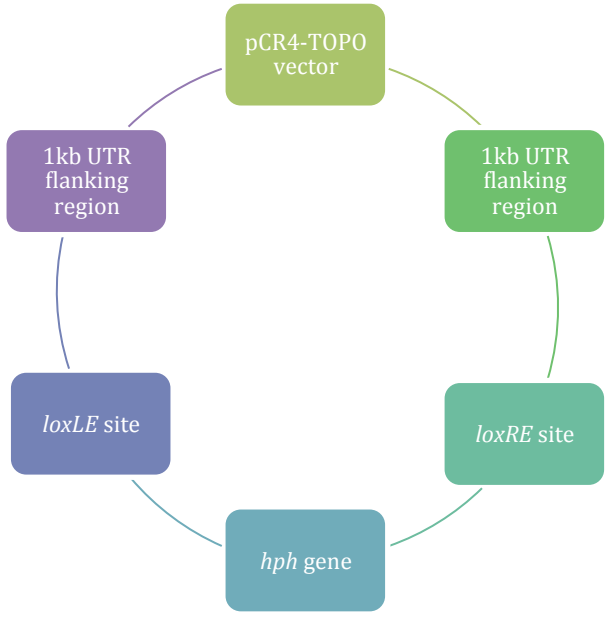

Figure 12: Knockout construct diagram. Note *hph* confers resistance to hygromycin B, and that the specialized *lox*P mutant sites are in use.

the sequence was replaced via homologous recombination through double crossover. The presence of this construct was verified by growth on YPD + hyg followed by verification of the location by PCR amplification. A consistent distribution of primer-binding sites (Figure 13) was designated that allow for the selective amplification of relevant products for all knockouts. Using this approach, three amplifications would be sufficient to conclusively demonstrate this homologous recombination displacing the target gene: 1) Amplification of HPH3→C. This amplification, entirely within the inserted construct,

will verify the integrity of the drug resistance cassette. 2) Amplification of HPH3→F. This amplification runs from the center of the construct out into the neighboring genome and will provide support that the recombination was correctly targeted. 3) Amplification of HPH4→E. Analogous to the second amplification, isolation of a properly sized PCR product will further support disruption of the intended locus by probing sequence adjacent to the opposite end of the construct.

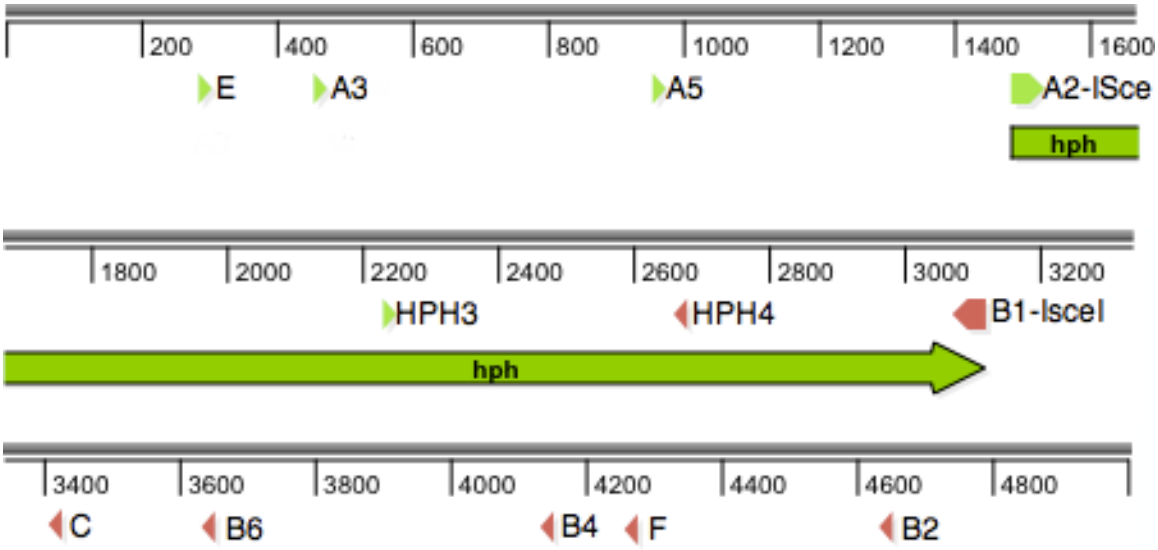

Figure 13: PCR primer sites in and around the knockout construct. Note that the construct extents 1kb from either end of the hph gene.

The remainder of the design summary, previously described herein, is summarized in Figure 14. The product pCre-AHAS* will be usable with any other gene knockout constructs using this same *hph*/*loxP* design. In addition, after loss of pCre-AHAS*, a knockout strain may then integrate a second *hph* construct through homologous recombination, which may in turn be excised through transformation with pCre-AHAS*. This iterative process is limited only by the number of *hph* constructs synthesized.

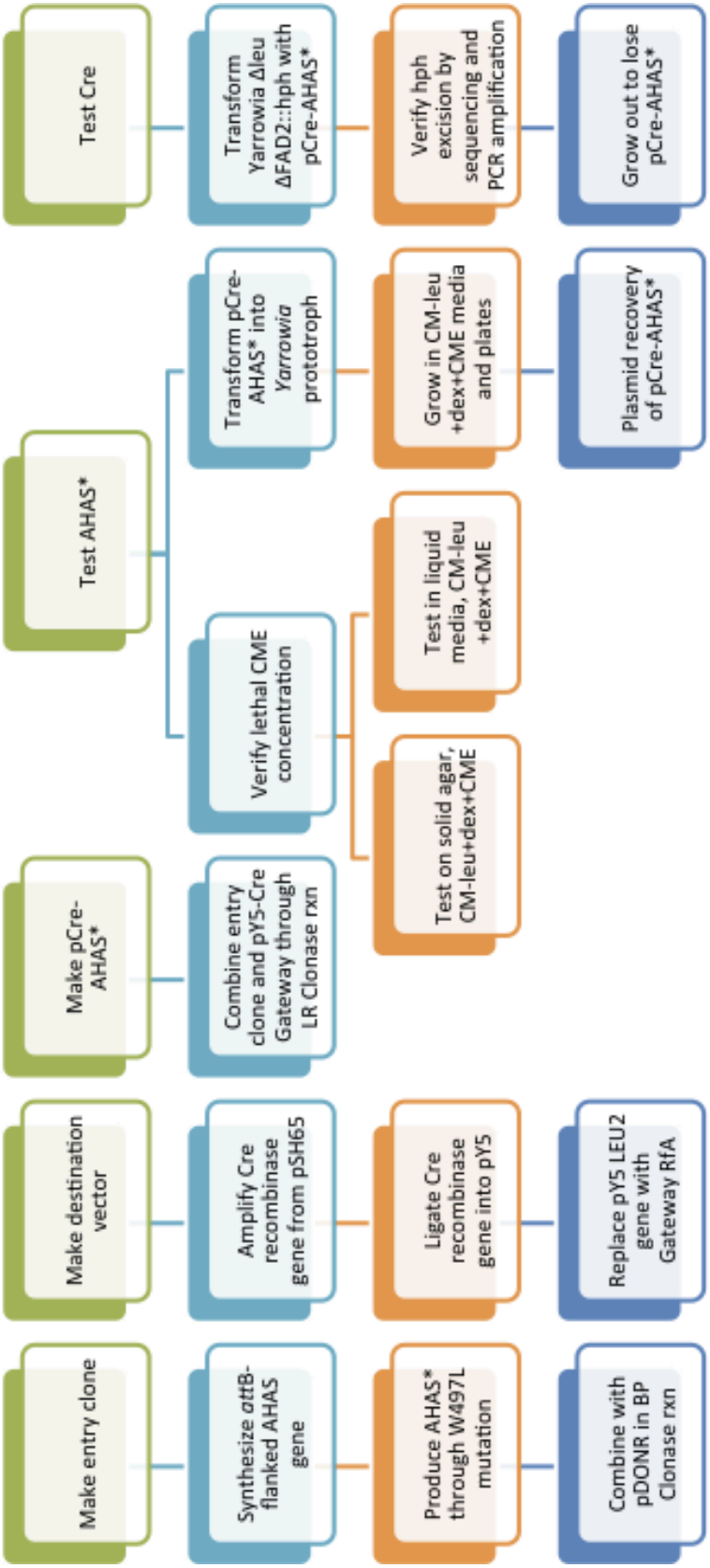

Figure 14: Plan of action for the construction, production, and testing of pCre-AHAS*. Intended sequence of events is left to right, top to bottom.

2.2 Materials and Methods

2.2.1 Production of Entry Clone

Wild type *Y. lipolytica* (ATCC 20460) was grown on YPD at 28°C. Genomic DNA was released from cells via NaOH preparation similar to that given by Wang et al. (73). A small clump of fresh cells (1 mm^3) were added to 10 µL of 20 mM NaOH and heated to 99 °C for 15 min. The cells were then rapidly centrifuged, resulting in a solution

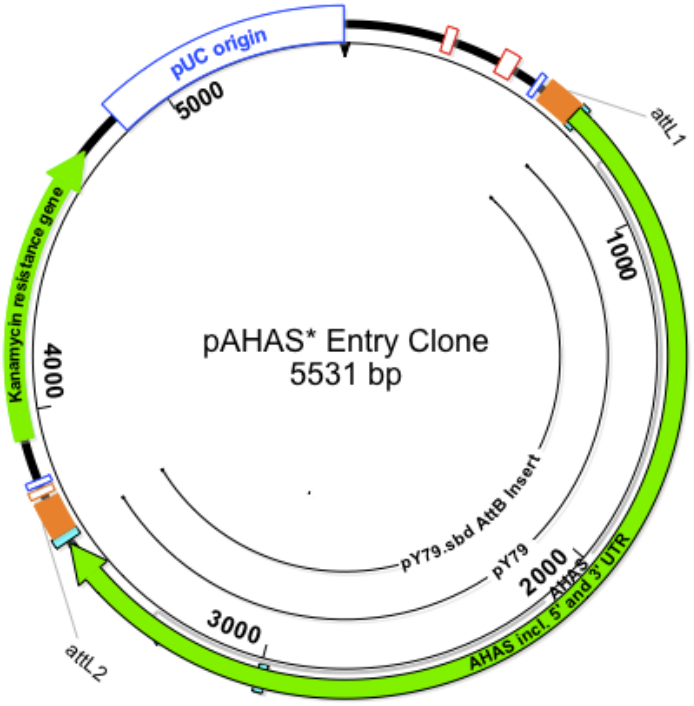

Figure 15: Map of pAHAS* after BP Clonase rxn.

containing the desired DNA. The W497L mutant *AHAS* was then amplified in two steps from the gDNA using specialized primers containing the *att*B sequence flanking either end of the gene and primers to install the point mutation. After sequencing to confirm its identity and the installation of the desired mutation, the *AHAS** gene was reacted with pDONR221 via the BP Clonase reaction (70) to produce the entry clone, as seen in Figure 15. This clone was prepared by Dr. Robert Minto, prior to my involvement in this project.

2.2.2 Preparation of Gateway Plasmid

Unless otherwise noted, each product plasmid was transformed back into $RbCl_2$ XL1 Blue chemically competent *E. coli* cells to prepare freezer stocks, then fresh cultures of each were grown and the plasmids were prepared using the alkaline lysis Wizard miniprep kit from Promega. The Cre recombinase gene had been PCR amplified from pSH65 (graciously provided by Prof. M. Goebl, IU School of Medicine, Indianapolis, IN) and ligated into the BamHI/NotI sites in the pY5 plasmid (a gift from E. Cahoon, Univ. Nebraska, Lincoln, NE) (Figure 16). While retaining the ARS 18 as the *Yarrowia* promoter sequence, it was advantageous to replace the no longer needed LEU2 gene with a Gateway linker sequence to allow the flexible installation of a new selectable marker. A mutation at position 2910 was added using the QuickChangeII procedure to inactivate the EcoRI restriction site, which was confirmed via digests with EcoRI (Figure 17). When initial attempts with EcoRI/SphI double digests were unsuccessful despite optimization of the digestion conditions and the addition of SphI restriction sites via mutagenesis, digestion with EcoRI alone only excised half of the LEU2 gene (positions 5545-6507), as shown in Figures 18-21. This was also shown via cycle sequencing (Figure 22). After repeated failures in digesting the plasmid with EcoRI and SphI, together or stepwise, other options were considered, leading to the ultimate installation of an EcoRI site adjacent to the ARS 18 promoter. With insertion of this site via a point mutation (T4309A), the product plasmid was checked via cycle sequencing (Figure 23).

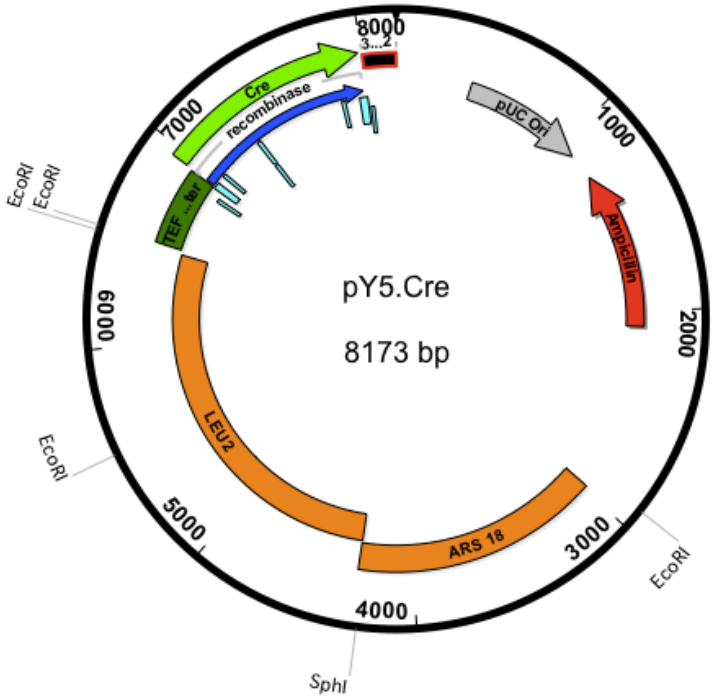

Figure 16: pY5-Cre plasmid map. This plasmid is the result of ligating Cre recombinase, excised from pSH65, into the standard *Yarrowia* plasmid pY5 (plasmid courtesy of R. Minto).

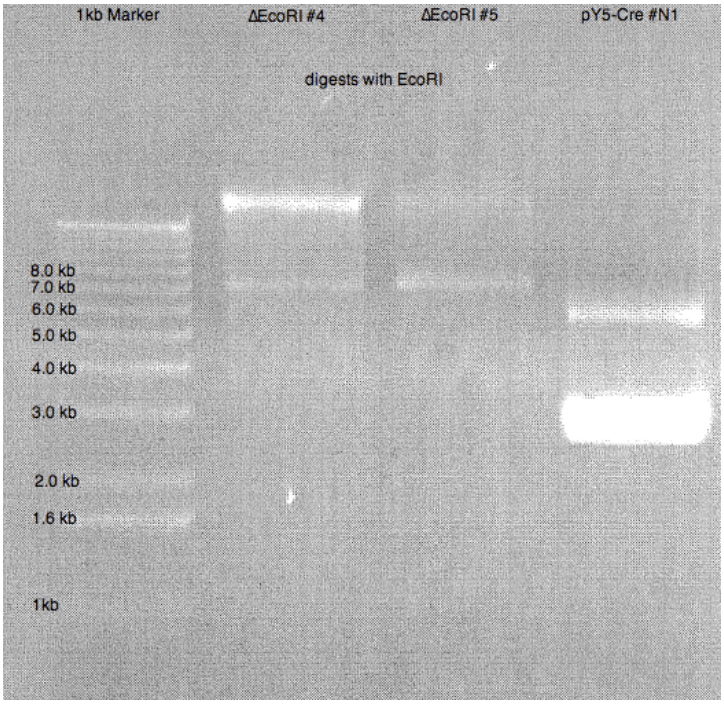

Figure 17: Confirmation of EcoRI site deletion. Note that in the deletion strains only one ~7 kb band is visible (the 1 kb band is too faint to be seen), but the plasmid prior to site directed mutagenesis led to two excision products (~2.6 kb and 5.5 kb).

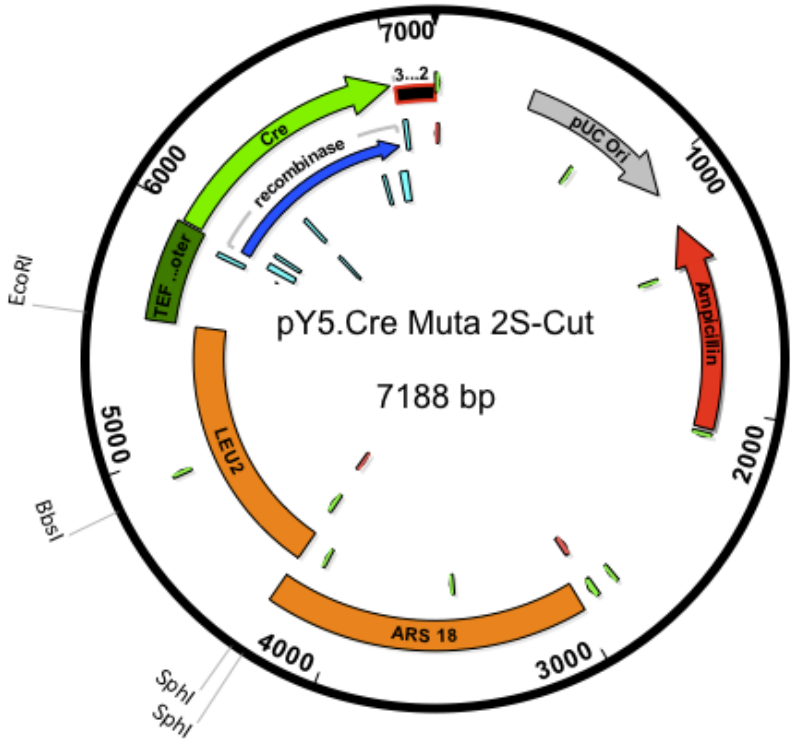

Figure 18: Plasmid resulting from the excision of half of the LEU2 gene from pY5-Cre. The Muta 2S title is derived from the second SphI site that was engineered into the LEU2 gene by site-directed mutagenesis.

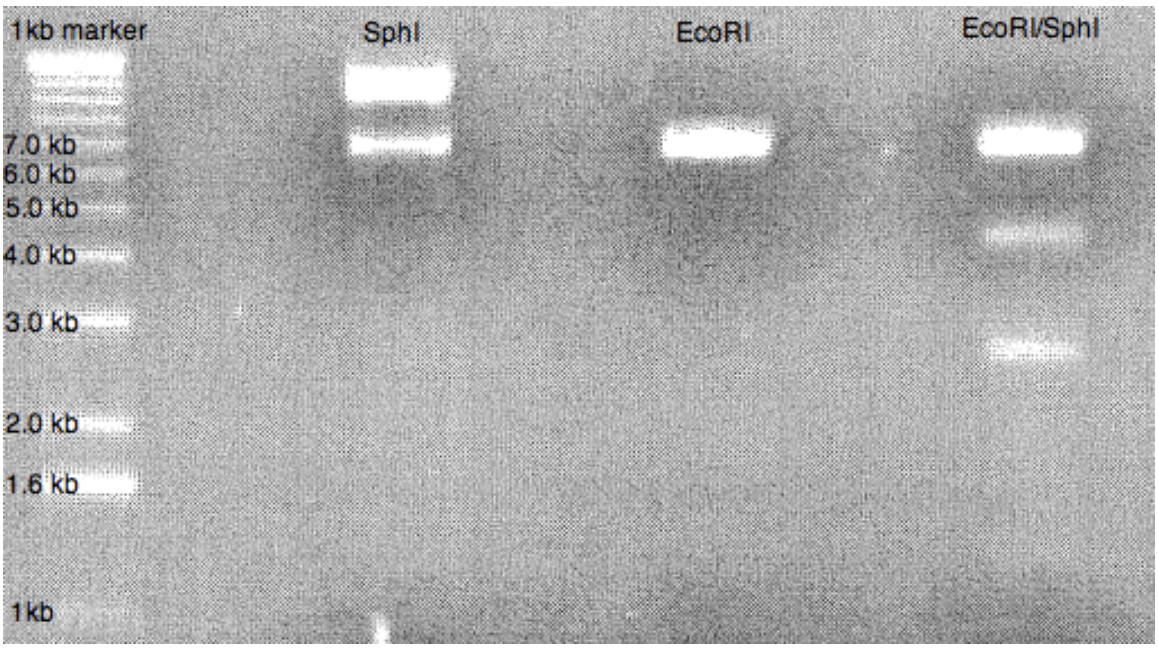

Figure 19: Restriction digests of pY5-Cre Muta 2S-Cut. Note the large amount of uncut plasmid from the SphI digest. Both SphI and EcoRI individually show effective digests, but the double digests led to aberrant bands. Due to this irregularity, the plasmid was also checked with a second battery of digests.

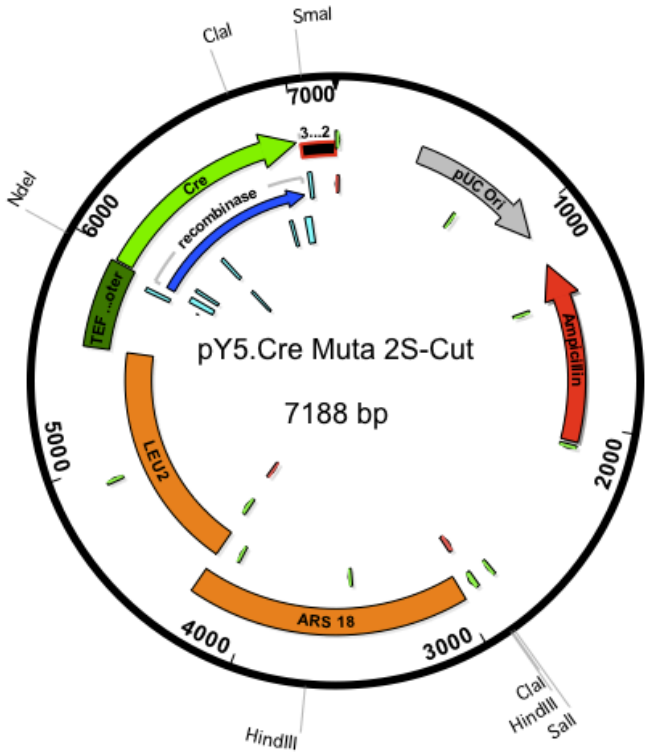

Figure 20: pY5-Cre Muta 2S-Cut with selected restriction sites denoted.

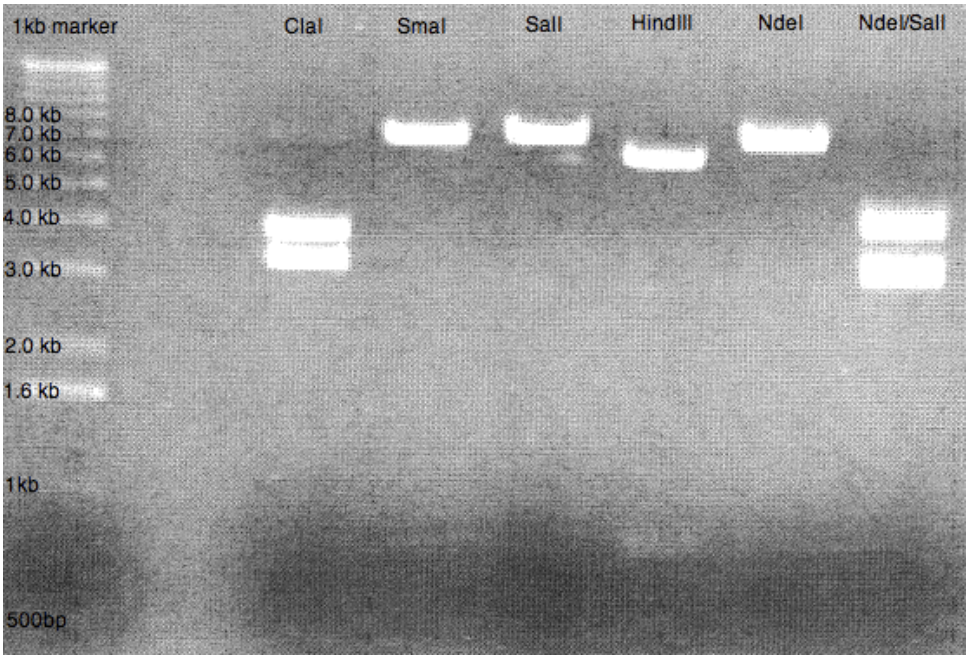

Figure 21: Alternative restriction digests of pY5-Cre Muta 2S-Cut. All of the fragment lengths correspond exactly with those predicted from the plasmid restriction map, thus supporting its identity.

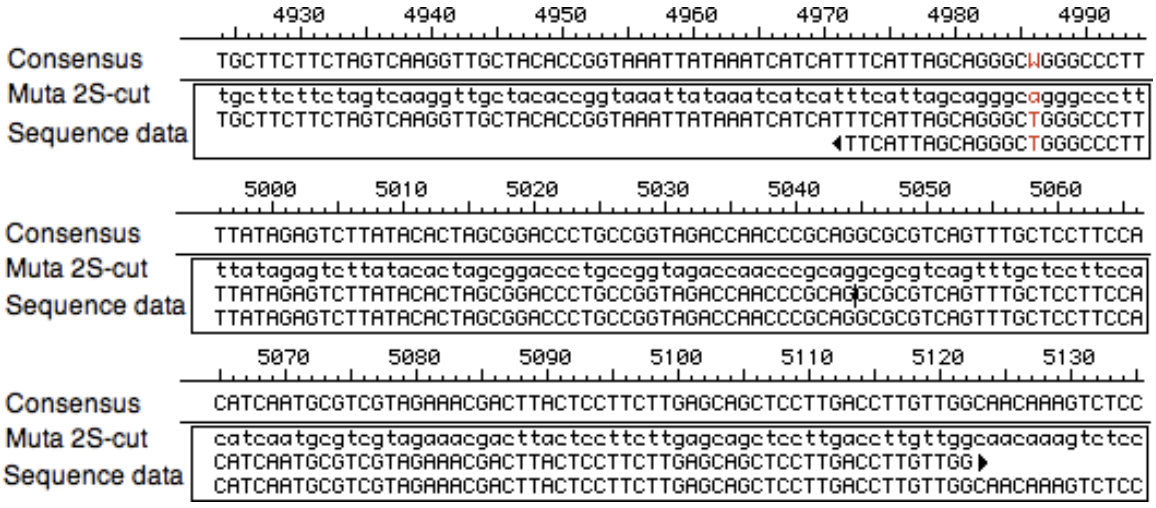

Figure 22: Selected sequencing data confirmed the pY5-Cre Muta 2S-Cut sequence. This region was selected due to the overlap of the two sequenced regions. Excepting the installed mutation, only 2-3 possible sequence changes versus the GenBank sequence for pY5-derived regions of the plasmid were observed throughout the total sequence area.

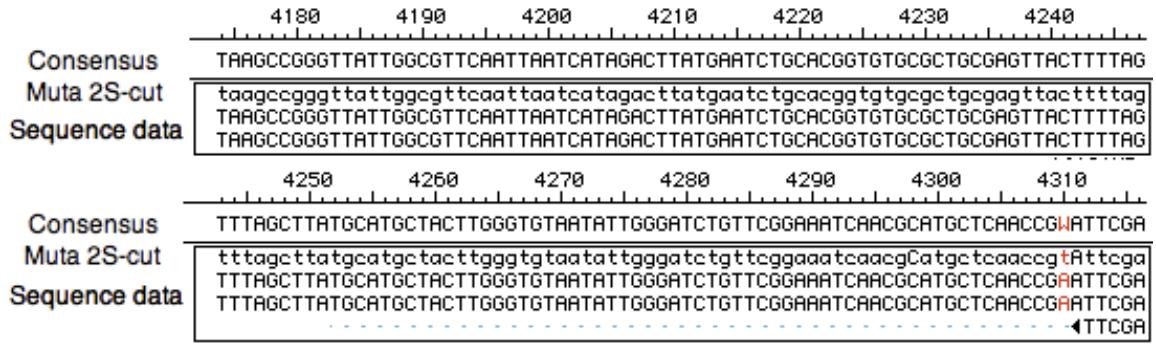

Figure 23: Sequencing of T4309A mutant demonstrated the insertion of the EcoRI site. This plasmid was denoted as pY5-Cre Muta 2E/2S, due to the two altered EcoRI and two SphI restriction sites. Note the presence of the desired mutation in red.

The resulting plasmid was also checked directly by an EcoRI digestion (Figure 24). To complete the replacement of the *LEU2* gene with the Gateway linker, this plasmid was digested in excess with EcoRI, heat inactivated, then the DNA ends were blunted. This final DNA strand was treated with Antarctic phosphatase to limit recircularization. Once the phosphatase was inactivated, the DNA was mixed with Gateway RfA from the Invitrogen Gateway Kit per published instructions (70), and the two were joined using T4 DNA ligase. The heat-inactivated ligation mixture was transformed into Invitrogen One Shot® *ccd*B Survival™ T1^{R} competent cells and plated on prewarmed LB+Amp+Chl

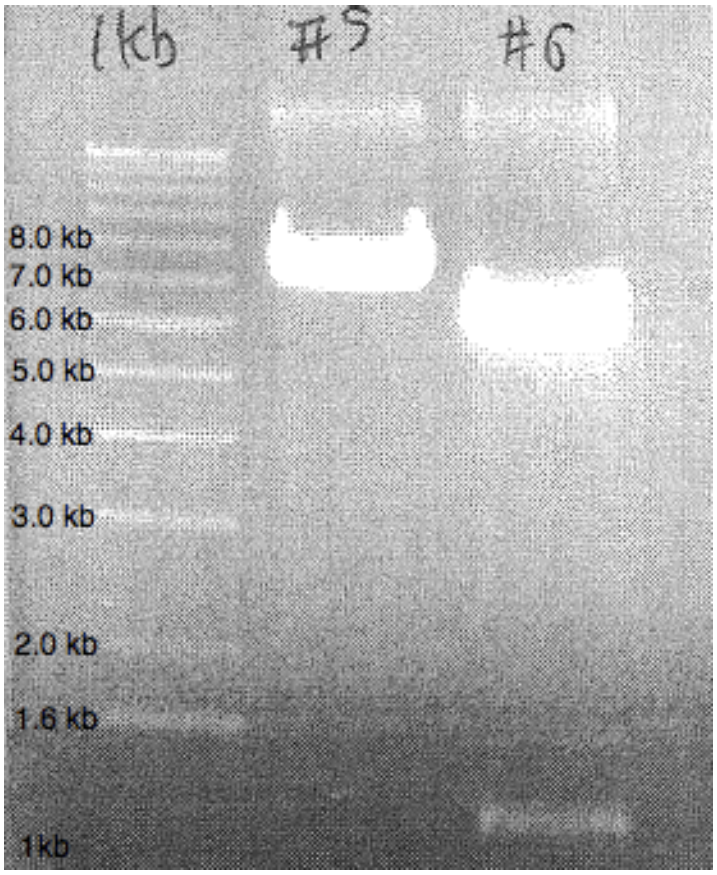

Figure 24: Digests of Muta 2E/2S strains with EcoRI. Plasmid #5, which was the precursor to the addition of the EcoRI site near base 4310, merely linearized, but DNA from plasmid #6 successfully produced two fragments of the correct size.

plates. Initial growth of 2 days at 37°C resulted in no colonies, likely due to the presence of 3 very strong selection factors (Amp, Chl, and ccdB). The plates were allowed to sit out at room temperature over two additional days, resulting in hundreds of colonies. Of these, 64 colonies were screened via shaken growth in LB+Amp+Chl liquid media overnight at 37 °C, 250 rpm. In total, 7 of these cultures grew, and the best four were analyzed via boiling miniprep. The final plasmid DNA was tested via digestion with MluI and SmaI (Figure 25), showing two plasmids (Gateway #8 and Gateway #9) with the RfA gateway in the correct orientation (Figure 26), and two (Gateway #15 and EG #24) with the RfA gateway ligated in the reverse direction (Figure 27). All four strains were cultured and duplicate freezer stocks of each were made and stored in the -80 °C freezer. After sequencing of the Cre recombinase gene to ensure no alterations and of the Gateway cloning site as final confirmation of positioning, Gateway #9 was chosen as the verified destination vector.

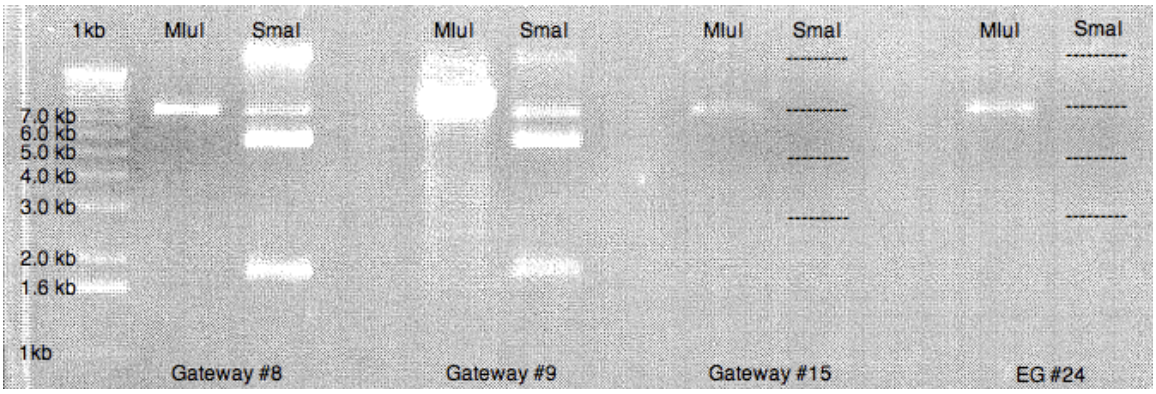

Figure 25: Confirmatory digests of the Gateway destination vectors. Due to lightness the bands for Gateway #15 and EG #24 are marked. SmaI appears to have poor activity because both the uncut and singly cut plasmid appeared for each digest.

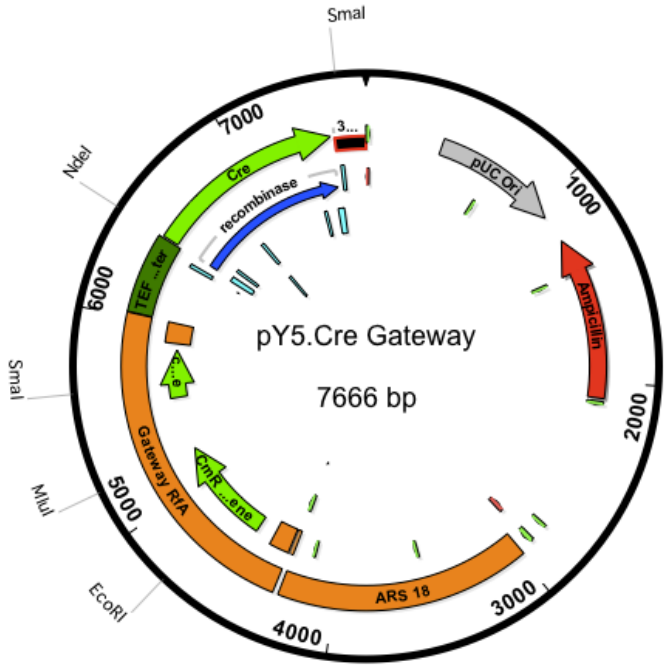

Figure 26: Map of the Gateway destination vector.

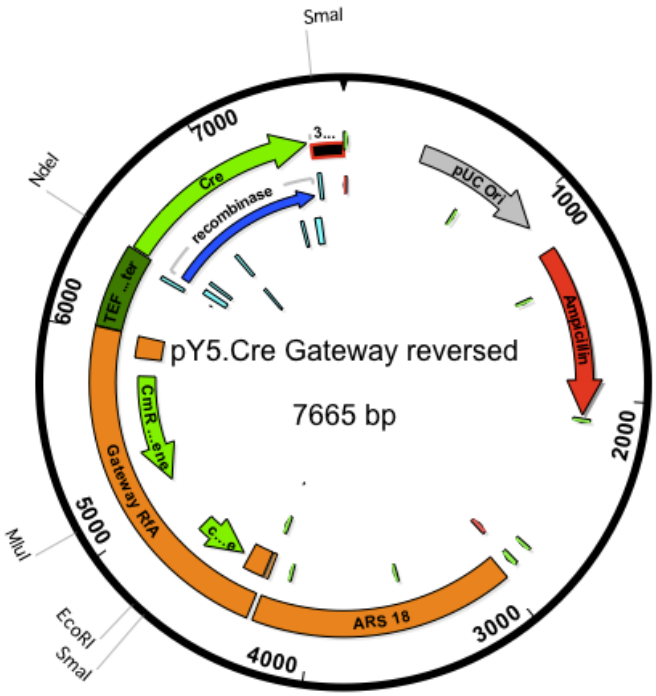

Figure 27: Map of Gateway destination vector with inverted Gateway cassette.

2.2.3 LR Clonase Reaction

The marker gene from pAHAS* #11 was transferred into pY5-Cre Gateway #9 with the LR Clonase reaction using the published procedure (70). The resulting reaction mixture was transformed into supercompetent Omnimax® 2 T1^{R} cells (Invitrogen) and plated on LB+Amp plates, which were incubated at 37 °C. A total of four colonies appeared overnight, all of which were picked and cultured in liquid LB+Amp overnight at 250 rpm, 37 °C. Plasmid DNA was isolated and digested with three restriction enzymes for characterization (Table 2; Figures 28, 29). Clone LR2 clearly showed the appropriate bands and was thus renamed pCre-AHAS*. Cycle sequencing of the LR2 product (pCre-AHAS*) was also used to verify the sequence fidelity (not shown).

Table 2: Expected band sizes for restriction digests of pCre-AHAS*.

Restriction Enzyme	NcoI	AflII	NotI
Expected bands (bp)	5635	7608	8998
	1947	1390	
	1290		
	126		

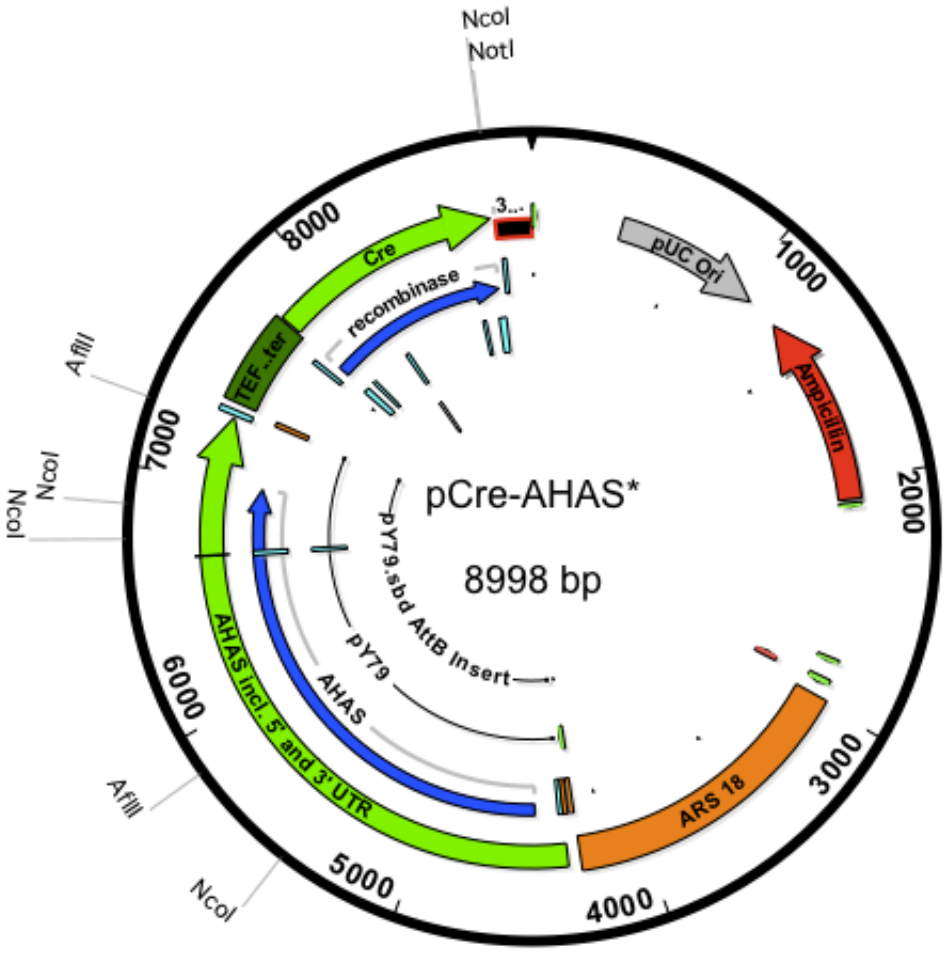

Figure 28: Map of pCre-AHAS* plasmid.

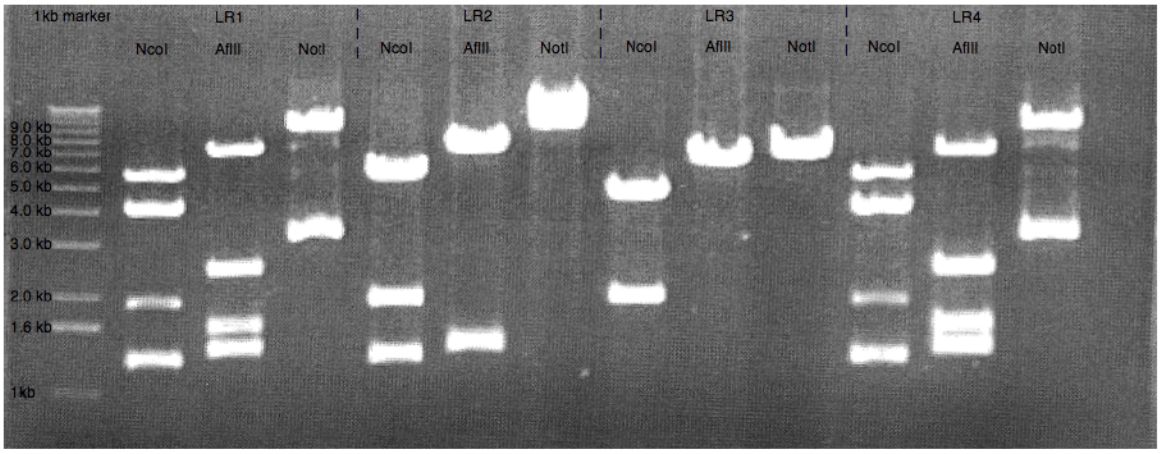

Figure 29: Characteristic digests of the product strains from the LR Clonase reaction. While LR1 and LR4 appeared to have the same product, its identity was not pCre-AHAS* based on the plasmid map. Only LR2 showed the appropriate bands.

2.2.4 Testing of CME Herbicide

To be able to utilize the AHAS* gene as a selection marker, an effective working concentration for CME needed to be determined. Since colonies will be grown in both liquid and solid cultures, both of these dosages were determined separately. With its high CME solubility of 70.5 mg/mL and low toxicity, acetone was chosen for the preparation of concentrated stock solutions (63). Other solvents capable of dissolving CME efficiently, such as methylene chloride (153 mg/mL), acetonitrile (31.0 mg/mL), and ethyl acetate (23.6 mg/mL) presented toxicity concerns for *in vivo* experiments, while the solubility in n-hexane was far too low for use as a stock solution (0.06 mg/mL). To avoid evaporation issues when pipetting small volumes of the CME in acetone, a secondary stock solution of CME in ethanol (reported solubility of 3.92 mg/mL (63)) was used for lower concentrations.

2.2.4.1 Liquid Cultures

In total, three studies were performed to determine the required CME concentration in liquid cultures. For each study, the prototrophic *Yarrowia* ATCC 20460 strain was cultured overnight in YPD at 28 °C, 240 rpm for use as a starter. The cell density of this starter was manually counted allowing the culture flasks to be inoculated with 4.0×10^3 cells per mL of CM-leu+dex. After inoculation with the cells, an appropriate amount of

CME was added to each flask and the culture was incubated at 28 °C, 240 rpm. The flasks were removed from the incubator at regular intervals and sampled, with the cell density measured spectrophotometrically. The sampled volume or, as necessary, a dilution of the sample to remain within the dynamic range of the spectrophotometer was analyzed by A_{600} absorption. The results of these studies are shown in Figures 30-32. In total, while dosing each set of replicates (prepared from the same starter), the only significant growth was seen for cultures with ≤1 µg/mL, and marginal growth in cultures at 5 µg/mL. To ensure absolutely no growth of contaminant colonies, 20 µg/mL was selected as the standard liquid culture CME concentration.

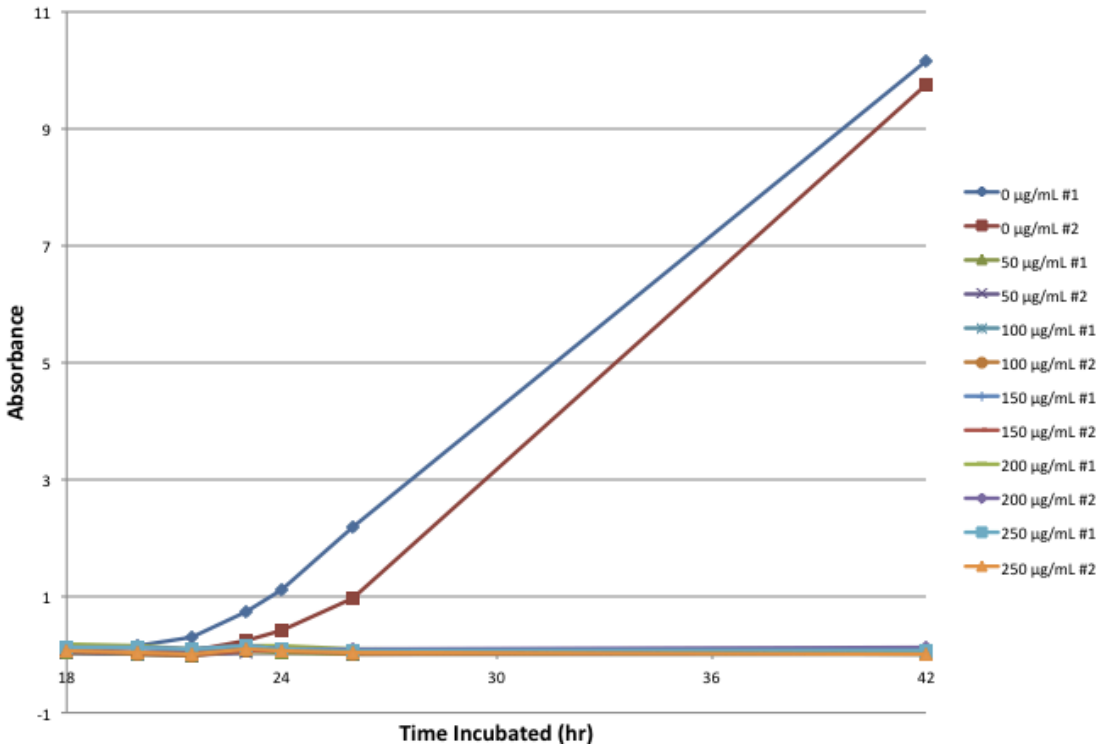

Figure 30: CME feeding in liquid media - trial #1. This trial used high [CME], with the CME stock solution in acetone. After 42 hours, no growth was seen from any of the CME-containing cultures.

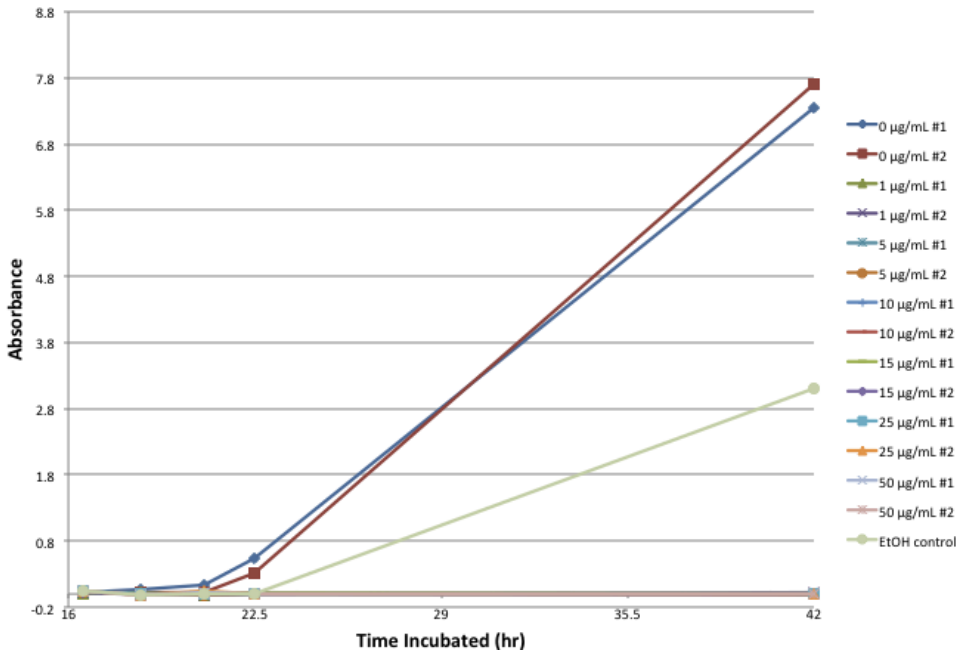

Figure 31: CME feeding in liquid media - trial #2. This trial used low [CME] and the CME stock solution in EtOH. The EtOH control was fed pure EtOH at the maximum concentration used. After 42 hours, no significant growth was seen from any of the CME-containing cultures.

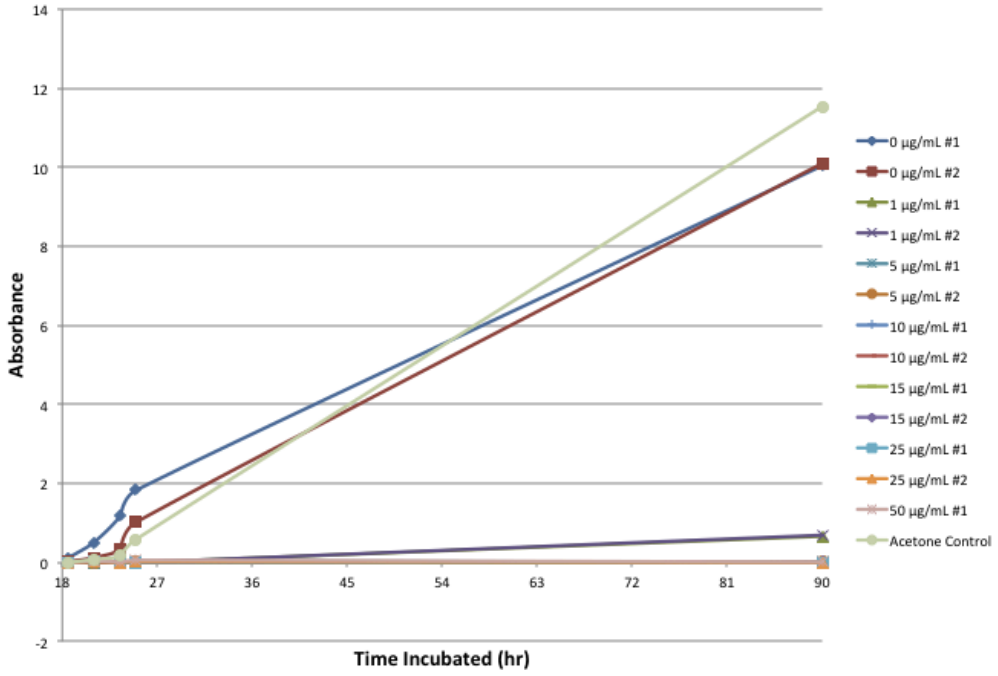

Figure 32: CME feeding in liquid media - trial #3. After 90 hours of culturing, significant growth was seen for [CME] ≤1 µg/mL, and detectable growth was observed for 5 µg/mL CME. As before, the acetone control was fed the same volume as present in the most concentrated flask.

2.2.4.2 Solid Agar Plates

To test the necessary CME concentration in solid media, a series of CM-leu+dex+CME plates were poured, with concentrations ranging between 1-150 µg/mL CME. A freshly cultured overnight *Yarrowia* prototroph starter was diluted 1:20 in TE, and 150 µL of the dilution was pipetted to each plate and spread across the surface via glass spreader bar. The plates were incubated 48 hours at 28 °C and the resulting colonies were counted (Table 3). Since 100 µg/mL marks the concentration that suppressed essentially all growth and allowed the preparation of homogeneous plates, it was selected as the standard concentration for CME in solid media.

CME concentration	Colony Count
1 µg/mL	Lawn – DNR
10 µg/mL	Lawn – DNR
25 µg/mL	≥400 colonies
50 µg/mL	≥100 colonies
100 µg/mL	6-8 colonies
150 µg/mL	0 colonies

Table 3: Growth of the *Yarrowia* prototroph on CME in solid agar. While the higher concentration of 150 µg/mL resulted in no colonies, both sets of plates contained precipitated CME crystals.

2.2.5 Testing of pCre-AHAS*

2.2.5.1 Production of *FAD2* KO

The synthesis of the *FAD2* KO construct, as with all of the other *Yarrowia* gene KOs, was completed in conjunction with the IUPUI Undergraduate Research Mentoring (URM) program. Several undergraduates, under the coordination of Dr. Brenda Blacklock, assisted in the synthesis, assembly, and transformation of these hyg-selected knockout cassettes, with the majority of the successful products produced by Dr. Blacklock and Paola Fernandez. The *FAD2* KO construct was synthesized and verified through PCR amplification and cycle sequencing by Dr. Blacklock. It was subsequently transformed into *Yarrowia* with homologous recombination, and the insertion site was verified by PCR amplification.

2.2.5.2 Confirmation of AHAS* Resistance to CME

To demonstrate the insensitivity of AHAS* to CME, the prototrophic *Yarrowia* strain was transformed with pCre-AHAS* via the procedure described by Mauersberger and Nicaud (74), and spread on a pair of CM-leu+dex+CME plates. Throughout the remainder of this thesis, CME was added to liquid and solid media at 20 µg/mL and 100µg/mL CME, respectively. After incubation at 28 ℃ for 4 days, the plates showed a total of ~400 colonies. Of these, 50 transformants were picked and cultured in liquid CM-leu+dex+CME at 28 °C, 240 rpm overnight. All cultures grew, with 48 of the tubes exhibiting near-saturated growth of the picked culture. To confirm that this survival was due to pCre-AHAS*, four of the cultures were subjected to rapid plasmid recovery through an abbreviated version of the method of Hoffman and Winston (75). The recovered DNA was transformed into *E. coli* under Amp selection and analyzed by restriction digest with NcoI (Figures 28 & 33, Table 4). Excepting a singular band attributed to star activity that can be seen brightly in four digests and dimly in two more, only one of the analyzed recovered plasmids was found to be inconsistent with pCre-AHAS*. This demonstrated the link between pCre-AHAS* and resistance to CME at the concentrations in use, both on solid and in liquid media.

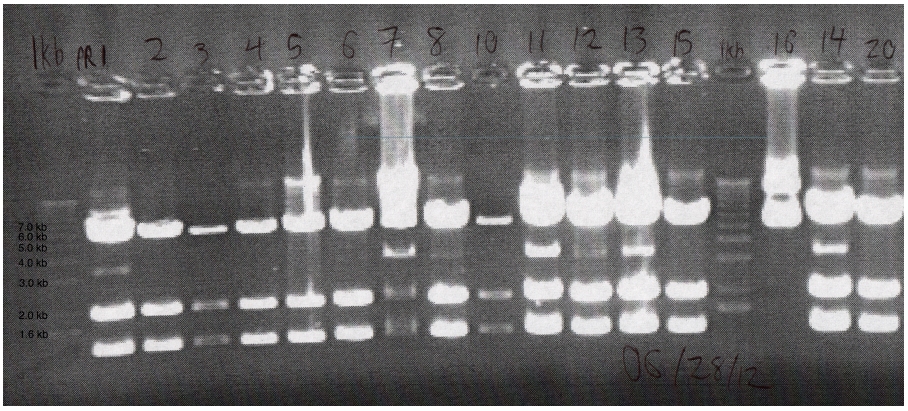

Figure 33: NcoI digests of recovered plasmids. While the plasmid analyzed in lane 16 produces the wrong fragments, the remainder had the correct pattern, occasionally with one star activity band at 3500 bp.

Table 4: Expected bands for NcoI digestion of recovered plasmids.

Expected Bands
5635 bp
1947 bp
1290 bp
126 bp

2.2.5.3 Transformation of pCre-AHAS* into Δ*FAD2*

The confirmed *FAD2* KO *Yarrowia* strain was cultured and transformed with pCre-AHAS* according to the method of Mauersberger and Nicaud (74), then spread on CM-leu+dex+CME plates. After incubation at 28 °C for 4 days, the pair of spread transformant plates showed ~500 colonies. Of these, a total of 50 were picked and cultured in liquid CM-leu+dex+CME overnight at 28 °C, 240 rpm. While thirteen of the colonies showed no growth, 20 showed low level and 17 showed extensive growth. Of these, four were analyzed via the same rapid plasmid recovery procedure performed on the prototroph (75). As before, NcoI digests of the recovered plasmids confirmed the presence of pCre-AHAS* (data not shown). All of the colonies that showed growth in CM-leu+dex+CME liquid media were replicate streaked in triplicate onto two paired plates of YPD+hyg and CM-leu+dex+CME, to test the excision rate of the hph resistance cassette (Table 5, Figure 34).

Table 5: Loss of hyg resistance vs. incubation time in CM-leu+dex+CME. Note that, as expected from culturing in CM-leu+dex+CME, all streaked colonies retained growth on the solid CME-containing agar. ++hyg denotes extensive growth on YPD+hyg, while +hyg indicates the presence of a few small colonies. After 48 hours incubation, ~96% of streaked colonies did not grow on YPD+hyg, indicating excision of the hph resistance cassette by Cre recombinase.

Incubated for 24 hours in CM-leu+dex+CME			Incubated for 48 hours in CM-leu+dex+CME	
Phenotype	Count		Phenotype	Count
++ hyg/ +CME	5		++ hyg/ +CME	5
+hyg/ +CME	12		+hyg/ +CME	0
-hyg/ +CME	97		-hyg/ +CME	109
-hyg/ -CME	0		-hyg/ -CME	0

Three of the colonies that most clearly showed loss of the hph gene (KO2-2, KO5-2, KO50-3) were then selected to be grown out and lose pCre-AHAS* plasmid. Fresh stocks of each were cultured overnight and freezer stocks were made in duplicate.

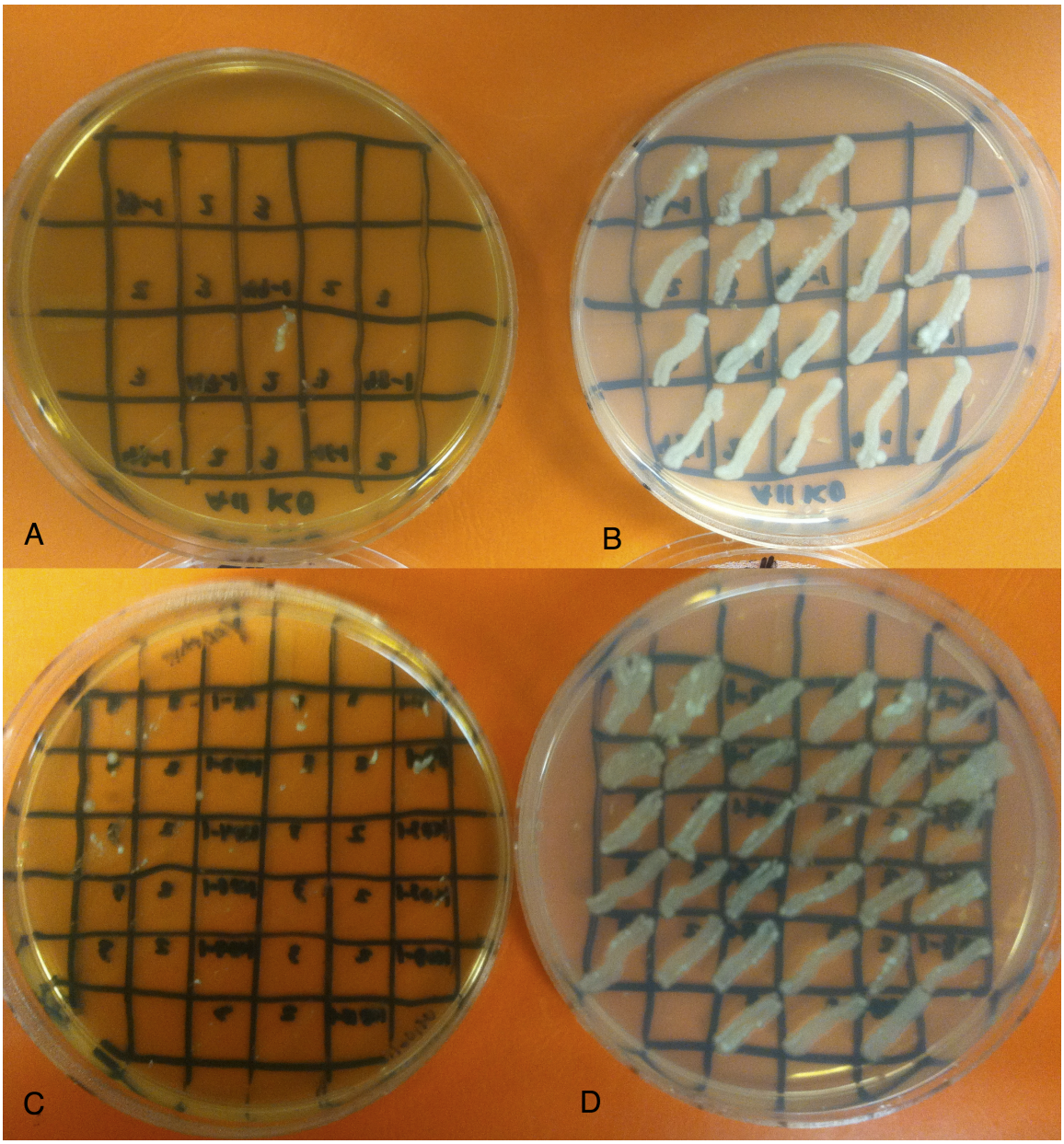

Figure 34: Pictures of replica plates for hph excision. Plates A & C show growth on YPD+hyg, while B & D show growth on CM-leu+dex+CME. The streak in the middle of A is ++hyg, while the isolated colonies on plate C were recorded as +hyg.

2.2.5.4 Grow out for Loss of pCre-AHAS*

Yeast, like bacteria (76), are capable of losing plasmids containing selection markers during extended growth in non-selective media if the plasmid loss confers no benefit to its viability without the selection challenge (77-79). For this project, these conditions were provided by culture in YPD. Initial colonies (KO2-2, KO5-2, KO50-3) were picked

from fresh streaks on CM-leu+dex+CME plates incubated overnight at 28 °C. Each colony was inoculated into YPD and incubated overnight at 28 °C, 240 rpm and then it was streaked onto CM-leu+dex+CME to test for plasmid loss. If the cells still grew, an aliquot of the YPD culture was reinoculated into fresh YPD and cultured again overnight at 28 °C, 240 rpm. After five cycles of this iterative growth (abbreviated as Gen1, Gen2, etc), each of the cultures in Gen3, 4, and 5 were replicate streaked 5 times on YPD and CM-leu+dex+CME plates. After incubation overnight at 28 °C, a total of only three colonies from the streaks showed no resistance to Cre-AHAS*. Freezer stocks of all three strains were made in duplicate and stored. Further investigation to determine the reason for this retention of the resistance plasmid concluded that since the AHAS* sequence was identical to the AHAS gene present in the gDNA, excessive incubation in CM-leu+dex+CME may result in homologous recombination of the mutant gene into the genome. If this were to happen, even upon loss of pCre-AHAS* the colony would retain resistance to CME. As a preventative measure, future transformants were transferred directly into YPD for grow outs from the original selection plate, mitigating the advantageousness of the recombination event.

2.2.5.5 KO Confirmation via FAME GC/MS Analysis

As a final confirmation, FAMEs (Fatty Acid Methyl Esters) were prepared from the prototroph and cured *FAD2* KO Yarrowia strains as previously described (80,81). Cells from each sample were pelleted and then resuspended in 2% H_2SO_4 in MeOH. After a 1 h incubation at 80 °C to produce the methyl esters, the mixture was extracted twice with H_2O/hexanes, and the organic layers were combined and dried down under a stream of N_2. The resulting concentrated FAME products were then analyzed by an Agilent Technologies GC-MS (7890A GC/ 5975C MS) using a VF-23 column (30 m x 250 µm x 0.25 µm). For “VF23FAME”, the oven program was: 60 °C starting temperature,

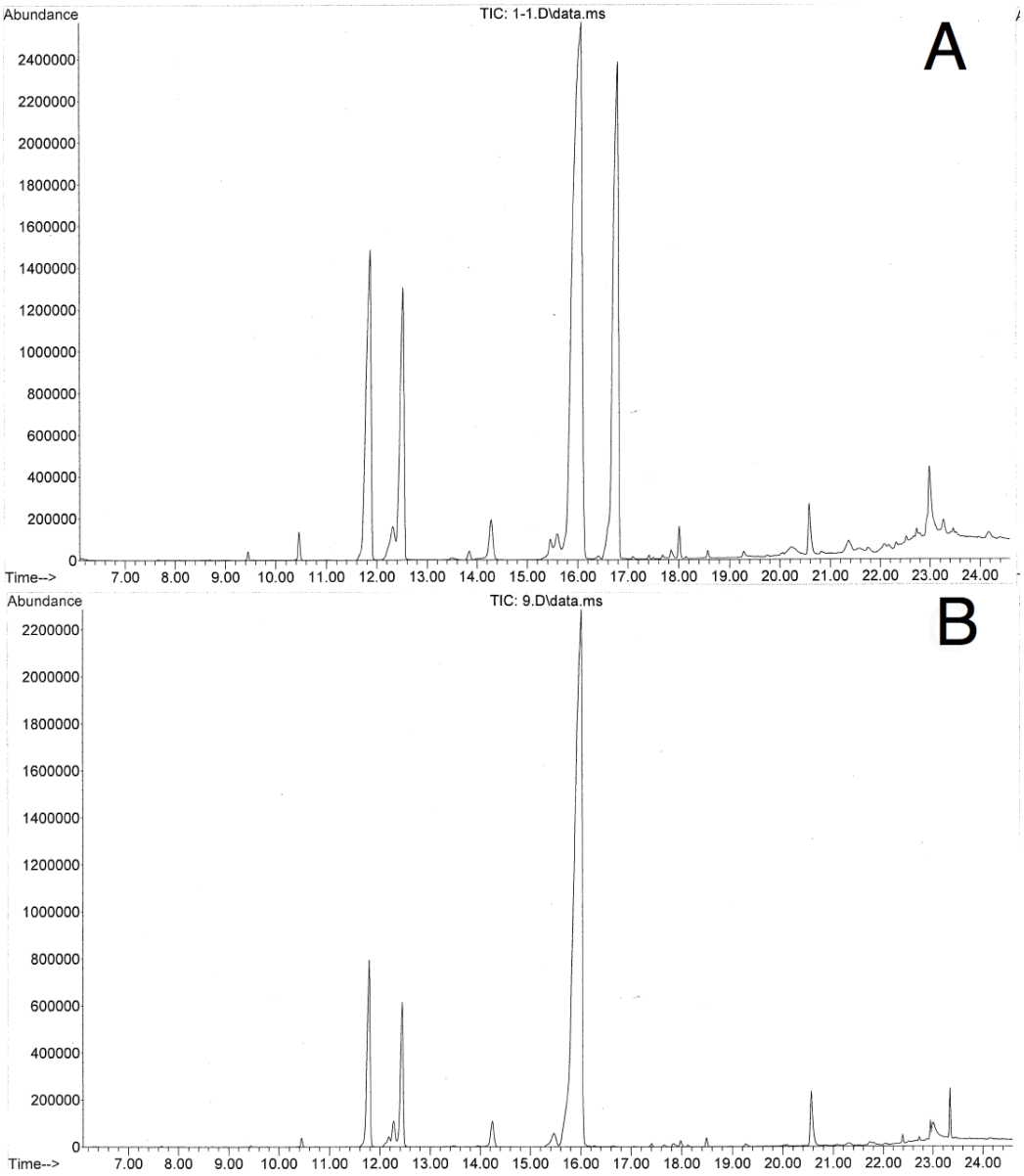

Figure 35: GC traces for FAMEs of *Y. lipolytica* strains. A shows the prototroph, while B is from FAD2 KO strains. The peak at 16.00 min is from $18{:}1^{\Delta 9}$, while the peak at 16.80 min is from $18{:}2^{\Delta 9,12}$(See Figure 36). Note the conspicuous absence of the peak at 16.80 min in plot B, indicating the loss of the Δ12 desaturase activity from FAD2.

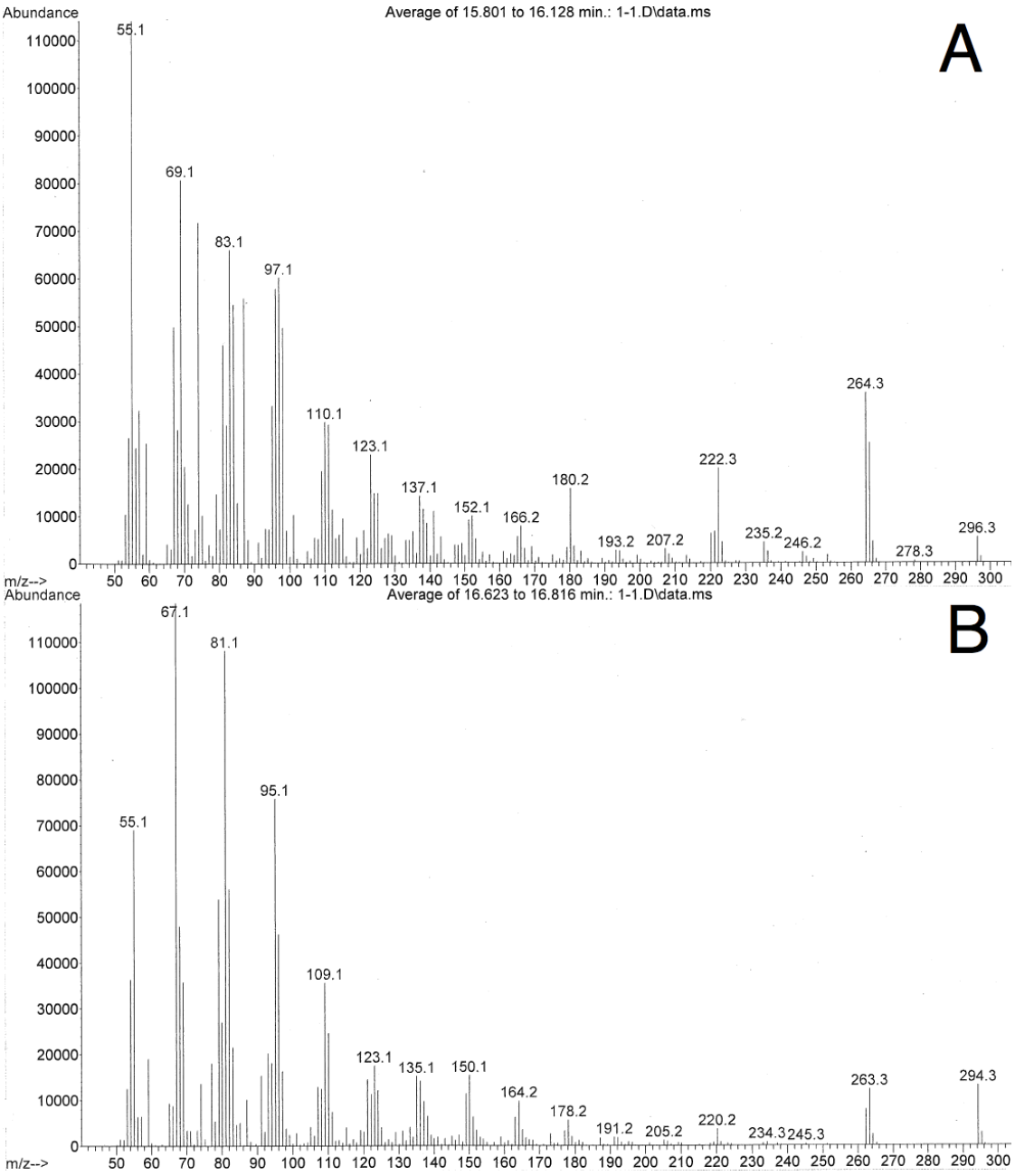

Figure 36: Mass spectra of oleic and linoleic acid. Image A shows the MS for 18:1$^{\Delta 9}$, while image B shows the trace for 18:2$^{\Delta 9,12}$. Note the smaller MacLafferty peaks at *m/z* 74, demonstrating the compounds are methyl esters. Identification was based on comparison to previous MS spectra of authentic standards (23)

ramp 10 °C/min to 150 °C, hold 5 min; ramp 10 °C/min to 220 °C, hold 1 min; and ramp 50 °C/min to 250 °C, hold 20 min. The injector was set to 250 °C with He flow rates

of 1.9 mL/min. After running the samples, analysis of the resultant spectra demonstrated complete loss of the Δ12-desaturase activity, providing final confirmation of the loss of the FAD2 gene (Figure 35, 36). This concluded the initial studies to demonstrate the capability of pCre-AHAS*.

2.3 Results

The *FAD2*::hygromycin knockout construct was assembled and transformed into prototrophic *Y. lipolytica.* The location of this construct was confirmed via PCR amplification, and the final strain was cultured for transformation. The AHAS gene was cloned out of *Yarrowia* and point mutated (W497L) to produce the sulfonyurea herbicide-resistant mutant AHAS*. The AHAS* sequence was then inserted into the pDONR221 donor vector via the BP Clonase reaction. Cre recombinase was transferred from pSH65 into pY5, then the pY5 *LEU2* gene was replaced with Gateway RfA. The final AHAS* entry vector and Cre-containing destination vector were combined through the LR Clonase reaction to produce pCre-AHAS*, the desired expression vector. Testing of pCre-AHAS* in the *Y. lipolytica* prototroph strain demonstrated effectiveness of the AHAS* gene in providing resistance to the CME herbicide, while transformation into a ΔFAD2::hph *Yarrowia* strain confirmed the effectiveness of the Cre recombinase activity in excising the hph resistance cassette. Subsequent iterative growth in nonselective media resulted in the loss of pCre-AHAS*, allowing for the knockout of additional genes using the *lox*P flanked hygromycin resistance cassette. The phenotype of this knockout was then reconfirmed through FAMEs analysis via GC/MS. Both pCre-AHAS* and *Y. lipolytica* Δ*FAD2* are complete and functional.

2.4 Discussion

This chapter details the cloning of *AHAS* and its mutation to *AHAS**, the production of the pDONR-AHAS* entry vector, the transfer of Cre recombinase to pY5 and subsequent insertion of the RfA gateway, the final production of pCre-AHAS*, and its testing on the *Yarrowia* Δ*FAD2*::*hph* strain. Surprisingly, the majority of difficulties in completion of the pY5-Cre Gateway destination vector came from improper digestion.

Despite possessing the proper sequence (confirmed through cycle sequencing), digests with single enzymes, and even the mutagenic insertion of a second SphI site, the anticipated band for excision and ligation constituted a comparatively small fraction of the double restriction digest products. This aberrant digestion pattern was maintained independent of enzyme concentration, substrate concentration, incubation time, buffer, and across a number of tested buffer concentrations. Whether this is an artifact as a result of the structure of the specific DNA sequence being digested or Star activity from EcoRI, SphI, or both (82) is unclear. However, since the aberrant digests occurred even with low enzyme concentration, low enzyme to DNA ratio, short digestion time, optimal buffers (listed as 100% activity per NEB), and Mg^{2+} as the divalent cation concurrently, Star activity is unlikely.

Excepting this singular aberration, integration of the Cre-AHAS* system for use in our lab was seamless. Excision of the *hph* resistance cassette by Cre recombinase was highly efficient, with ~86% showing excision after 24 hours incubation time, and ~96% showing excision after 48 hours incubation. In addition, selection in liquid cultures by CME was extremely effective, with cell death seen for all [CME] ≥ 5µg/mL. Growth on solid media was more challenging because the effective concentration approached the maximum solubility of CME in the media. Regardless, every step of the selection process had high specificity and high efficiency. pCre-AHAS* is a specialized plasmid for single resistance serial gene knockout, showing excellent results (See also Chapter 3 for *POX* gene knockouts).

While the core idea of Cre-lox resistance excision stems from Fickers et al. (54), previous studies have not implemented the secondary resistance of AHAS* as a selection factor. A number of these studies focus on using metabolic auxotroph strains, such as *Yarrowia* Δ*LEU* or Δ*URA* phenotypes, and then transforming with the pCre that also contains the complementary amino acid synthesis gene, allowing growth on CM knockout media. While this previous system is effective, use of pCre-AHAS* requires no alterations to the original metabolic genotype. The only mutations required are those implemented through the hygromycin-based knockout constructs, and the final resulting strain contains a minimal residual DNA scar from the replacement of the knocked-out

gene with an inactive *lox*P site. In addition to this, CME is an excellent selection marker in liquid media and acceptable selection marker on solid media for *Yarrowia lipolytica* However, since CME is effective against a wide range of lifeforms (plants, fungi, bacteria, and algae), yet shows little to no toxicity against higher organisms like fish and mammals, this modified system may be transferred for use in a wide range of organisms. Since its discovery, Cre recombinase has been implemented for gene excision and insertion in a number of organisms, ranging from knockout mice (83), to plants like bananas (84), rice (85), and rapeseed (86), bacteria like *Coxiella burnetii* (87), and yeasts like *Yarrowia*. So long as the organism in question contains a characterized AHAS gene with a known resistance mutation for sulfonylurea herbicides, use of this alternate Cre-AHAS* system may be easily implemented for the organism with minimal alteration from the methods described in this thesis. The only notable difference is that Cre recombinase and the Gateway must be implemented into an organism specific plasmid, with appropriate origin of replication, promoter, terminator, etc. Should these conditions be satisfied, this effective system may be generalized for research and industrial use.

While the current results are very positive, this final pCre-AHAS* may be improved through a number of additional mutations to the AHAS* gene which leave its function and activity unaltered. Since the potential for integration of the AHAS* gene is nonzero, and increased by the length of incubation in selective media, additional alterations which do not affect its effectiveness but might reduce this eventuality's likeliness are desirable. Implementation would likely be dependent on the utility of the plasmid to the scientific community at large.

In short, this chapter demonstrates the production of a Cre-lox recombinase system in novel conjunction with the AHAS* CME-resistant mutant gene, its assembly via the Gateway® cloning system, and its testing on a Δ*FAD2*::*hph Yarrowia* knockout strain. Testing demonstrates high specificity, high efficiency, and excellent selection.

2.5 Future Uses

2.5.1 Epa955 and Epa2161

A number of acetylenases have been previously characterized, including the landmark study of *Crep1* (18), the first Δ12-acetylenase ever cloned and functionally characterized. More recent studies have identified new plant acetylenases and expanded the range into fungal acetylenases (16), moss acetylenases (88), and even acetylenases from moths (89). Many of these characterized acetylenases contain multifunctional activities, such as the Δ12 *cis* and *trans* desaturation activity of *Crep1* (90), the Δ11 desaturase/acetylenase activity and Δ13 desaturase activity from *Thaumetopoea pityocampa* (89), and the Δ6 desaturase/acetylenase activity from *Ceratodon purpureus* (88). Despite the presence of Δ14-desaturation activity on $18{:}1^{\Delta 9,12a}$ fatty acid products in *CfACET Yarrowia* expression clones, no other Δ14-desaturation products were observed (unpublished research) (16). Similar results are seen with the Δ13 desaturase activity of *Tpi-PGFAD* (89), as well as many others. This secondary activity is proposed to be a result of the insertion of the short alkyne bond, allowing access of the to-be conjugated position to the original desaturase active site (89,91,92). However, in most cases this desaturation and the original desaturation step may be attributed to endogenous FAD2 or potentially FAD3 activities instead of the acetylenase. Acetylenic natural products are derived from three major biosynthetic pathways: the crepenynic acid pathway, the stearolic acid pathway, and the tariric acid pathway. These pathways differ based on the regioselectivity of the desaturation/acetylenation of the oleic acid precursor, producing crepenynic acid ($18{:}1^{\Delta 9,12a}$), stearolic acid ($18{:}0^{\Delta 9a}$), and tariric acid ($18{:}0^{\Delta 6a}$), respectively. The vast majority of acetylenic metabolites are produced via the crepenynic acid pathway (seen in part in Figure 4, and in full in Figure 37). A recent study by the Minto lab has resulted in the cloning and characterization of two enzymes involved in the crepenynic acid pathway, named Epa955 and Epa2161 (23). A TBlastX search of the publically available *E.*

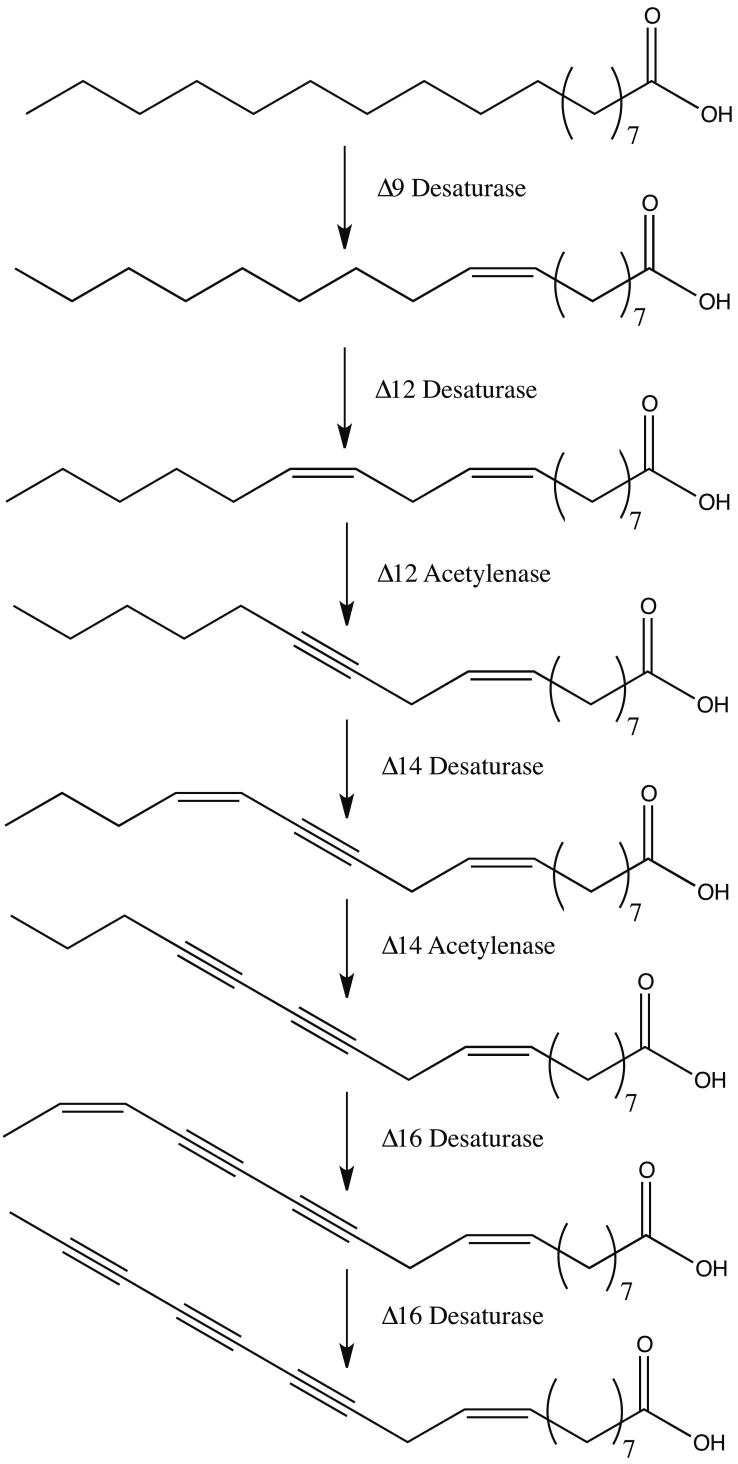

Figure 37: The crepenynic acid pathway, as originally proposed by Bu'Lock (24)

purpurea transcriptome against the sequences of 48 known and putative acetylenases and diverged desaturases resulted in the identification of these two Δ12-acetylenase homologs. After confirmation of the ORF via RACE (Rapid Amplification of cDNA Ends) amplification, the full-length targets were synthesized in four codon-optimized; Epa955 RACE opt 2 (Epa955R2), Epa955 RACE opt 3 (Epa955R3), Epa955 trans opt (Epa955T), and Epa2161 trans opt (Epa2161T) and expressed in *Y. lipolytica*. Products were adjusted to the consensus RACE transcripts (RACE opt) or the transcriptomic sequence (trans opt). Characterization of the activities of both enzymes in *Yarrowia* (ATCC 76982) demonstrated production of crepenynate from linoleic acid via a Δ12 acetylenase activity. These cultures also produced of dehydrocrepenynate, indicating a Δ14 desaturase activity. While this may be consistent with both of these enzymes being in fact bifunctional Δ12 desaturases/acetylenases, the *Yarrowia* strain used contained a *FAD2* Δ12-desaturase that could have been the source of this "Δ14 desaturase" activity. With the production of the *Yarrowia* ΔFAD2 knockout, a reinvestigation of this potential secondary activity has now become possible. Future work will seek to characterize whether Epa955 and Epa2161 do indeed possess a Δ12- and/or Δ14-desaturase activities.

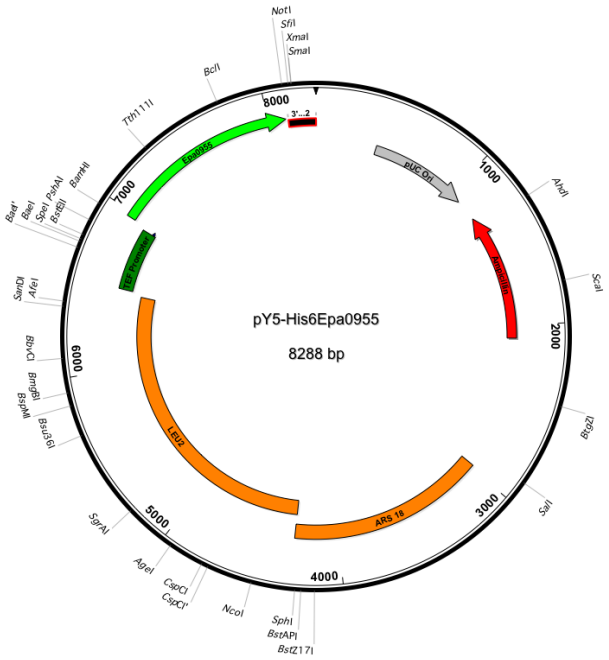

Figure 38: Epa955 plasmid map.

2.5.2 Lipid Degradation

While chapter three deals with the initial work of a study on lipid degradation in Δ*POX2 Yarrowia* strains, a number of other knockouts are of interest. Since effective

production of lipids for biodiesel requires optimization for superior fuels, understanding the mechanism present for degradation and alteration is key in tailoring the product lipid pool. Initial studies have marked out $18:1^{\Delta 9}$ as a product of interest with good fit for viscosity, cold flow, oxidative stability, and lubricity, maintaining many of the key qualities seen in current fuels (93). Ergo, knockouts that amplify the amount of this product in the stored lipid are desirable. The specific activities of POX4 and POX5, if any, remain unknown. The effects of knockouts at distinct points during lipid degradation (*MFE1*, *POT1*) on the lipid profile remain uninvestigated. Many previous studies in *Yarrowia* seek to maximize total lipid output, rather than examine the lipid profile in detail. The system developed here allows for this examination without the presence of any metabolic mutations with excellent selection.

2.5.3 Gene Knock-Ins with pCre-AHAS*

Simple modifications to the knockout constructs in use allow for the easy insertion of exogenous genes in place of those knocked out within the genome. By inserting the gene sequence within the construct but outside of the mutant *loxP* sites, selection using the *hph* marker and excision of this resistance via the method previously descried is unaltered (see Figure 39). Instead of leaving only the *loxLR* scar in the DNA, the gene is now replaced by the knock-in, allowing this inserted gene to use the promoter, terminator, and other metabolic machinery already in place. While assembly of a test knock-in construct was initiated, final testing of the product was not yet completed. Should the test be successful, the pCre-AHAS* methodology will provide an efficient means for both deletion and insertion of chosen genes and the biochemical characterization of metabolic pathways.

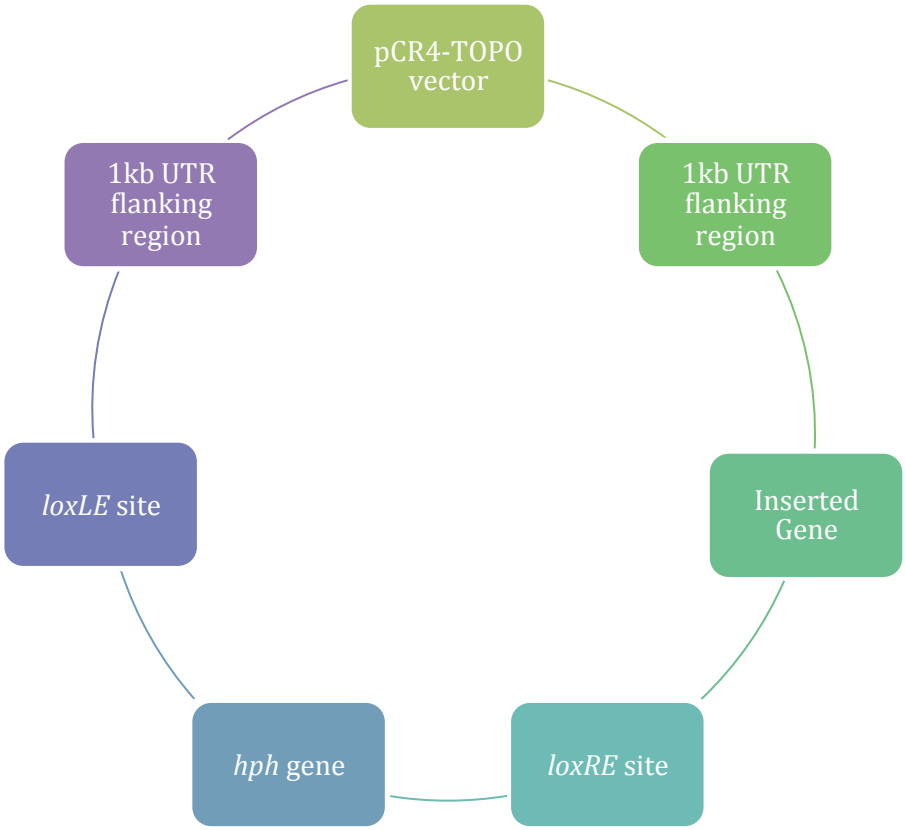

Figure 39. Gene knock-in construct diagram.

CHAPTER 3. LIPID UPTAKE AND DEGRADATION IN POX KO STRAINS

3.1 Background

While the general mechanisms for the degradation of lipids by *Yarrowia* are reasonably well understood, a number of open questions still remain. Several researchers have investigated the uptake of common lipids by *Yarrowia*, such as $18{:}1^{\Delta 9}$, $18{:}2^{\Delta 9,12}$, and $18{:}3^{\Delta 9,12,15}$ (94,95) but little to no research has been performed on the uptake of less common lipids, the effects of the degrees of unsaturation on lipid accumulation, and the selectivity of the exogenous fatty acid uptake. This same exploration of selectivity extends throughout the lipid degradation. Past research showed the specificity for POX2 and POX3 oxidases (48-50) for medium and short fatty acid chains, respectively, while recent research has shown POX1 and POX6 preferentially degrade dicarboxylic acids. To date, POX4 and POX5 are reported as having nonspecific binding across saturated FAs between C_4 and C_{16} (51,52); however, a recent study looking at the viability of PHA production demonstrated a high activity of POX5 against the odd chain MUFA $17{:}1^{\Delta 10}$ (32). While of great use in the general determination of the activity of relevant POX genes, these studies lack an assessment of a number of relevant topics. None of the activity studies cited here look at any desaturated compounds (excepting the PHA study which looked at three). As such, none look at the importance of alkene stereochemistry, the preferential degradation or integration of desaturated lipids, or activities against mixed substrates which are not dominantly even-chain saturated FAs (such as stearin and other animal fats). This chapter seeks to rectify this information void with a preliminary analysis of lipid uptake and degradation in the *Yarrowia* prototroph and *POX* knockouts.

To properly analyze the lipid content for the purposes of this study, a method is required that allows for quantitation of the lipid present in the cells not only after growth, but of that which remains in the media and which has not been taken up by the cell. This

is complicated by the presence of the detergent NP-40 in the growth media. While exogenously fed free lipids may be easily taken up, growth above a characteristic concentration of lipid results in the formation of micelles, limiting the availability of the lipid to the cells. To mitigate this difficulty, a small amount of detergent is added, which prevents the formation of these lipid-lipid interactions. However, when this NP-40-containing media is mixed with hexanes, the result is a heterogenous emulsion. No hexane may be successfully recovered. In addition, the procedure must be highly efficient to process the number of product fatty acid profiles necessary for the analysis. The resulting protocol is detailed in Figure 39.

3.2 Materials and Methods

3.2.1 Preparation and Setup

To find a useful concentration of NP-40 that did not result in an emulsion, hexane extraction was tested across a range of reasonable NP-40 concentrations. Since the critical micelle concentration for NP-40 was reported by the manufacturer as 0.0232% (w/v) (96), the sample was tested by serial dilutions of the stock 1% NP-40 solution. Concentrated 50 mM stocks were made of each fatty acid for feeding, with the FAs dissolved in DMSO. To determine the retention time of each of the fed lipids, about 10 µL of each stock solution was prepped and converted into FAMEs, which were then analyzed by GC/MS. To quantitate the amount of lipid taken up by the cell, 11-Br 11:0 was added to each sample prior to the preparation of FAMEs.

3.2.2 Prototroph

As previously stated, the prototrophic *Yarrowia* strain grows with 85-90% of the total lipid content comprised of five fatty acids: 16:0, $16:1^{\Delta 9}$, 18:0, $18:1^{\Delta 9}$, and $18:2^{\Delta 9,12}$ (31). While this fact remains unchanged regardless of the identity of any of the lipids fed in this experiment, the ratios of these key lipids shift in response to the identity of the

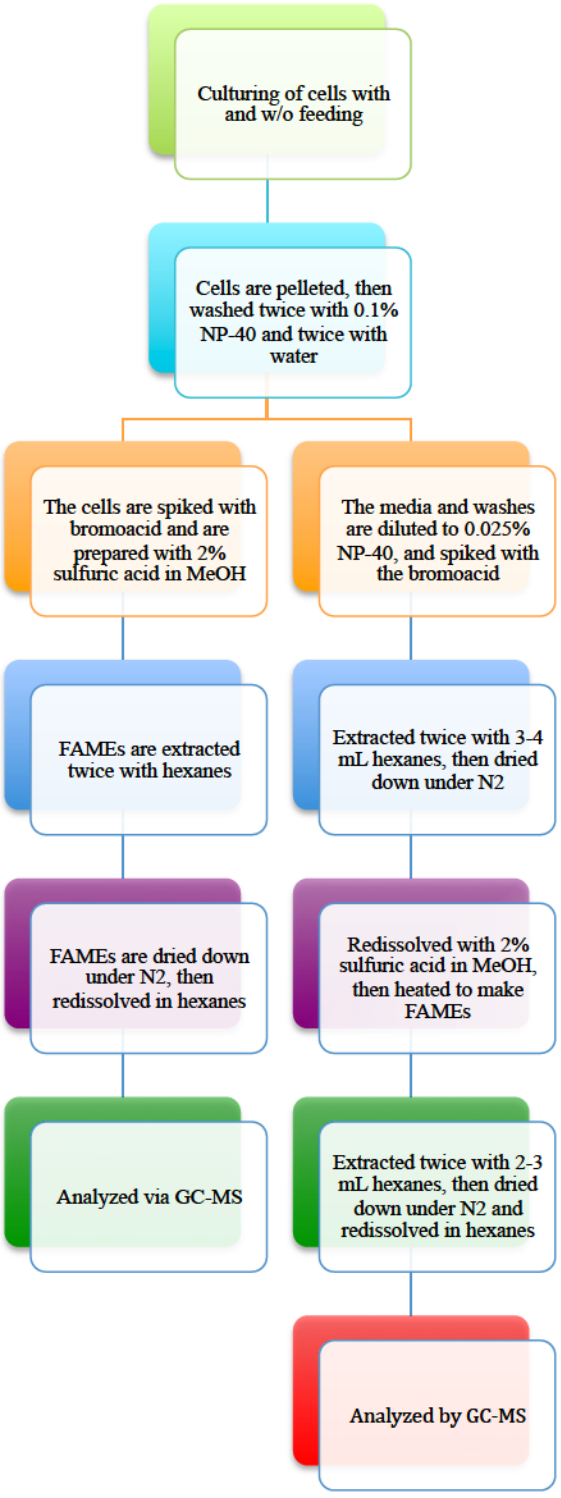

Figure 40: Separation and preparation scheme for prototroph/Δ*POX* strains, with feeding.

lipids that have been exogenously fed. Cultures were prepared using 3 mL of YPD+0.1% NP-40 inoculated with 30 µL of freshly cultured cells and 30 µL of the appropriate ~50 mM FA solution stock. The resulting culture tubes were incubated 24 hours at 28 °C, 240 rpm and FAMEs were prepared using 250 µL of the final grown culture according to the method described in Figure 39. Once complete, these FAME spectra were tabulated and analyzed via statistical analysis for determination of relevant results.

3.2.3 *POX2* Knockout Strain

The Δ*POX2* knockout construct was produced by Dr. Brenda Blacklock and transformed by her into the *Yarrowia* prototroph. Streaks of the positive transformants were made on YPD+hyg, and given to me for use. The positioning of the Δ*POX2* construct was verified through PCR amplification, then the sample was cultured and prepared in the fashion as the prototroph.

3.3 Results

3.3.1 Stocks, Sample Spectra, and Preparatory Work

Table 6: Stock solutions of fatty acids. Each FA was dissolved in DMSO, then stored at -80 ℃ to limit air oxidation.

Identity	Stock concentration (mmol/L)	Retention Time (min)
$11{:}1^{\Delta 10}$	51.6	7.33 min
$15{:}1^{\Delta 10}$	53.3	11.05 min
$17{:}1^{\Delta 10}$	51.8	14.23 min
$17{:}1^{\Delta 10t}$	51.8	13.94 min
$19{:}1^{\Delta 7}$	49.6	16.94 min
$19{:}1^{\Delta 10}$	48.1	16.98 min
$19{:}1^{\Delta 10t}$	49.6	16.83 min
$14{:}1^{\Delta 9}$	53.9	9.86 min
$14{:}1^{\Delta 9t}$	53.9	9.70 min
$16{:}1^{\Delta 9}$	50.3	12.31 min
$16{:}1^{\Delta 9t}$	51.1	12.09 min
$18{:}2^{\Delta 9,12}$	53.3	16.56 min
$18{:}3^{\Delta 9,12,15}$ (α)	51.4	17.41 min
$18{:}3^{\Delta 6,9,12}$ (γ)	51.4	17.05 min
11-Br 11:0	51.1	16.00 min

The actual stock FA solution concentrations may be seen in Table 6, along with the retention times for the FAME of each lipid. When working to find an internal standard, initial attempts with 9:0 and 13:0 were fruitless, since the lipids evaporated completely out of solution prior to analysis. Clearly, neither of these two options would be useful through two separate drying steps in quantitation of the lipid in the wash solution. Instead, 11-Br-11:0 was selected. Not only did it occupy an open space in the normal lipid profile, falling between $18:1^{\Delta 9}$ (15.73 min) and $18:2^{\Delta 9,12}$ (16.56 min), but it showed minimal degradation, minimal evaporation, and excellent quantitation (Figure 45).

The acquisition of the feeding data was most hindered by the colloid formation caused by the presence of NP-40. Since initial trial cases using the traditional 1% NP-40 for washes and YPD+1% NP-40 for feeding resulted in the formation of a heterogeneous sludge-like colloid upon addition of hexanes, the extraction was tested across a range of reasonable NP-40 concentrations. The emulsion was seen for all wash mixtures with concentrations of NP-40 greater than 0.025%, a value extremely close to the critical micelle concentration of 0.0232%. While using a higher concentration would ensure the prevention of micelle formation, the increasing NP-40 concentration would require substantial dilution of the washes for subsequent extraction. To compensate for this, the media and wash solution were made with 0.1% NP-40 and then diluted later as necessary, resulting in a final 3 mL of the wash solution. This volume could be extracted with 3 mL hexanes without overfilling the FAMEs tubes used while still maintaining an acceptable mass balance for useful extraction.

3.3.2 Prototroph

3.3.2.1 Lipid Uptake, Incorporation, and Degradation

While previous studies have investigated preferential degradation of certain lipids in natural mixtures (animal fats, plant oils, etc.), this study looks at the feeding of singular lipids. The generalized results of the feeding may be seen in table 7.

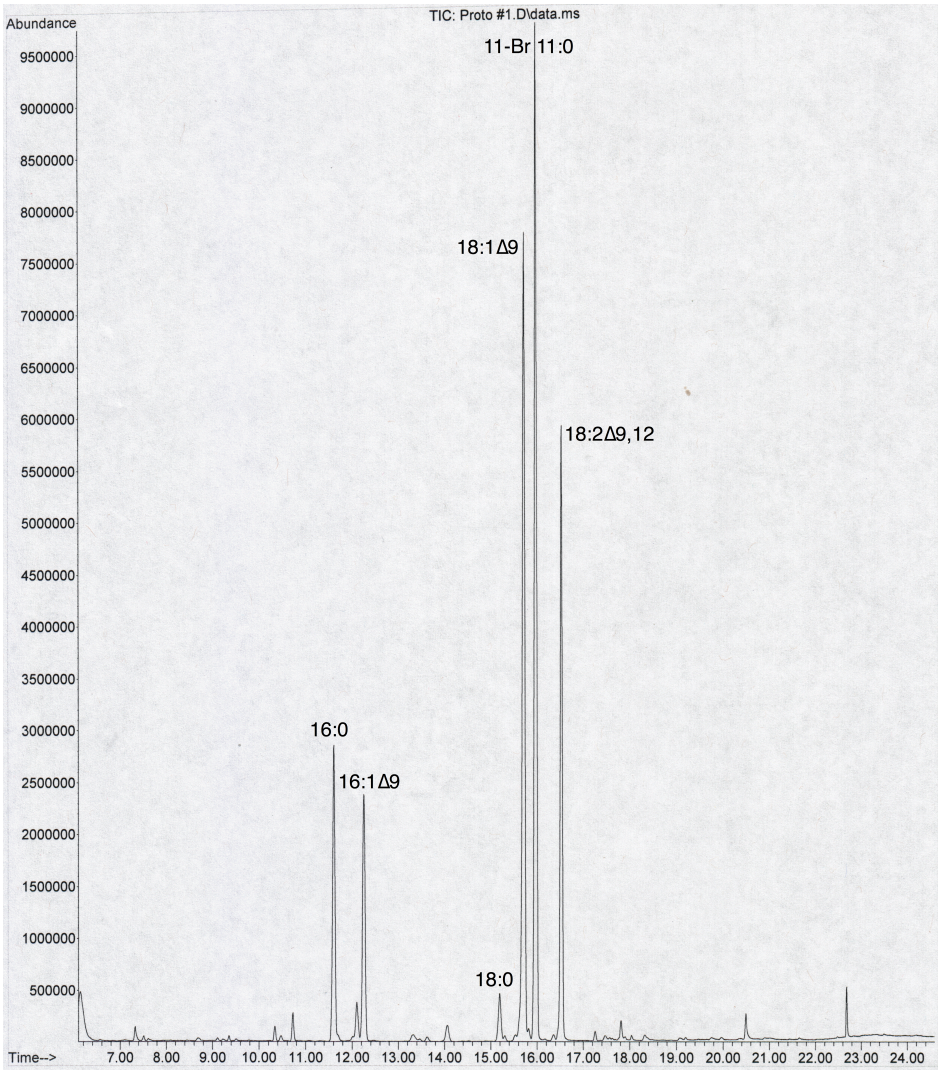

Figure 41: Prototroph *Yarrowia* FAMEs spectrum with 11-Br-11:0 added as an internal standard.

Equation 1: Equation set for the calculated values seen in Table 7.

$$Exogenously\ fed\ lipid\ = [FA\ stock] * \frac{30\ \mu L}{3.0\ mL\ media} * 0.25\ mL\ media\ harvested$$

$$Imported\ exogenous\ lipid = Exogenously\ fed\ lipid - \mu mol\ lipid\ in\ wash$$

$$Lipid\ accumulated = Feeding\ mol\ of\ FA - Prototroph\ mol\ of\ FA$$

$$Lipid\ accumulated = \frac{Feeding\ mol\ of\ FA - Prototroph\ mol\ of\ FA}{Exogenously\ fed\ lipid} * 100\%$$

$$Degraded\ fed\ lipid = Imported\ exogenous\ lipid - Lipid\ accumulated$$

Despite an incubation time of only one day in rich media, the majority of the lipids exogenously fed in each trial were taken up by the *Yarrowia* prototroph strain. Of the results found, only $15{:}1^{\Delta 10}$ had a high standard deviation, with all other µmol results accurate to the fourth decimal place. The results seen for lipid uptake do not indicate a selectivity based on chain length, lipid desaturation, or configuration of the double bonds among the FAs studied. Accumulation of the fed lipid in the prototroph heavily favors the LCFAs studied, with greatest accumulation seen for $16{:}1^{\Delta 9}$, $18{:}2^{\Delta 9,12}$, $18{:}3^{\Delta 9,12,15}$, $18{:}3^{\Delta 6,9,12}$, and $17{:}1^{\Delta 10}$. Due to the variability in the values measured, no significant alteration is seen for $11{:}1^{\Delta 10}$, $14{:}1^{\Delta 9t}$, $14{:}1^{\Delta 9,}$ or $15{:}1^{\Delta 10}$, indicating the degradation of all of the exogenous lipid which was taken up by the cells. Every one of the lipids of size C_{16} or greater with a Δ9 alkene bond show accumulation in excess of 7%, implying that this bond may enhance accumulation rates. The *cis* alkene configuration is favored for accumulation in $16{:}1^{\Delta 9}$ and $17{:}1^{\Delta 10}$, while the larger $19{:}1^{\Delta 10}$ and smaller $14{:}1^{\Delta 9}$ show minimal difference between the isomers.

Table 7: Lipid feedings of prototroph, with quantified uptake, incorporation, and degradation. While the first four fed lipids showed accumulation within the standard deviation of their values (an insignificant change), the remainder all accumulated significantly.

Lipid uptake	Exogenously fed lipid (µmol)	Imported exogenous lipid (µmol)	Lipid accumulated (µmol)	Lipid Accumulated (%)	Degraded fed lipid (µmol)
$11{:}1^{\Delta 10}$	0.129	0.126	trace	-0.33	0.127
$14{:}1^{\Delta 9}$	0.135	0.134	0.001	0.39	0.133
$14{:}1^{\Delta 9t}$	0.135	0.133	0.001	0.89	0.132
$15{:}1^{\Delta 10}$	0.133	0.129	0.004	3.0	0.125
$16{:}1^{\Delta 9t}$	0.128	0.126	0.009	7.1	0.117
$16{:}1^{\Delta 9}$	0.126	0.124	0.046	36.3	0.078
$17{:}1^{\Delta 10t}$	0.129	0.129	0.011	8.7	0.118
$17{:}1^{\Delta 10}$	0.129	0.129	0.018	13.8	0.112
$18{:}2^{\Delta 9,12}$	0.133	0.131	0.015	11.5	0.116
$18{:}3^{\Delta 9,12,15}$ (α)	0.128	0.125	0.039	30.5	0.086
$18{:}3^{\Delta 6,9,12}$ (γ)	0.128	0.127	0.027	21.2	0.100
$19{:}1^{\Delta 7}$	0.124	0.124	0.004	3.1	0.120
$19{:}1^{\Delta 10}$	0.120	0.120	0.004	3.0	0.116
$19{:}1^{\Delta 10t}$	0.124	0.124	0.004	2.9	0.120

3.3.2.2 Lipid Profiles

The results for the overall lipid profiles may be seen in Table 8. A number of interesting alterations present themselves upon close inspection. Accumulation of $11{:}1^{\Delta 10}$ is relatively uniform across all the feedings performed. However, $15{:}1^{\Delta 10}$ shows

Table 8: Lipid profiles from prototroph feeding experiments. Note that the giving of a value as 0 indicates no peak or a peak more than 4 orders of magnitude below the internal standard. All values given are in µmol.

Retention time	Compound	Prototroph	11:1Δ10	14:1Δ9	14:1Δ9t	15:1Δ10	16:1Δ9	16:1Δ9t	17:1Δ10	17:1Δ10t	19:1Δ10	19:1Δ10t	19:1Δ7	18:2Δ9,12	alpha 18:3	gamma 18:3
7.33 min	$11:1^{\Delta 10}$	0.0032	0.0028	0.0020	0.0020	0.0030	0.0020	0.0018	0.0029	0.0024	0.0025	0.0028	0.0022	0.0020	0.0020	0.0021
9.70 min	$14:1^{\Delta 9t}$	0	0	0	0.0012	0	0	0	0	0	0	0	0	0	0	0
9.86 min	$14:1^{\Delta 9}$	0	0	0.0005	0	0	0	0	0	0	0	0	0	0	0	0
11.05 min	$15:1^{\Delta 10}$	0	0	0	0	0.0040	0	0	0.0022	0	0.0239	0.0010	0	0	0	0
11.61 min	16-0	0.0679	0.0518	0.0628	0.1180	0.0719	0.0960	0.0702	0.0631	0.0892	0.0577	0.1000	0.0625	0.0748	0.0591	0.0791
12.09 min	$16:1^{\Delta 9t}$	0.0085	0.0064	0.0102	0.0161	0.0085	0.0145	0.0176	0.0071	0.0122	0.0078	0.0126	0.0087	0.0110	0.0076	0.0097
12.31 min	$16:1^{\Delta 9}$	0.0628	0.0466	0.0581	0.1042	0.0541	0.1084	0.0609	0.0336	0.0664	0.0430	0.0355	0.0481	0.0578	0.0503	0.0712
13.94 min	$17:1^{\Delta 10t}$	0	0	0	0	0	0	0	0	0.0112	0	0.0066	0	0	0	0
14.23 min	$17:1^{\Delta 10}$	0	0	0	0	0	0	0	0.0179	0	0.0161	0	0	0	0	0
15.20 min	18-0	0.0118	0.0095	0.0129	0.0241	0.0132	0.0218	0.0161	0.0203	0.0190	0.0115	0.0278	0.0114	0.0147	0.0101	0.0135
15.73 min	$18:1^{\Delta 9}$	0.2129	0.1807	0.2033	0.3491	0.2532	0.2898	0.2349	0.1843	0.2647	0.1577	0.2826	0.1666	0.2314	0.1848	0.3011
16.56 min	New $18:2^{\Delta 9,12}$	0.1185	0.0905	0.1003	0.1723	0.0953	0.1105	0.1011	0.0924	0.1455	0.0831	0.1338	0.0902	0.1338	0.0643	0.0822
16.83 min	$19:1^{\Delta 10t}$	0	0	0	0	0	0	0	0	0	0	0.0035	0	0	0	0
16.94 min	$19:1^{\Delta 7}$	0	0	0	0	0	0	0	0	0	0	0	0.0038	0	0	0
16.98 min	$19:1^{\Delta 10}$	0	0	0	0	0	0	0	0	0	0.0037	0	0	0	0	0
17.05 min	$18:3^{\Delta 6,9,12}$ (γ)	0	0	0	0	0	0	0	0	0	0	0	0	0	0	0.0272
17.41 min	$18:3^{\Delta 9,12,15}$ (α)	0	0	0	0	0	0	0	0	0	0	0	0	0	0.0392	0
20.49 min	24-0	0.0061	0.0054	0.0086	0.0149	0.0179	0.0175	0.0156	0.0284	0.0106	0.0071	0.0234	0.0094	0.0090	0.0058	0.0148

increased accumulation with the feedings of 17:1$^{\Delta 10}$ and 19:1$^{\Delta 10}$, both with the *cis* and *trans* isomers. Also, 17:1$^{\Delta 10}$ shows accumulation from feeding with 19:1$^{\Delta 10}$. This increasing accumulation could be due to β-oxidation of the FA acyl chain with isomerization of the double bond, or it could be a result of omega-oxidation, as seen in yeasts such as *Candida cloacae* (97). Feedings with α-18:3 resulted in decreased accumulation for all lipids studied, including most notably a decrease of nearly 50% in the amount of accumulated 18:2$^{\Delta 9,12}$. Feedings with γ-18:3, however, resulted in increased accumulation for all lipids studied excepting 18:2$^{\Delta 9,12}$, which showed ~30% decrease in accumulation. Feedings with 14:1$^{\Delta 9}$ resulted in a lipid profile very similar to the prototroph, while feedings with 14:1$^{\Delta 9t}$ showed an increase in lipid accumulation across those investigated. Feeding 16:1$^{\Delta 9}$ resulted in enrichment of only 16:1$^{\Delta 9}$ and 18:1$^{\Delta 9}$, implying the action of an elongase, while feeding 16:1$^{\Delta 9t}$ resulted only in enrichment of the 16:1$^{\Delta 9t}$ lipid. This indicates that the enrichment seen with 14:1$^{\Delta 9t}$ is not exclusively caused by the stereochemistry, but is specific to that compound for unknown reasons.

3.3.3 Δ*POX2* Strain

As shown in Table 9, the *Yarrowia* Δ*POX2* mutant deviates from the prototrophic strain in several key ways. The most notable and obvious difference is that the amount of accumulated lipid has increased dramatically, with increases of between 20-50% for 16:0, 16:1$^{\Delta 9}$, 16:1$^{\Delta 9t}$, 18:1$^{\Delta 9}$, and 18:2$^{\Delta 9,12}$, and a decrease of ~40% for 18:0. While not unexpected due to the double nature of *POX2* as a regulatory factor in the assembly of the *POX* complex and as a medium-chain oxidase, the increased accumulation is strikingly. This increase in lipid accumulation is relatively uniform across all of the Δ*POX2* feedings. Similar to the prototroph, feedings with α-18:3 resulted in decreased accumulation for all lipids studied, including most notably a decrease of nearly 25% in the amount of accumulated 18:2$^{\Delta 9,12}$. Unlike in the prototroph, feedings with γ-18:3 also resulted in decreased accumulation for the lipids studied. The Δ*POX2* 15:1$^{\Delta 10}$ no longer shows increased accumulation with the feedings of 17:1$^{\Delta 10}$ and 19:1$^{\Delta 10}$, with either the *cis* or *trans* isomers. This implies the loss of the enzyme aiding in this conversion, supporting

the idea that this accumulation in the prototroph could be due to β-oxidation of the FA acyl chain by *POX2*, followed by isomerization of the double bond.

Table 9: The Δ*POX2* lipid profiles. Note that, as before, the giving of a value as 0 indicates no peak or a peak more than 4 orders of magnitude below the internal standard.

Retention time	Compound	ΔPox2	11:1Δ10	14:1Δ9	14:1Δ9t	15:1Δ10	16:1Δ9	16:1Δ9t	17:1Δ10	17:1Δ10t	19:1Δ10	19:1Δ10t	19:1Δ7	18:2Δ9,12	alpha 18:3	gamma 18:3
7.33 min	$11{:}1^{\Delta 10}$	0.0019	0.0019	0.0019	0.0018	0.0020	0.0016	0.0017	0.0015	0.0018	0.0017	0.0017	0.0018	0.0015	0.0013	0.0016
9.70 min	$14{:}1^{\Delta 9t}$	0	0	0	0	0	0	0	0	0	0	0	0	0	0	0
9.86 min	$14{:}1^{\Delta 9}$	0.0013	0	0	0	0	0	0	0	0	0	0	0	0	0	0
11.05 min	$15{:}1^{\Delta 10}$	0	0	0	0	0.0011	0	0	0	0	0	0	0	0	0	0
11.61 min	16-0	0.0938	0.0760	0.0536	0.0630	0.0555	0.0844	0.0973	0.0845	0.0934	0.0644	0.0780	0.0913	0.0799	0.0768	0.0685
12.09 min	$16{:}1^{\Delta 9t}$	0.0104	0.0094	0.0061	0.0070	0.0063	0.0081	0.0101	0.0078	0.0107	0.0079	0.0085	0.0105	0.0071	0.0077	0.0086
12.31 min	$16{:}1^{\Delta 9}$	0.0942	0.0552	0.0660	0.0765	0.0644	0.1054	0.1137	0.0844	0.1084	0.0815	0.0934	0.0955	0.0857	0.0784	0.0892
13.94 min	$17{:}1^{\Delta 10t}$	0	0	0	0	0	0	0	0	0.0052	0.0028	0	0	0	0	0
14.23 min	$17{:}1^{\Delta 10}$	0	0	0	0	0	0	0.0062	0	0	0	0	0	0	0	0
15.20 min	18-0	0.0065	0.0051	0.0031	0.0044	0.0040	0.0072	0.0061	0.0055	0.0090	0.0053	0.0052	0.0119	0.0064	0.0053	0.0044
15.73 min	$18{:}1^{\Delta 9}$	0.3119	0.2879	0.2084	0.2421	0.2087	0.3537	0.3700	0.3030	0.3257	0.2013	0.2793	0.2933	0.3369	0.3177	0.2786
16.56 min	New $18{:}2^{\Delta 9,12}$	0.2237	0.1931	0.1443	0.1601	0.1455	0.2018	0.2361	0.2014	0.2034	0.1399	0.1746	0.1786	0.2004	0.1760	0.1628
16.83 min	$19{:}1^{\Delta 10t}$	0	0	0	0	0	0	0	0	0	0	0.0017	0	0	0	0
16.94 min	$19{:}1^{\Delta 7}$	0	0	0	0	0	0	0	0	0	0	0	0.0030	0	0	0
16.98 min	$19{:}1^{\Delta 10}$	0	0	0	0	0	0	0	0	0	0.0016	0	0	0	0	0
17.41 min	$18{:}3^{\Delta 6,9,12}$ (γ)	0	0	0	0	0	0	0	0	0	0	0	0	0	0	0.0078
17.05 min	$18{:}3^{\Delta 9,12,15}$ (α)	0	0	0	0	0	0	0	0	0	0	0	0	0	0.0183	0
20.49 min	24-0	0.0117	0.0051	0.0031	0.0034	0.0041	0.0176	0.0116	0.0126	0.0100	0.0037	0.0109	0.0118	0.0167	0.0156	0.0049

3.4 Discussion

While the information contained here is new, it is by no means complete. Our preliminary data set encompasses the prototroph and one of the six *POX* genes, leaving the remaining five for completion. As of this time, verified constructs exist for all 6 of the *POX* genes with verified transformants of *POX2*, *POX3*, and *POX4*. While not completed in time for inclusion within this thesis, it is our intention to complete analysis of all six *POX* genes. The main limiting factor is the sizable time commitment to be able to complete each data set and analyze the results. While the method shown in Figure 44 was the most efficient sequence to produce the FAMEs of both the cells and wash solution, it is worth noting that preparation of large sets of feedings rapidly increases the time scale to complete the method. For reference, the completion of a set of 48 feedings required 2-3 days of exclusive attention to complete, with approximately 21.5-22 hours to acquire each set of GC/MS results from the FAMEs samples. This problem is a tractable one, but one that will require far more time invested. Of the remaining genes to investigate, the one of most interest is *POX5*. Previous studies have shown it had a demonstrable and specific activity against $17{:}1^{\Delta 10}$, indicating the possibility of a specific activity, perhaps against desaturated FAs. Until the data is collected and analyzed, however, this remains speculation.

CHAPTER 4. MATERIALS AND METHODS

4.1 Materials

Yeast and *E. coli* media components (peptone, tryptone, yeast extract, yeast nitrogenous base, agar) were manufactured by Becton Dickinson & Co. (Franklin Lakes, NJ). Tris base, PEG4000, Tergitol NP-40, lysozyme, DMSO, and all amino acids used for CM dropout powder were purchased from Sigma-Aldrich (St. Louis, MO). Dextrose, NaCl, NaOH, agarose, sodium acetate, EDTA, lithium acetate, and ammonium sulfate were all purchased from Fisher Scientific or ACROS Organic (Fair Lawn, NJ). For the fatty acid feedings, 9:0, 13:0, and 11-Br-11:0 were all purchased from Sigma-Aldrich (St. Louis, MO), while the remainder were purchased from Nu-Chek-Prep (Elysian, MN). All restriction enzymes and buffers were purchased from New England Biolabs (Ipswich, MA). All primers were obtained from Integrated DNA Technologies (Coralville, IA) and synthetic genes were purchased from Genscript (Piscataway, NJ). The pSH65 plasmid, containing the Cre recombinase gene, was graciously provided by Prof. Mark Goebl of the IU School of Medicine, Indianapolis, IN. The pY5 plasmid was graciously provided by E. Cahoon from the University of Nebraska, Lincoln, NE. All the materials for the Gateway® reactions, including pDONR, Gateway RfA, and all associated buffers and reaction mixes and the 1-kb ladder were obtained from Invitrogen (Grand Island, NY). Chlorsulfuron (98%) and chlorimuron ethyl (95%) were both purchased from AK Scientific, Inc. (Mountain View, CA). The Wizard® *Plus* SV Minipreps DNA Purification System for plasmid purification was purchased from Promega (Madison, WI). Terminator cycle sequencing was performed using the BigDye® Direct Cycle Sequencing Kit from Invitrogen, through Life Technologies (Grand Island, NY). PCR mutagenesis was performed using the Quikchange II Site Directed Mutagenesis kit from Agilent (Santa Clara, CA). DNA amplification was performed using the GoTaq® DNA Polymerase kit from Promega. A QIAEX II DNA Extraction Kit was purchased from QIAGEN (Germantown, MD).

4.2 Instrumentation

DNA concentration was measured using a Thermo Scientific Nanodrop 2000 spectrophotometer using 1 μL of the plasmid DNA dissolved in TE. All PCR reactions were performed on a Eppendorf Mastercycler Gradient thermocycle. Cell counting was performed using a Nikon Eclipse TS100 Confocal microscope with visual counting on a Hausser Scientific Bright-line hemacytometer. A Glenmills Inc. Mini Beadbeater was used to lyse yeast cells, while centrifugation was performed with a IEC HN-SII high speed centrifuge and Eppendorf 5415R microcentrifuge. Absorbance readings for cell growth were taken using a Thermo Scientific Genesys 10 UV/Vis spectrophotometer. All GCMS spectra were taken using an Agilent Technologies GC (7890A) and MS (5979C), with the samples run through a VF23 30 m X 0.39 mm X 0.25 μm GC column. All FAMEs were run using the program VF23FAME: 60 °C starting temperature, ramp 10 °C/min to 150 °C, hold 5 min; ramp 10 °C/min to 220 °C, hold 1 min; ramp 50 °C/min to 250 °C, hold 2 min.

4.3 Media

4.3.1 LB

When making liquid media, approximately 200 mL of Millipure-filtered microbiology grade water was added with a magnetic stirbar to a 500-mL graduated cylinder. To this was added 5 g tryptone, 2.5 g yeast extract, and 5.0 g NaCl. The graduated cylinder was filled to the 500-mL line, and allowed to mix thoroughly on a stirring plate. The media was transferred to a screw-top bottle and then autoclaved for 15 min at 15 psig (121 °C). After cooling, the media was stored for use. If an antibiotic was required (e.g., Amp, Kan), it was added individually to each culture prior to inoculation.

When making solid agar plates, 500 mL of Millipure-filtered microbiology grade water was measured using a 500-mL graduated cylinder and then approximately half of it was added to a 1-L flask. To this, 5 g tryptone, 2.5 g yeast extract, 5.0 g NaCl, and one NaOH pellet were added with stirring. The remainder of the water was added, the solution was transferred to a flask, 10 g of agar were added, and mixed briefly in the

solution. The flask was capped with an aluminum foil sheath and autoclaved for 15 min at 15 psig. After autoclaving, the media was allowed to slowly cool with stirring on the magnetic stir plate. If an antibiotic was needed, the appropriate amount (500 µl of a 1000x premade stock) was added after the flask was cool enough to lightly touch by hand (~60-70 °C). After mixing, the media was poured in a series of plates, and allowed to cool and dry on the benchtop overnight. The next morning the plates were bagged, and stored in the 4 °C fridge.

4.3.2 YPD

When making liquid media, 5 g yeast extract, 10 g peptone, and 10 g dextrose were added to 500-mL graduated cylinder, and water was added to the 500 mL line. The media was mixed, bottled, and autoclaved 15 minutes at 15 psig in the same fashion as for LB. After cooling, the media was stored for use. If liquid media required the addition of an antibiotic (e.g. hyg), it was added individually to each culture prior to inoculation. When making solid agar plates, 5 g yeast extract, 10 g peptone, 10 g dextrose, one NaOH pellet, and 10 g agar were added to a 1-L flask with 500 mL of water and mixed thoroughly. The flask was capped with an aluminum foil sheath and autoclaved 15 minutes at 15 psig. After autoclaving, the media was allowed to slowly cool with stirring on the magnetic stir plate. If hyg was needed, 667 µL of the 300 mg/mL hygromycin stock was added after the flask was cool enough to lightly touch by hand (~60-70 °C). After mixing, the media was poured in a series of plates, and allowed to cool and dry on the benchtop overnight. The next morning the plates were bagged, and stored in the 4 °C fridge.

4.3.3 CM-leu+dex

When making liquid media, 1.30 g CM–leu dropout powder, 1.70 g yeast nitrogenous base (-amino acids, -ammonium sulfate), and 5.0 g ammonium sulfate were added to 1-L graduated cylinder. The graduated cylinder was filled with water to the 900-mL line, and allowed to mix thoroughly. After the media was well mixed, it was poured into an appropriate bottle, labeled, and autoclaved. After cooling, the media was stored for use.

To minimize issues with storage, 20% (w/v) dex solution was produced separately and stored. Before use, an appropriate volume of CM-leu media was mixed with 1/9 of its volume in 20% dex solution, and, if needed, CME from an acetone or ethanol stock to 20 µg/mL. The final media was mixed thoroughly then dispensed to each culture tube/flask.

When making solid agar plates, 0.65 g CM–leu dropout powder, 0.85 g yeast nitrogenous base (-amino acids, -ammonium sulfate), 2.5 g ammonium sulfate, one NaOH pellet, 50 mL of 20% (w/v) dextrose solution, 10 g agar, and 450 mL of water were added to a 1-L flask with stirring. The flask was capped with an aluminum foil sheath and autoclaved. After autoclaving, the media was allowed to slowly cool with stirring on the magnetic stir plate. If CME was needed, it was added from an acetone or ethanol stock to 100 µg/mL after the flask was cool enough to lightly touch without burning (~60-70 °C). After mixing, the media was poured in a series of plates, and allowed to cool and dry on the benchtop overnight. The next morning the plates were bagged, and stored in the 4 °C fridge.

4.3.3.1 CM Dropout Powder

To produce CM knockout powder, all of the nutrients in Table 10 were mixed together in the masses specified, excepting the nutrient(s) specified as the dropout. For CM-leu, appropriate masses of all the listed nutrients except L-leucine were mixed together and ground together by pestle in a mortar until smooth and homogenous. The resulting knockout powder was stored in an airtight jar.

4.3.3.2 20% (w/v) Dextrose Solution

Dextrose solution was produced in 50-mL portions for ease of use. Dextrose (10g) was massed and then added to a sterile 50-mL Falcon tube. Millipure microbiology grade water was added to about the 45-mL line and the dextrose was dissolved by repeated agitation of the Falcon tube. Once the dextrose was fully dissolved, the tube was filled to the 50-mL line with Millipure water and shaken to mix. The mixture was sterilized by syringe-driven Millipore filtration into a second sterile 50-mL Falcon tube,

then stored on the bench top. Two 50-mL tubes were made for each batch of liquid CM-leu+dex media, while one was made for each run of plates.

Table 10: CM Dropout Powder Recipe showing all possible components.

Nutrient	Amount in dropout powder (g)	Final concentration in prepared media (µg/mL)
Adenine (hemisulfate salt)	2.5	40
L-Arginine (HCl)	1.2	20
L-Aspartic acid	6.0	100
L-Glutamic acid (free acid)	5.21	100
L-Histidine	1.2	20
L-Leucine	3.6	60
L-Lysine (mono-HCl)	1.8	30
L-Methionine	1.2	20
L-Phenylalanine	3.0	50
L-Serine	22.5	375
L-Threonine	12.0	200
L-Tryptophan	2.4	40
L-Tyrosine	1.8	30
L-Valine	9.0	150
Uracil	1.2	20

4.4 General Methods

4.4.1 DNA Preparation

4.4.1.1 Rapid NaOH *Yarrowia* gDNA Prep

The method in use is similar to that described by Wang et al. (73). A small amount of cells from a single colony on a fresh YPD agar plate grown overnight, approximately enough to cover the very end of a 200 µL micropipette tip, was added to a PCR tube with 10 µL of 20 mM NaOH. The tube was then incubated for 15 min at 99 °C on an Eppendorf Mastercycler gradient thermocycle, and spun down at ~ 3k rpm on a microcentrifuge for approximately 30 sec. The resulting aqueous layer over the pelleted cell debris contained *Yarrowia* gDNA, and was used directly for PCR amplifications without purification.

4.4.1.2 Wizard® *Plus* Minipreps Plasmid DNA Prep

This system, available as a kit from Promega, is used for the rapid acquiring of high purity plasmid DNA from *E. coli* hosts via alkaline lysis. Between 1 and 3 mL of fresh liquid culture of the cells were used as the plasmid source and prepared according to the published method. Improved results were seen by increasing the incubation time when adding the final solution for elution from 1 minute to five minutes. The final plasmid DNA was redissolved in 30-50 µL of TE buffer and the concentration was then determined with the Nanodrop UV/Vis spectrophotometer.

4.4.1.3 Boiling Minipreps

Boiling minipreps are used for crude preparation of plasmid DNA from *E. coli*, typically for use in characteristic digests and for colony screening. Approximately 1.5 mL of fresh cell culture were transferred to a microfuge tube, and pelleted at maximum speed for five minutes. The supernatant was removed, and the cells were resuspended in a mixture of 300 µL STET with fresh lysozyme (1 mg/mL). This mixture was then incubated 90 seconds at 100 °C and then microfuged at maximum speed for 15 minutes to pellet the cell debris. This cell debris pellet was removed with a toothpick and discarded.

Next, the DNA was precipitated by the addition of 300 µL isopropanol and mixed by inverting the tube. The DNA was then pelleted by microcentrifugation at maximum speed for 15 minutes. The supernatant was removed, and the pellet was rinsed with 500-µL ice cold 70% EtOH. The ethanol was removed, the tube centrifuged 5 minutes at max speed, then any remaining EtOH was again removed from the tube. The tubes were then allowed to dry, either upside down at room temperature for 15-20 minutes or on a 37 °C heating block for 5-8 minutes. The resulting DNA was redissolved in 40 µL TE + 0.4 µL 1 mg/mL heat-treated RNAse A and incubated 15 minutes at 37 °C to destroy any RNA contaminants. The DNA concentration was then determined with the Nanodrop UV/Vis spectrophotometer.

4.4.1.4 DNA Extraction from Agarose Gels

If recovery of a specific DNA restriction digest band was necessary, the band was selected from a 0.8% agarose gel and cleanly excised with a minimal amount of excess gel, then extracted using the QIAGEN Qiaex II kit. The gel slice was transferred into a premassed clear plastic tube, and its mass was determined. As all extracted bands were in excess of 4 kb, 3 volumes of buffer QX1 and two volumes of water were added (1 volume is 100 µL/mg gel). The QIAEX II resin was resuspended by vortexing 30 seconds, then an appropriate amount was added to the tube. Where the total DNA was less than 2 µg, 10 µL of the QIAEX II were added, while 2-10 µg of DNA resulted in the addition of 30 µL of QIAEX II. The resulting mixture was mixed thoroughly and incubated at 50°C for 10 minutes, with vortexing every two minutes to keep the QIAEX II in suspension. The sample was then centrifuged for 30 seconds and the supernatant was removed. The pellet was then washed twice with 500 µL of buffer QX1 to remove any residual agarose, then washed twice with 500 µL of buffer PE to remove any salt. The pellet was resuspended by vortexing, and then incubated 5 minutes at 50°C. The mixture was then centrifuged one last time, and the removed supernatant contained the purified DNA band.

4.4.2 PCR Reactions

4.4.2.1 PCR GoTaq Amplification

All amplifications were performed according to the published method, using 2/5 of the described reaction mixture volume to maximize efficient use of reagents.

Table 11: GoTaq PCR Amplification reaction mixture.

Component	Final Volume (per reaction)	Final Concentration
5X Green GoTaq reaction buffer	4.0 µL	1X
dNTPs, 10 mM	0.4 µL of each dNTP	0.2 mM each dNTP
$MgCl_2$, 25 mM	1.6 µL	1.5 mM $MgCl_2$
Upstream Primer, 5 mM	2 µL	0.01 µM
Downstream Primer, 5 mM	2 µL	0.01 µM
GoTaq DNA Polymerase (5 U/µL)	0.1 µL	0.5 U
Template DNA (<0.5 µg/mL)	1-8 µL	Variable
Nuclease–Free water	To 20 µL final volume	

Since PCR amplifications tend to be performed in batches to ensure uniform concentrations of most reagents, a master mix containing everything except the primers and template DNA was made with enough for each trial plus about 10% reserve (e.g. 40 trials→Master Mix for 44 trials). This Master Mix was mixed thoroughly. In very large cases, such as amplifications with >10 samples with the same primer pair, this Master Mix was subdivided into secondary Master Mixes and the primer stocks were added, then these were dispensed into PCR tubes. Otherwise, the Master Mix was distributed to PCR tubes, then each had its primers added separately. Once the Master Mix and primer pairs were distributed, the template DNA was added to each tube and they were capped for amplification.PCR amplification was performed on an Eppendorf Mastercycler gradient

thermocycler under the program GTAQTDOV, shown in Table 12. After completion of the amplification run, the product DNA was either used directly or stored in the -20°C freezer until use.

Table 12: PCR Program parameters.

program GTAQTDOV CNTRL TUBE LID=105° NOWAIT AUTO 1T=94.0°00:05:00 2T=94.0°00:00:30 3T=65.0°00:00:30 -1.0°+0:00 R=3.0°/s+0.0°/s G=0.0° 4T=72.0°00:05:00 5GOTO2REP15 6T=94.0° 00:00:30 7T=50.0°00:00:30 8T=72.0°00:05:00 9GOTO6REP30 10T=72.0°00:05:00 11HOLD4.0°ENTER end	program BIG CNTRLTUBE LID=105° WAITAUTO 1T=96.0°00:01:00 2T=96.0°00:00:10 3T=50.0°00:00:05 4T=60.0°00:04:00 5GOTO2REP24 6HOLD4.0°ENTER end	program HYMUT CNTRLBLOCK LID=105° NOWAIT AUTO 1 T=95.0° 0:0:30 2 T=95.0° 0:0:30 3 T=55.0° 0:1:00 4 T=68.0° 0:6:00 5 GOTO 2 REP24 6HOLD 4.0° ENTER end

4.4.2.2 PCR Mutation

Mutation with Quikchange II kit was performed according to the published method, while using half of the recommended reaction volume to maximize reagent efficiency. The reaction was set up in a PCR tube according to the recipe seen in Table 13 and amplified using the program HYMUT, shown in Table 12.

Table 13: PCR Mutagenesis reaction mixture.

Component	Final Volume
10X reaction buffer	2.5 µL
DNA template (25 ng)	Variable, optimal 1-5 µL
Forward primer (20 ng/µL)	3.125 µL
Reverse primer (20 ng/µL)	3.125 µL
dNTP mix	0.5 µL
H_2O	To 25 µL

4.4.2.3 PCR Cycle Sequencing

The procedure was performed according to the kit's published manual. The reaction was set up in a PCR tube according to the recipe seen in Table 14. PCR cycle sequencing was performed using the program BIG, shown in Table 12. After completion, the products were spun down and transferred to 1.7 mL microcentrifuge tubes. One µL of 1.5 M NaOAc/ 0.25 M Na_2EDTA was added, and the liquid was pipetted to mix. Next, 40 µL of room temperature 95% EtOH were added to precipitate the DNA. The tube was flicked to mix, and then centrifuged at maximum speed for 15 minutes. The supernatant was removed, then the tube was spun down a second time for 5 minutes, and the remaining supernatant was removed. Finally, 63 µL of ice cold 70% EtOH were added, and the tube was spun once more at maximum speed for 5 minutes. The supernatant was then removed, and the sequencing products were allowed to air dry with heating on a 37°C block for ~10 min or until dry. Reactions were shipped to Miami University (Xiaoyun Deng, Microbiology) for sequencing by capillary electrophoresis.

Table 14: PCR Cycle sequencing reaction mixture

Component	Final Volume
Template	0.5-5 µL, need 150 ng
Primer (100 mM)	0.80 µL
5X Buffer	1.50 µL
Reaction Mix	1.00 µL
H_2O	To 10 µL

4.4.3 DNA Digestion

The DNA for digestion was prepared by either a Wizard miniprep or a boiling miniprep of a fresh cell culture. Digestion of the DNA occurred in two recurring scales (Table 15). The buffers used were chosen to provide optimum activity for the enzymes, according to the reported values given by NEB. The resulting fragments were run on 0.8% agarose gels stained with ethidium bromide for UV visualization.

Table 15: Standard DNA restriction digest conditions. Note that analytical digests are designed to minimize the amount of enzyme used, while preparative reactions for gel band excision are designed to ensure complete digestions.

Analytical digests	Digests for agarose gel band excision
2.0 µL miniprep DNA	~1 µg DNA in 1-8 µL TE
2.0 µL NEBuffer	2.0 µL NEBuffer
2.0 µL BSA (as needed)	2.0 µL BSA (as needed)
0.5 µL enzyme (each)	1.0 µL enzyme (each)
Water to 20 µL total volume	Water to 20 µL total volume

4.4.4 Additional Common Methods

4.4.4.1 Freezer Stocks

When a valuable plasmid or strain of interest was produced, short-term storage options such as Wizard Miniprep DNA solution or regular streak plates were insufficient to archive the DNA or cells. To allow for long-term (nearly indefinite) storage, these colonies were cultured and prepared using the following methods.

4.4.4.1.1 Yeast Freezer Stock Method

Fresh overnight cultures of the desired strain were incubated overnight to near-saturation, determined visually. From each culture, 1 mL was removed and added to each of two labeled 2.0-mL conical screw-cap tubes. Next, 80 µL of DMSO was added to the dispensed cell culture, and the tubes were sealed and vortexed to mix. The tubes were then placed into a prechilled EtOH/dry ice bath and allowed to cool until the cell culture was visibly frozen. The tubes were stored at -80 °C.

4.4.4.1.2 *E. coli* Freezer Stock Method

Fresh overnight cultures of the desired strain were incubated overnight to near-saturation, determined visually. From each culture, 700 µL were removed and added to each of two labeled 2.0-mL conical screw-cap tubes. Next, 700 µL of *E. coli* storage buffer (65% glycerol (v/v), 0.1 M $MgSO_4$, and 0.025 M Tris□ l) was added to the dispensed cell culture, and the tubes were sealed and vortexed to mix. The tubes were then placed into a prechilled EtOH/dry ice bath and allowed to cool until the cell culture was visibly frozen. The tubes were stored in the -80 °C freezer.

4.4.4.1.3 Inoculation from a Freezer Stock

The freezer stock from the -80 °C freezer was chilled on dry ice. Cells were scraped from the top of the freezer stock, either using a sterile 200-µL micropipette tip or a flame-sterilized inoculation loop and were then inoculated into a culture tube of appropriate media, and the fresh inoculation was incubated at 37 °C or 28 °C for *E. coli* and *Y. lipolytica*, respectively.

4.4.4.2 Yeast Transformation

This method is an adaptation of the method of Mauersberger and Nicaud (74). Three flasks of 25 mL YPD were inoculated from a starter of the cells at $5*10^4$, $1*10^5$, and $2*10^5$ cells/mL and cultured overnight at 28 °C. After ~14-18 hours incubation, 10 mL of the culture between $9*10^7$ and $1*10^8$ cells/mL was harvested. The cells were centrifuged 5 min at 3k rpm, rinsed twice with 10 mL TE, then resuspended at $5*10^7$ cells/mL in 0.1 M LiOAc, pH 6.0 and incubated one hour at 28°C with gentle shaking. The cells were then centrifuged and resuspended in 1/10th of the volume of 0.1 M LiOAc pH 6.0. Carrier DNA (salmon sperm) was incubated at 95 °C for 5 min, and put on ice. Next, 5 µL carrier DNA, 0.5-1 µg transforming DNA, and 100 µL competent cells were mixed and incubated 15 min at 28 °C. The cells were mixed gently, then 700 µL 40% PEG 4000 in 0.1 M LiOAc, pH 6.0 was added, and the mixture was again mixed gently. The cells were incubated 1 hour at 28 °C, 250 rpm, then 80 µL DMSO were added and the cells were heat shocked in a water bath 10 min at 39 °C. Lastly, 0.6 mL of 0.1 M LiOAc were added twice and mixed by inverting and 200 µL of the transformed cells were spread on selective plates.

4.5 Experimental Methods

4.5.1 pCre-AHAS* Assembly

4.5.1.1 Production of pY5-Cre Muta 2E/2S

The pY5-Cre plasmid and pDONR-AHAS* were provided by Dr. Robert Minto for assembly. Plasmid DNA of pY5-Cre2*-01 was prepared using Wizard miniprep and the concentration was checked by Nanodrop. An EcoRI site was removed by site-directed mutagenesis using primers pY5 G2908Cs and pY5 G2908Ca under the HYMUT program. The product plasmid was transformed into $RbCl_2$ chemically competent XL1Blue *E. coli* cells and spread on LB+Amp plates. The plates were incubated overnight at 37 °C, and 8 colonies were picked and cultured in LB+Amp liquid media at 37°C, 250 rpm. The resulting plasmids were prepared by boiling miniprep, and screened through restriction digests with EcoRI. The four strains containing the proper plasmid were then cultured

for fresh growth overnight in LB+Amp, then plasmid DNA was prepared from each using the Wizard Miniprep Kit. A segment of the LEU2 gene was then excised through digestion with EcoRI and the fragment was ligated to form the plasmid. The plasmid identity was checked by characteristic digests with EcoRI, SphI, EcoRI/SphI, ClaI, SaI, SalI, HindIII, NdeI, and SalI/NdeI. Additionally, the plasmid was sequenced at and around the deletion site (primers pY5@4150s, pY5@4900s). A second EcoRI site was mutationally inserted (primers T4309A EcoRI insertion a and T4309A EcoRI insertion s) into the pY5-Cre Muta 2S-cut plasmid. The resulting plasmid DNA was confirmed by digestion with EcoRI.

4.5.1.2 Production of the Gateway Entry Clone

To create the entry clone, 7.0 µL of fresh Muta 2E/2S #6 DNA (207.1 ng/µL) was digested with 2.0 µL EcoRI (additionally 1.0 µL NEBuffer EcoRI, 10 µL water) for 2 hours at 37 °C. The enzyme was heat inactivated 20 minutes at 65 °C, then the digested DNA was blunted using the NEB Quick Blunting Kit. The resulting DNA was purified away from the enzymes using a serial phenol/chloroform/isoamyl alcohol extraction. The digest was mixed with 25 µL of equilibrated phenol, vortexed briefly to mix and centrifuged to separate the layers. The phenol (bottom) layer was then removed. Next, 12.5 µL of equilibrated phenol and 12.5 µL of a 24:1 chloroform:isoamyl alcohol mixture were combined and mixed thoroughly, then added to the blunting reaction. This new mixture was vortexed briefly, spun down to separate the layers, and the organic (bottom) layer was removed. Lastly, 25 µL of 24:1 chloroform:isoamyl alcohol were added, the mixture was vortexed, spun down, and the aqueous (top) layer was transferred to a separate tube. The DNA was then precipitated by the addition of 2.26 µL of NaAc and 60 µL of ice cold 100% EtOH. The mixture was flicked, then incubated 5 minutes on crushed dry ice. After its incubation, the tube was spun down 5 minutes at maximum speed and the supernatant was removed. One mL of 70% EtOH was added, the tube was mixed by inversion, and the sample was centrifuged at maximum speed for 5 minutes. The supernatant was removed and the DNA was allowed to dry with light heat at 37 °C. The DNA was then redissolved in 17.0 µL water and 2.0 µL of 10X Antarctic

phosphatase buffer; 1.0 µL of Antarctic phosphatase (NEB) was added. The modification reaction was incubated 15 minutes at 37 °C, then heat inactivated 15 minutes at 65 °C. This blunted and phosphatased product was finally ligated with Gateway RfA from the Gateway Kit.

Table 16: Gateway ligation mixture. Note that the T4 ligase is not provided with the kit and must be purchased separately.

Gateway Ligation Mixture
5 µL phosphatase-treated DNA
2 µL Gateway RfA
2 µL 5X T4 ligase buffer
1 µL T4 ligase

The mixture was combined as described in Table 16, and allowed to incubate for 1 hour at room temperature. After ligation was complete, 1 µL of the ligation mixture was added to a vial of *ccd*B survival $T1^R$ competent cells and gently mixed. This tube was kept on ice 30 minutes, then heat shocked 30 seconds at 42 °C and returned immediately to ice for 2 minutes. Next, 250 mL of SOC media was added and the tube was incubated with shaking 1 hour at 37 °C. The final transformed cells were spread on LB+Amp+Chl prewarmed plates, and incubated at 37 °C. The colonies were screened via growth in LB+Amp+Chl media, followed by confirmation of the plasmid by digests MluI and SmaI.

4.5.1.3 The LR Clonase Reaction

Approximately 0.5 µL of the entry clone AHAS* 11-2 (400.2 ng/µL) was mixed with 5.0 µL of the destination vector Gateway #9 (35.1 ng/µL) and 2.50 µL TE. The LR Clonase enzyme mix was thawed, vortexed, and 2 µL were added. After 1 hour incubation at room temperature, the solution was treated with 1 µL Proteinase K solution and was incubated 10 min at 37 °C. The product was then transformed into high efficiency Omnimax 2 $T1^R$ cells per the published method. The transformed cells were then plated on LB+Amp, and the plasmid identity as confirmed by digests with NcoI, AflII, and NotI and cycle sequencing into the AHAS* gene using primer pY5@4150s.

4.5.1.4 Testing CME Concentrations

Two CME stock solutions were prepared in acetone (50 mg/mL) and ethanol (2.5 mg/mL). For growth in liquid media, 25 mL of CM-leu+dex were inoculated with 10 µL of a fresh overnight culture of the *Yarrowia* prototroph (ATCC 20460) and the appropriate amount of CME stock (0-250 µg/mL), then incubated at 28 °C, 240 rpm. For each reading ~500 µL of the culture was removed, diluted as necessary, and quantitated using A_{600} values. For the solid agar, CM-leu+dex+CME plates were made (0-150 µg/mL) and freshly cultured *Yarrowia* prototroph cells (ATCC 20460) were spread on the plates. After incubation for 2 days at 28 °C, the resulting colonies were counted visually.

4.5.1.5 Testing pCre-AHAS*

The pCre-AHAS* plasmid was transformed into prototrophic *Yarrowia* (ATCC 20460) and spread on CM-leu+dex+CME plates. The resulting colonies were also cultured in liquid CM-leu+dex+CME media. The presence and identity of the plasmid in the surviving colonies was confirmed by rapid plasmid recovery (75) with restriction digests of the recovered plasmids.

The pCre-AHAS* plasmid was also transformed into the *Yarrowia* ΔFAD2::hph gene knockout strain and spread on CM-leu+dex+CME plates. The resulting colonies were cultured in liquid CM-leu+dex+CME at 28°C, and then replica plated onto YPD+hyg and CM-leu+dex+CME plates. The presence and identity of pCre-AHAS* was again confirmed via rapid plasmid recovery with restriction digests. Once selected, the final colonies were inoculated in triplicate into 5-mL tubes of YPD and incubated 24 hours. After incubation, each tube was replicate streaked on YPD and CM-leu+dex+CME plates for selection based on loss of pCre-AHAS*, and then inoculated into another tube of fresh YPD for another round of growth. After obtaining the new *Yarrowia* Δ*FAD2* without pCre-AHAS*, this final strain was cultured in YPD overnight at 28 °C, 240 rpm. Approximately 1 mL of this culture was harvested for the preparation of FAMEs. The supernatant was removed from the culture, then the cells were washed twice with water

and brought up in 1 mL 2% H_2SO_4 in MeOH. The tubes were tightly capped and incubated 1 hr at 80 °C, then 1 mL of water was added and the FAMEs were extracted twice with 2-3 mL of hexanes. The hexanes mixture was evaporated to dryness by heating under a steady stream of nitrogen, then redissolved in 200 µL of hexanes and analyzed by GC-MS.

4.5.2 Lipid Degradation with *POX* Knockouts

4.5.2.1 Preparation

Stocks of all fatty acids in use were prepared at 50 µM in DMSO, and stored at -80 °C to limit air oxidation. The *Yarrowia* Δ*POX2*::*hph* strain was obtained from Dr. Brenda Blacklock, and the positioning of the knockout construct in the gDNA was confirmed by PCR amplification of HPH3→Pox2 C, Pox2 A5→Pox2 C, and HPH3 →Pox2 F2. Since quantitation of lipids in the media and washes was required, the maximum concentration of Tergitol NP-40 that allowed for proper extraction with hexanes was determined via serial dilution with attempted extraction. FAMEs were prepared of each of the fatty acids to be fed, to determine location in the resulting spectra. Additionally, the area of the peak relative to FAME present was determined for the 11-Br 11:0 internal standard.

4.5.2.2 Feedings

Fresh starter stocks of the *Yarrowia* prototroph and Δ*POX2*::*hph* were incubated in YPD overnight at 28 °C, 240 rpm. Each 3-mL feeding culture was grown in YPD+0.1% NP-40 inoculated with 30 µL of the 50 mM fatty acid stock, and 30 µL of the starter culture. The feedings were incubated 24 hours at 28 °C, 240 rpm, and then prepared as FAMEs. About 0.25 mL of each culture was harvested, then washed twice with 0.25 mL of 0.1% NP-40, and twice with 0.25 mL H_2O. The washes were stored in a separate FAME tube. The cells were then brought up with 1 mL of 2% H_2SO_4 in MeOH and spiked with 5 µL of the 11-Br 11:0 internal standard. The tubes were tightly capped and incubated 1 hr at 80 °C, then 1 mL of water was added and the FAMEs were extracted twice with 2-3 mL of hexanes. The hexanes mixture was evaporated to dryness by

heating under a steady stream of nitrogen, then redissolved in 200-500 µL of hexanes and analyzed by GC-MS. Next, the wash solutions were diluted with ~ 1.75 mL of H_2O, spiked with 5 µL of the 11-Br 11:0 internal standard, and extracted twice with ~3-4 mL of hexanes. The resulting solution was evaporated to dryness with heating under a stream of nitrogen, then redissolved in 1 mL 2% H_2SO_4 in MeOH. The tubes were tightly capped and incubated 1 hr at 80 °C, then 1 mL of water was added and the FAMEs were extracted twice with 2-3 mL of hexanes. The hexanes mixture was evaporated to dryness by heating under a steady stream of nitrogen, then redissolved in 200-500 µL of hexanes and analyzed by GC-MS.

REFERENCES

REFERENCES

1. Rustan, A., and Drevon, C. (2005) Fatty Acids: Structures and Properties. in *eLS2005*. pp 1-7.
2. Alberts, B., Johnson, A., Lewis, J., Raff, M., Roberts, K., and Walter, P. (2002) The Lipid Bilayer. in *Molecular Biology of the Cell*, 4th Ed., Garland Science, New york. pp 1463
3. Fujimoto, T., Ohsaki, Y., Cheng, J., Suzuki, M., and Shinohara, Y. (2008) Lipid droplets: a classic organelle with new outfits. *Histochem Cell Biol* **130**, 263-279.
4. Resh, M. D. (1999) Fatty acylation of proteins: new insights into membrane targeting of myristoylated and palmitoylated proteins. *BBA-Mol Cell Res* **1451**, 1-16.
5. Christie, W. (2012) Eicosanoids and related compounds - An introduction. in *The Lipid Library*, AOCS.
6. Demopoulos, C. A., Pinckard, R. N., and Hanahan, D. J. (1979) Platelet activating factor: Evidence for 1-O-alkyl-2-acetyl-*sn*-glyceryl-3-phosphorylcholine as the active component (A new class of lipid chemical mediators). *J Biol Chem* **254**, 9355-9358.
7. Haemmerle, G., Moustafa, T., Woelkart, G., Büttner, S., Schmidt, A., Weijer, T., Hesselink, M., Jaeger, D., Kienesberger, P. C., Zierler, K., Schreiber, R., Eichmann, T., Kolb, D., Kotzbeck, P., Schweiger, M., Kumari, M., Eder, S., Schoiswohl, G., Wongsiriroj, N., Pollak, N. M., Radner, F. P. W., Preiss-Landl, K., Kolbe, T., Rülicke, T., Pieske, B., Trauner, M., Lass, A., Zimmermann, R., Hoefler, G., Cinti, S., Kershaw, E. E., Schrauwen, P., Madeo, F., Mayer, B., and Zechner, R. (2011) ATGL-mediated fat catabolism regulates cardiac mitochondrial function via PPAR-α and PGC-1. *Nature Medicine* **17**, 1076-1085.

8. IUPAC. (2012) Compendium of Chemical Terminology: Gold Book. in *Pure Appl Chem*. pp 554.
9. Kolattukudy, P. (1976) Introduction to natural waxes. in *Chemistry and Biochemistry of Natural Waxes* (Kolattukudy, P. ed.), Elsevier Scientific Pub. Co. pp 1-15.
10. Ohlrogge, J., and Browse, J. (1995) Lipid Biosynthesis. *The Plant Cell* **7**, 957-970.
11. Christie, W. (2013) Fatty acids: straight-chain monoenoic. in *The Lipid Library*, AOCS.
12. Behrouzian, B., and Buist, P. (2003) Mechanism of fatty acid desaturation: a bioorganic perspective. *Prostag Leukotr Ess* **68**, 107-112.
13. Okuley, J., Lightner, J., Feldmann, K., Yadav, N., Lark, E., and Browse, J. (1994) Arabidopsis FAD2 gene encodes the enzyme that is essential for polyunsaturated lipid synthesis. *Plant Cell* **6**, 147-158.
14. Zaloga, G., and Marik, P. (2001) Lipid modulation and systemic inflammation. *Crit Care Clin* **17**, 201-217.
15. Periera, S., Leonard, A., and Mukerji, P. (2003) Recent advances in the study of fatty acid desaturases from animals and lower eukaryotes. *Prostaglandins Leukot Essent Fatty Acids* **68**, 97-106.
16. Blacklock, B. J., Scheffler, B. E., Shepard, M. R., Jayasuriya, N., and Minto, R. E. (2010) Functional Diversity on Fungal Fatty Acid Synthesis: The first acetylenase from the Pacific golden chanterelle, *Cantharellus formosus*. *J Biol Chem* **285**, 28442-28449.
17. Cahoon, E., Schnurr, J., Huffman, E., and Minto, R. E. (2003) Fungal responsive fatty acid acetylenases occur widely in evolutionarily distant plant families. *Plant J* **34**, 671-683.
18. Lee, M., Lenman, M., Banas, A., Bafor, M., Singh, S., Schweizer, M., Nilsson, R., Liljenberg, C., Dahlqvist, A., Gummerson, P., Sjodahl, S., Green, A., and Stymne, S. (1998) Identification of non-heme diiron proteins that catalyze triple bond and epoxy group formation. *Science* **280**, 915-918.

19. Minto, R. E., Adhikari, P., and Lorigan, G. (2004) A 2H solid-state NMR spectroscopic investigation of biomimetic bicelles containing cholesterol and polyunsaturated phosphatidylcholine. *Chem Phys Lipids* **132**, 55-64.
20. Minto, R. E., Gibbons Jr., W. J., Cardon, T., and Lorigan, G. (2002) Synthesis and conformational studies of a transmembrane domain from a diverged microsomal Δ12-desaturase. *Anal Biochem* **308**, 134-140.
21. Shanklin, J., and Cahoon, E. (1998) Eight histidine residues are catalytically essential in a membrane associated iron enzyme, stearoyl-CoA desaturase, and are conserved in alkane hydroxylase and xylene monooxygenase. *Biochemistry* **33**, 12787-12794.
22. Reed, D. W., Polichuk, D. R., Buist, P. H., Ambrose, S. J., Sasata, R. J., Savile, C. K., Ross, A. R. S., and Covello, P. S. (2003) Mechanistic Study of an Improbable Reaction: Alkene Dehydrogenation by the Δ12 Acetylenase of *Crepis alpina*. *J Am Chem Soc* **125**, 10635-10640.
23. Ransdell, A. S. (2012) Investigating the biosynthetic pathways to polyacetylenic natural products in *Fistulina hepatica* and *Echinacea purpurea*. Purdue University.
24. Bu'Lock, J., and Smith, G. (1967) The origin of naturally-occuring acetylenes. *J Chem Soc*, 332-336.
25. Barth, G., and Gaillardin, C. (1997) Physiology and gentics of the dimorphic fungus *Yarrowia lipolytica*. *FEMS Microbiol Rev* **19**, 219-237.
26. Barth, G., Beckerich, J., Dominguez, A., Kerscher, S., Ogrydziak, D., Titorenko, V., and Gaillardin, C. (2003) Functional Genetics of *Yarrowia lipolytica*. in *Functional genetics of industrial yeasts, vol 1. Topics in current genetics.*, Springer, Berlin. pp 227-271.
27. Bankar, A., Kumar, A., and Zinjarde, S. (2009) Environmental and industrial applications of *Yarrowia lipolytica*. *Appl Microbiol Biotechnol* **84**, 847-865.
28. Ratledge, C. (2005) Chapter 1. Single Cell Oils for the 21st Century. in *Single Cell Oils* (Ratledge, C., and Cohen, Z. eds.), AOCS Publishing. pp.

29. Papanikolaou, S., and Aggelis, G. (2010) *Yarrowia lipolytica*: A model microorganism used for the production of tailor-made lipids. *Eur J Lipid Soc Technol* **112**, 639-654.

30. Tsigie, Y. A., Chun-YuanWang, Kasim, N. S., Diem, Q.-D., Huynh, L.-H., Ho, Q.-P., Truong, C.-T., and Ju, Y.-H. (2012) Oil Production from *Yarrowia lipolytica* Po1g Using Rice Bran Hydrolysate. *J Biomed Biotechnol* **2012.**

31. Beopoulos, A., Mrozova, Z., Thevenieau, F., Dall, M.-T. L., Hapala, I., Papanikolaou, S., Chardot, T., and Nicaud, J.-M. (2008) Control of Lipid Accumulation in the Yeast *Yarrowia lipolytica*. *Appl Environ Microbiol.* **74**, 7779-7789.

32. Haddouche, R., Delessert, S., Sabirova, J., Neuvéglise, C., Poirier, Y., and Nicaud, J.-M. (2010) Roles of multiple acyl-CoA oxidases in the routing of carbon flow towards ß-oxidation and polyhydroxyalkanoate biosynthesis in *Yarrowia lipolytica*. *FEMS Yeast Res* **10**, 917-927.

33. Rabenhorst, J., and Gatfield, I. (2002) Method of Producing ɣ-decalactone using *Yarrowia lipolytica* strain HR 145 (US 6451565). United States of America.

34. Pagot, Y., Endrizzi, A., Nicaud, J.-M., and Belin, J. (1997) Utilization of an auxotrophic strain of the yeast Yarrowia lipolytica to improve gamma-decalactone production yields. *Lett Appl Microbiol* **25**, 113-116.

35. Kamzolova, S. V., Morgunov, I. G., Aurich, A., Perevoznikova, O. A., Shishkanova, N. V., Stottmeister, U., and Finogenova, T. V. (2005) Lipase secretion and citric acid production in *Yarrowia lipolytica* yeast grown on animal and vegetable fat. *Food Technol Biotechnol* **43**, 113-122.

36. Dulermo, T., and Nicaud, J.-M. (2011) Involvement of the G3P shuttle and β-oxidation pathway in the control of TAG synthesis and lipid accumulation in *Yarrowia lipolytica*. *Metab Eng* **13**, 482-491.

37. Vorapreeda, T., Thammarongtham, C., Cheevadhanarak, S., and Laoteng, K. (2012) Alternative routes of acetyl-CoA synthesis identified by comparative genomic analysis: involvement in the lipid production of oleaginous yeast and fungi. *Microbiology+* **158**, 217-228.

38. Sharma, R., Chisti, Y., and Banerjee, U. (2001) Production, purification, characterization and application of lipases. *Biotechnol Adv* **19**, 627-662.

39. Dominguez, A., Deive, F., Sanromán, M., and Longo, M. (2003) Effect of lipids and surfactants on extracellular lipase production by *Yarrowia lipolytica*. *J Chem Technol Biotechnol* **78**, 1166-1170.

40. Hong, S.-P., Seip, J., Walters-Pollak, D., Rupert, R., Jackson, R., Xue, Z., and Zhu, Q. (2012) Engineering *Yarrowia lipolytica* to express secretory invertase with strong FBAIN promoter. *Yeast* **29**, 59-72.

41. Beopoulos, A., Nicaud, J.-M., and Gaillardin, C. (2011) An overview of lipid metabolism in yeasts and its impact on biotechnological processes. *Appl Microbiol Biotechnol* **90**, 1193-1206.

42. Beopoulos, A., Nicaud, J.-M., and Gaillardin, C. (2011) An overview of lipid metabolism in yeasts and its impact on biotechnological processes. *Appl Microbiol Biotechnol* **90**, 1193-1206

43. Bartz, R., Li, W.-H., Venables, B., Zehmer, J. K., Roth, M. R., Welti, R., Anderson, R. G. W., Liu, P., and Chapman, K. D. (2007) Lipidomics reveals that adiposomes store ether lipids and mediate phospholipid traffic. *J Lipid Res* **48**, 837-847.

44. Zweytick, D., Athenstaedt, K., and Daum, G. (2000) Intracellular lipid particles of eukaryotic cells. *BBA-Rev Biomembranes* **1469**, 101-120.

45. Ratledge, C., and Wynn, J. (2002) The biochemistry and molecular biology of lipid accumulation in oleaginous microorganisms. *Adv Appl Microbiol* **51**, 1-51.

46. Gibbons, G. F., Islam, K., and Pease, R. J. (2000) Mobilization of triacylglycerol stores. *Biochem Biophys Acta* **1483**, 37-57.

47. Titorenko, V. I., Nicaud, J.-M., Wang, H., Chan, H., and Rachubinski, R. A. (2002) Acyl-CoA oxidase is imported as a heteropentameric, cofactor-containing complex into peroxisomes of *Yarrowia lipolytica*. *J Cell Biol* **156**, 481-494.

48. Wang, H., Clainche, A. L., Dall, M.-T. L., Wache, Y., Pagot, Y., Belin, J.-M., Gaillardin, C., and Nicaud, J.-M. (1998) Cloning and characterization of the peroxisomal acyl CoA oxidase ACO3 gene from the alkane-utilizing yeast *Yarrowia lipolytica*. *Yeast* **14**, 1373-1386.

49. Luo, Y.-S., Wang, H.-J., Gopalan, K. V., Srivastava, D. K., Nicaud, J.-M., and Chardot, T. (2000) Purification and characterization of the recombinant form of acyl CoA oxidase 3 from the yeast *Yarrowia lipolytica*. *Arch Biochem Biophys* **384**, 1-8.

50. Luo, Y.-S., Nicaud, J.-M., Veldhoven, P. P. V., and Chardot, T. (2002) The acyl–CoA oxidases from the yeast *Yarrowia lipolytica*: characterization of Aox2p. *Arch Biochem Biophys* **407**, 32-38.

51. Wang, H. J., Dall, M.-T. L., Waché, Y., Laroche, C., Belin, J.-M., Gaillardin, C., and Nicaud, J.-M. (1999) Evaluation of acyl coenzyme A oxidase (Aox) isozyme function in the n-alkane-assimilating yeast *Yarrowia lipolytica*. *J Bacteriol* **181**, 5140-5148.

52. Mlíčkova, K., Roux, E., Athenstaedt, K., d'Andrea, S., Daum, G., Chardot, T., and Nicaud, J.-M. (2004) Lipid accumulation, lipid body formation, and acyl coenzyme A oxidases of the yeast *Yarrowia lipolytica*. *Appl Environ Microbiol.* **70**, 3918-3924.

53. Pignède, G., Wang, H., Fudalej, F., Gaillardin, C., Seman, M., and Nicaud, J.-M. (2000) Characterization of an Extracellular Lipase Encoded by LIP2 in *Yarrowia lipolytica*. *J Bacteriol* **182**, 2802-2810.

54. Fickers, P., Dalla, M. L., Gaillardin, C., Thonart, P., and Nicaud, J.-M. (2003) New disruption cassettes for rapid gene disruption and marker rescue in the yeast *Yarrowia lipolytica*. *J Microbiol Method* **55**, 727-737.

55. Savická, D., and Šilhánková, L. (1995) Drug resistance in *Yarrowia lipolytica*. *Folia Microbiologica* **40**, 89-94.

56. Madzak, C., Nicaud, J.-M., and Gaillardin, C. (2005) *Yarrowia lipolytica*. in *Production of Recombinant proteins* (Gellissen, G. ed.). pp 163-189.

57. Cordero, O. R., and Gaillardin, C. (1996) Efficient selection of hygromycin-B-resistant *Yarrowia lipolytica* transformants. *Appl Microbiol Biotechnol* **46**, 143-148.

58. Abremski, K., and Hoess, R. (1984) Bacteriophage P1 site-specific recombination. Purification and properties of the Cre recombinase protein. *J Biol Chem* **259**, 1509-1514.

59. Metzger, D., and Feil, R. (1999) Engineering the mouse genome by site-specific recombination. *Curr Opin Biotech* **10**, 470-476.

60. The Jackson Laboratory. (2013). creintro_fig2 ed., http://cre.jax.org/introduction.html. Accessed 06/15/2013.

61. Nagy, A. (2000) Cre recombinase: The universal reagent for genome tailoring. *Genesis* **26**, 99-109.

62. Carter, Z., and Delneri, D. (2010) New generation of *loxP*-mutated deletion cassettes for the genetic manipulation of yeast natural isolates. *Yeast* **27**, 765-775.

63. Taylor, R. U. (1986) Chlorimuron ethyl (DPX F6025) Herbicide Profile 4/86. (EPA ed.

64. Protection, D. C. (2010) Material Safety Data Sheet: DuPont™ Classic® Herbicide.

65. Ross, M. A., and Childs, D. J. (1996) Herbicide Mode-Of-Action Summary. Purdue University, Department of Botany and Plant Pathology.

66. Duggleby, R. G., and Pang, S. S. (2000) Acetohydroxyacid Synthase. *J Biochem Mol Biol* **33**, 1-36.

67. Lee, Y.-T., and Duggleby, R. G. (2006) Mutations in the regulatory subunit of yeast acetohydroxyacid synthase affect its activation by MgATP. *Biochem J* **395**, 331-336.

68. Kolkman, J. M., Slabaugh, M. B., Bruniard, J. M., Berry, S., Bushman, B. S., Olungu, C., Maes, N., Abratti, G., Zambelli, A., Miller, J. F., Leon, A., and Knapp, S. J. (2004) Acetohydroxyacid synthase mutations conferring resistance to imidazolinone or sulfonylurea herbicides in sunflower. *Theor Appl Genet* **109**, 1147-1159.

69. Landy, A. (1989) Dynamic, Structural, and Regulatory Aspects of Lambda Site-specific Recombination. *Ann Rev Biochem* **58**, 913-949.

70. Invitrogen. (2010) Gateway® Technology: A universal technology to clone DNA sequences for functional analysis and expression in multiple systems.

71. Katzen, F. (2007) Gateway® recombinational cloning: a biological operating system. *Expert Opin Drug Dis* **2**, 571-589.

72. Maki, S., Takiguchi, S., Horiuchi, T., Sekimizu, K., and Miki, T. (1996) Partner switching mechanisms in inactivation and rejuvenation of Escherichia coli DNA gyrase by F plasmid proteins LetD (CcdB) and LetA (CcdA). *J Mol Bio* **256**, 473-482.

73. Wang, H., Kohalmi, S. E., and Cutler, A. J. (1996) An Improved Method for Polymerase Chain Reaction Using Whole Yeast Cells. *Anal Biochem* **237**, 145-146.

74. Mauersberger, S., and Nicaud, J.-M. (2003) Tagging of Genes by Insertional Mutagenesis in the Yeast *Yarrowia lipolytica*. in *Springer Lab Manual: Non-Conventional Yeasts in Genetics, Biochemistry and Biotechnology* (Wolf, K., Breunig, K., and Barth, G. eds.). pp 343-356

75. Hoffman, C. S., and Winston, F. (1987) A ten-minute DNA preparation from yeast efficiently releases autonomous plasmids for transformation of *Escherichia coli*. *Gene* **57**, 267-272.

76. Smith, M., and Bidochka, M. (1998) Bacterial fitness and plasmid loss: the importance of culture conditions and plasmid size. *Can J Microbiol* **44**, 351-355.

77. Kawahata, M., Amari, S., Nishizawa, Y., and Akada, R. (1999) A positive selection for plasmid loss in *Saccharomyces cerevisiae* using galactose-inducible growth inhibitory sequences. *Yeast* **15**, 1-10.

78. Gupta, J., and Mukherjee, K. (2001) Stable maintenance of plasmid in continuous culture of yeast under non-selective conditions. *J Biosci Bioeng* **92**, 317-323.

79. Hjortso, M. A., and Bailey, J. E. (2004) Plasmid stability in budding yeast populations: Dynamics following a shift to nonselective medium. *Biotechnol Bioengineer* **26**, 814-819.

80. Minto, R. E., Blacklock, B. J., Younus, H., and Pratt, A. C. (2009) Artypical biosynthetic properties of a Δ12/v+3 desaturase from the model basidiomycete *Phanaerochaete chrysosporium*. *Appl Environ Microbiol* **2009.**

81. Christie, W. (1998) Mass spectroscopy of fatty acids with methylene-interrupted ene-yne systems. *Chem Phys Lipids* **94**, 35-41.

82. Wei, H., Therrien, C., Blanchard, A., Guan, S., and Zhu, Z. (2008) The Fidelity Index provides a systematic quantitation of star activity of DNA restriction endonucleases. *Nucl Acids Res* **36.**

83. Feil, S., Valtcheva, N., and Feil, R. (2009) Inducible Cre Mice. *Methods Mol Biol* **530**, 343-363.

84. Chong-Pérez, B., Reyes, M., Rojas, L., Ocaña, B., Ramos, A., Kosky, R., and Angenon, G. (2013) Excision of a selectable marker gene in transgenic banana using a Cre/lox system controlled by an embryo specific promoter. *Plant Mol Biol.*

85. Srivastava, V. (2013) Site-specific gene integration in rice. *Methods Mol Biol*, 83-93.

86. Kopertekh, L., Broer, I., and Schiemann, J. (2012) A developmentally regulated Cre-lox system to generate marker-free transgenic Brassica napus plants. *Methods Mol Biol*, 335-350.

87. Beare, P., LArson, C., Gilk, S., and Heinzen, R. (2012) Two systems for targeted gene deletion in Coxiella burnetii. *Appl Environ Microbiol* **78**, 4580-4589.

88. Sperling, P., Lee, M., Girke, T., Zahringer, U., Stymne, S., and Heinz, E. (2000) A bifunctional Δ6-fatty acid acetylenase/desaturase from the moss Ceratodon purpureus. *Eur J Biochem* **267**, 3801-3811.

89. Serra, M., Pina, B., Abad, J., Camps, F., and Fabrias, G. (2007) A multifunctional desaturase involved in the biosynthesis of the processionary moth sex pheromone. *Proc Natl Acad Sci U S A* **104**, 16444-16449.

90. Carlsson, A., Thomaeus, S., Hamberg, M., and Stymne, S. (2004) Properties of two multifunctional plant fatty acid acetylenase/desaturase enzymes. *Eur J Biochem* **271**, 2991-2997.

91. Abad, J.-L., Serra, M., Camps, F., and Fabriàs, G. (2007) Synthesis and Use of Deuterated Palmitic Acids to Decipher the Cryptoregiochemistry of a $\Delta 13$ Desaturation. *J Org Chem* **72**, 760-764.

92. Abad, J.-L., Villorbina, G., Fabriàs, G., and Camps, F. (2004) Synthesis and Use of Stereospecifically Deuterated Analogues of Palmitic Acid To Investigate the Stereochemical Course of the $\Delta 11$ Desaturase of the Processionary Moth. *J Org Chem* **69**, 7108-7113.

93. Knothe, G. (2005) Dependence of biodiesel fuel properties on the structure of fatty acid alkyl esters. *Fuel Processing Technology* **86**, 1059-1070.

94. Papanikolaou, S., and Aggelis, G. (2003) Selective uptake of fatty acids by the yeast *Yarrowia lipolytica*. *Eur J Lipid Sci Technol* **105**, 651-655

95. Najjar, A., Robert, S., Guérin, C., Violet-Asther, M., and Carrière, F. (2011) Quantitative study of lipase secretion, extracellular lipolysis, and lipid storage in the yeast *Yarrowia lipolytica* grown in the presence of olive oil: analogies with lipolysis in humans. *Appl Microbiol Biotechnol* **89**, 1947-1962

96. Sigma-Aldrich. (2013) Tergitol® solution.

97. Vanhanen, S., West, M., Kroon, J., Lindner, N., Casey, J., Cheng, Q., Elborough, K., and Slabas, A. (2000) A consensus sequence for long-chain fatty-acid alcohol oxidases from Candida identifies a family of genes involved in lipid omega-oxidation in yeast with homologues in plants and bacteria. *J Biol Chem* **275**, 4445-4552

APPENDICES

Appendix A pCre-AHAS* Primers, Sequences, and GC/MS

Table 17: FAD2 Knockout primer list

Primer Name	Sequence (From 5' to 3')
Fad2-A1	AGG TGT TTC GGA AGA AGG TAT T
Fad2-A2	GTA TAG CAT ACA TTA TAC GAA CGG TAA GCT AGA AAT GTT ATT TGA T
Fad2-B1	GTA TAA TGT ATG CTA TAC GAA CGG TAT TCT ATG GTC GGT CTG TT
Fad2-B2	CGG CGG CAG GCA GGC AGA CCA A
Fad2-C	GTG GCG GTT AGG AGA GGC GGG G
Fad2-E	AGG TGC TCT CCT AGT CTG AAC T
Fad 2-F	CCG TTC CTG TAG CGG GCG GTT G
D1	TAC CGT TCG TAT AAT GTA TGC TAT ACG AAG TTA TAG AGA CCG GGT TGG CGG C
A1'	TTA GAA GTG AGC TGT CCA AGG TCG CA
A2'	AGC TAG AAA TGT TAT TTG ATT GTG TT
D2	TAC CGT TCG TAT AGC ATA CAT TAT ACG AAG TTA TTT TAC AAC AAT ATC TGG T
HPH1	GAC CTG CCT GAA ACC GAA CTG C
HPH2	ATG CCT CCG CTC GAA GTA GCG C

Table 18: pY5-Cre Sequencing and Mutagenesis primers. Note that the location for sequencing primers is based on the position in the original pY5-Cre plasmid, prior to excision or Gateway insertion (see Figure 15)

Primer Name	Amplification Use	Sequence (From 5' to 3')
pY5@1s	Sequencing	GGT GGA GCT CCA GCT TTT GT
pY5@1a	Sequencing	ACA AAA GCT GGA GCT CCA CC
pY5@700s	Sequencing	GCT CCA AGC TGG GCT GTG TG
pY5@1400s	Sequencing	AAA CCA GCC AGC CGG AAG GG
pY5@2100s	Sequencing	TAT TAT TGA AGC ATT TAT CA
pY5@2800s	Sequencing	GTC ACG ACG TTG TAA AAC GA
pY5@3500s	Sequencing	GAT TAT TAT TGG ACG AGA AT
pY5@4150s	Sequencing	GTA TAC CTA CTT GTA CTT GT
pY5@4900s	Sequencing	TCC ACT ACA AAC ACA CCC AA
pY5@5600s	Sequencing	GCA CGT TGG CCT TGT CAA GA
pY5@6300s	Sequencing	CGC ACT TTT GCC CGT GCT AT
pY5 G2908Cs	Mutagenesis, ΔEcoRI site	CGA TAA GCT TGA TAT CCA ATT CAT GTC ACA CA
pY5 G2908Ca	Mutagenesis, ΔEcoRI site	TGT GTG ACA TGA ATT GGA TAT CAA GCT TAT CG
pY5-leu@4201s	Sequencing	ATA GAC TTA TGA ATC TGC ACG G
pY5-leu@4378a	Sequencing	TCA ATT TGG GGT CAA TTG GGG CAA
C4296G SphI insertion-s	Mutagenesis, ::SphI site	GGA TCT GTT CGG AAA TCA ACG CAT GCT CAA CCG AT
C4296G SphI insertion-a	Mutagenesis, ::SphI site	ATG GGT TGA GCA TGC GTT GAT TTC CGA ACA GAT CC
pY5-leu repair s	Mutagenesis	TTG ACC TTG TTG GCA ACA AGT CTC CGA CCT CGG AGG TGG
pY5-leu repair a	Mutagenesis	CCA CCT CCG AGG TCG GAG ACT TGT TGC CAA CAA GGT CAA
pY5Cre polylinker-s	Original linker to preserve ARS18	CTA CTT GGG TGT AAT ATT GGG ATC TGT TCG GCT AGC GTT TAA ACG
pY5Cre-polylinker-a	Original linker to preserve ARS18	AAT TCG TTT AAA CGC TAG CCG AAC AGA TCC CAA TAT TAC ACC CAA GTA GCA TG
T4309A EcoRI insertion-s	Mutagenesis, ::EcoRI site	ATG CTC AAC CGA ATT CGA CAG TAA TAA TTT GAA TC
T4309A EcoRI insertion-a	Mutagenesis, ::EcoRI site	GAT TCA AAT TAT TAC TGT CGA ATT CGG TTG AGC AT

Table 19: Cre recombinase and AHAS Sequencing and Mutagenesis primers.

Primer Name	Amplification Use	Sequence (From 5' to 3')
Cre – seq 1	Sequencing	ACA TGT CCA TCA GGT TCT TGC G
Cre – seq 2	Sequencing	CCC GCG CTG GAG TTT CAA TAC C
Cre – As	PCR Amplification	CAA AGG ATC CGG CAT ATG TCC AAT TTA CTG ACC GTA CAC C
Cre – Aa	PCR Amplification	CCG CGG TGG CGG CCG CCC ATG GCT AAT CGC CAT CTT CCA GCA GGC GCA
Cre – Bs	Mutagenesis, ΔBamHI site	ATG CGG CGA ATC CGA AAA GAA AAC
Cre – Ba	Mutagenesis, ΔBamHI site	CGT TTT CTT TTC GGA TTC GCC GCA T
AHAS – As	PCR Amplification	GGG GAC AAG TTT GTA CAA AAA AGC AGG CTT TCC CTA GTC CCA GTG TAC ACC CGC
AHAS – Aa	PCR Amplification	AGA GAG ACT GCA GCT GGG TGA CCA T
AHAS – Bs	PCR Amplification	ATG GTC ACC CAG CTG CAG TCT CTC T
AHAS – Ba	PCR Amplification	GGG GAC CAC TTT GTA CAA GAA AGC TGG GTG AGG TGT GCT GGA TTC ATG ACC ACA
AHAS – Seq 1	Sequencing	GTC GGG CGA GTC GCG ATT GCA TGT T
AHAS – Seq 2	Sequencing	ACG TCC ACC AGA CCA CCT TTG AGA A
AHAS – Seq 3	Sequencing	CGA CAC CCT CGA ACC ATG ATC ACT T

Nucleotide Sequence for *AHAS* from *Yarrowia lipolytica*

ATGCAATCGCGACTCGCCCGACGGGCCACTAACCTGGCCAGAATCTCCAGAT
CCAAGTATTCTCTTGGTCTGCGATATGTTTCCAACACAAAAGCCCCTGCTGCC
CAGCCGGCAACTGCTGAGTGAGTATTCCTTGCCATAAACGACCCAGAACCAC
TGTATAGTGTTTGGAAGCACTAGTCAGAAGACCAGCGAAAACAGGTGGAAA
AAACTGAGACGAAAAGCAACGACCAGAAATGTAATGTGTGGAAAAGCGACA
CACACAGAGCAGATAAAGAGGTGACAAATAACGACAAATGAAATATCAGTA
TCTTCCCACAATCACTACCTCTCAGCTGTCTGAAGGTGCGGCTGATATATCCA
TCCCACGTCTAACGTATGGAGTGTGATAGAATATGACGACACAAGCATGAGA
ACTCGCTCTCTATCCAACCACCGAAACACTGTCACTACAGCCGTTCTTGTTGC
TCCATTCGCTTTTGTGATTCCATGCCTTCTCTGGTGACTGACAACATTCCTTCC
TTTTCTCCAGCCCTGTTGTTATCTGCTCATGACCTACGGCCACTCTCTATCGCA
TACTAACATAGACGATCCCAGCCCGCTCCCCACTTCCAGGGCACCGTTGGCA
AGCCTCCTATCCTCAAGAAGGCTGAGGCTGCCAACGCTGACATGGACGAGTC
CTTCATCGGAATGTCTGGAGGAGAGATCTTCCACGAGATGATGCTGCGACAC
AACGTCGACACTGTCTTCGGTTACCCCGGTGGAGCCATTCTCCCCGTCTTTGA
CGCCATTCACAACTCTGAGTACTTCAACTTTGTGCTCCCTCGACACGAGCAGG
GTGCCGGCCACATGGCCGAGGGCTACGCTCGAGCCTCTGGTAAGCCCGGTGT
CGTTCTCGTCACCTCTGGCCCCGGTGCCACCAACGTCATCACCCCCATGCAGG
ACGCTCTTTCCGATGGTACCCCCATGGTTGTCTTCACCGGTCAGGTCCTGACC
TCCGTTATCGGCACTGACGCCTTCCAGGAGGCCGATGTTGTCGGCATCTCCCG
ATCTTGCACCAAGTGGAACGTCATGGTCAAGAACGTTGCTGAGCTCCCCCGA
CGAATCAACGAGGCCTTTGAGATTGCTACTTCCGGCCGACCCGGTCCCGTTCT
CGTCGATCTGCCCAAGGATGTTACTGCTGCCATCCTGCGAGAGCCCATCCCCA
CCAAGTCCACCATTCCCTCGCATTCTCTGACCAACCTCACCTCTGCCGCCGCC
ACCGAGTTCCAGAAGCAGGCTATCCAGCGAGCCGCCAACCTCATCAACCAGT
CCAAGAAGCCCGTCCTTTACGTCGGACAGGGTATCCTTGGCTCCGAGGAGGG
TCCTAAGCTGCTTAAGGAGCTGGCTGAGAAGGCCGAGATTCCCGTCACCACT
ACTCTGCAGGGTCTTGGTGCCTTTGACGAGCGAGACCCCAAGTCTCTGCACAT
GCTCGGTATGCACGGTTCCGGCTACGCCAACATGGCCATGCAGAACGCTGAC
TGTATCATTGCTCTCGGCGCCCGATTTGATGACCGAGTTACCGGCTCCATCCC
CAAGTTTGCCCCCGAGGCTCGAGCCGCTGCCCTTGAGGGTCGAGGTGGTATT
GTTCACTTTGAGATCCAGGCCAAGAACATCAACAAGGTTGTTCAGGCCACCG
AAGCCGTTGAGGGAGACGTTACCGAGTCTGTCCGACAGCTCATCCCCCTCAT
CAACAAGGTCTCTGCCGCTGAGCGAGCTCCCTGGACTGAGACTATCCAGTCC
TGGAAGCAGCAGTTCCCCTTCCTCTTCGAGGCTGAAGGTGAGGATGGTGTTAT
CAAGCCCCAGTCCGTCATTGCTCTGCTCTCTGACCTGACAGAGAACAACAAG
GACAAGACCATCATCACCACCGGTGTTGGTCAGCATCAGATGTGGACTGCCC
AGCATTTCCGATGGCGACACCCTCGAACCATGATCACTTCTGGTGGTCTTGGA
ACTATGGGTTACGGCCTGCCCGCCGCTATCGGCGCCAAGGTTGCCCGACCTG
ACTGCGACGTCATTGACATCGATGGTGACGCTTCTTTCAACATGACTCTGACC
GAGCTGTCCACCGCCGTTCAGTTCAACATTGGCGTCAAGGCTATTGTCCTCAA
CAACGAGGAACAGGGTATGGTCACCCAGCTGCAGTCTCTCTTCTACGAGAAC
CGATACTGCCACACTCATCAGAAGAACCCCGACTTCATGAAGCTGGCCGAGT
CCATGGGCATGAAGGGTATCCGAATCACTCACATTGACCAGCTGGAGGCCGG

TCTCAAGGAGATGCTCGCATACAAGGGCCCTGTGCTCGTTGAGGTTGTTGTCG
ACAAGAAGATCCCCGTTCTTCCCATGGTTCCCGCTGGTAAGGCTTTGCATGAG
TTCCTTGTCTACGACGCTGACGCCGAGGCTGCTTCTCGACCCGATCGACTGAA
GAATGCCCCCGCCCCTCACGTCCACCAGACCACCTTTGAGAACTAA

Predicted translation of coding sequence for *AHAS* from *Y. lipolytica*:
MQSRLARRATNLARISRSKYSLGLRYVSNTKAPAAQPATAE.VFLAINDPEPLYSV
WKH.SEDQRKQVEKTETKSNDQKCNVWKSDTHRADKEVTNNDK.NISIFPQSLPL
SCLKVRLIYPSHV.RMECDRI.RHKHENSLSIQPPKHCHYSRSCCSIRFCDSMPSLVT
DNIPSFSPALLLSAHDLRPLSIAY.HRRSQPAPHFQGTVGKPPILKKAEAANADMD
ESFIGMSGGEIFHEMMLRHNVDTVFGYPGGAILPVFDAIHNSEYFNFVLPRHEQG
AGHMAEGYARASGKPGVVLVTSGPGATNVITPMQDALSDGTPMVVFTGQVLTS
VIGTDAFQEADVVGISRSCTKWNVMVKNVAELPRRINEAFEIATSGRPGPVLVDL
PKDVTAAILREPIPTKSTIPSHSLTNLTSAAATEFQKQAIQRAANLINQSKKPVLYV
GQGILGSEEGPKLLKELAEKAEIPVTTTLQGLGAFDERDPKSLHMLGMHGSGYA
NMAMQNADCIIALGARFDDRVTGSIPKFAPEARAAALEGRGGIVHFEIQAKNINK
VVQATEAVEGDVTESVRQLIPLINKVSAAERAPWTETIQSWKQQFPFLFEAEGED
GVIKPQSVIALLSDLTENNKDKTIITTGVGQHQMWTAQHFRWRHPRTMITSGGL
GTMGYGLPAAIGAKVARPDCDVIDIDGDASFNMTLTELSTAVQFNIGVKAIVLNN
EEQGMVTQLQSLFYENRYCHTHQKNPDFMKLAESMGMKGIRITHIDQLEAGLKE
MLAYKGPVLVEVVVDKKIPVLPMVPAGKALHEFLVYDADAEAASRPDRLKNAP
APHVHQTTFEN

Nucleotide sequence for Cre recombinase

ATGTCCAATTTACTGACCGTACACCAAAATTTGCCTGCATTACCGGTCGATGC
AACGAGTGATGAGGTTCGCAAGAACCTGATGGACATGTTCAGGGATCGCCAG
GCGTTTTCTGAGCATACCTGGAAAATGCTTCTGTCCGTTTGCCGGTCGTGGGC
GGCATGGTGCAAGTTGAATAACCGGAAATGGTTTCCCGCAGAACCTGAAGAT
GTTCGCGATTATCTTCTATATCTTCAGGCGCGCGGTCTGGCAGTAAAAACTAT
CCAGCAACATTTGGGCCAGCTAAACATGCTTCATCGTCGGTCCGGGCTGCCA
CGACCAAGTGACAGCAATGCTGTTTCACTGGTTATGCGGCGAATCCGAAAAG
AAAACGTTGATGCCGGTGAACGTGCAAAACAGGCTCTAGCGTTCGAACGCAC
TGATTTCGACCAGGTTCGTTCACTCATGGAAAATAGCGATCGCTGCCAGGAT
ATACGTAATCTGGCATTTCTGGGGATTGCTTATAACACCCTGTTACGTATAGC
CGAAATTGCCAGGATCAGGGTTAAAGATATCTCACGTACTGACGGTGGGAGA
ATGTTAATCCATATTGGCAGAACGAAAACGCTGGTTAGCACCGCAGGTGTAG
AGAAGGCACTTAGCCTGGGGGTAACTAAACTGGTCGAGCGATGGATTTCCGT
CTCTGGTGTAGCTGATGATCCGAATAACTACCTGTTTTGCCGGGTCAGAAAAA
ATGGTGTTGCCGCGCCATCTGCCACCAGCCAGCTATCAACTCGCGCCCTGGA
AGGGATTTTTGAAGCAACTCATCGATTGATTTACGGCGCTAAGGATGACTCTG
GTCAGAGATACCTGGCCTGGTCTGGACACAGTGCCCGTGTCGGAGCCGCGCG
AGATATGGCCCGCGCTGGAGTTTCAATACCGGAGATCATGCAAGCTGGTGGC
TGGACCAATGTAAATATTGTCATGAACTATATCCGTACCCTGGATAGTGAAA
CAGGGGCAATGGTGCGCCTGCTGGAAGATGGCGATTAG

Predicted translation of coding sequence for Cre recombinase

MSNLLTVHQNLPALPVDATSDEVRKNLMDMFRDRQAFSEHTWKMLLSVCRSW
AAWCKLNNRKWFPAEPEDVRDYLLYLQARGLAVKTIQQHLGQLNMLHRRSGLP
RPSDSNAVSLVMRRIRKENVDAGERAKQALAFERTDFDQVRSLMENSDRCQDIR
NLAFLGIAYNTLLRIAEIARIRVKDISRTDGGRMLIHIGRTKTLVSTAGVEKALSLG
VTKLVERWISVSGVADDPNNYLFCRVRKNGVAAPSATSQLSTRALEGIFEATHR
LIYGAKDDSGQRYLAWSGHSARVGAARDMARAGVSIPEIMQAGGWTNVNIVM
NYIRTLDSETGAMVRLLEDGD

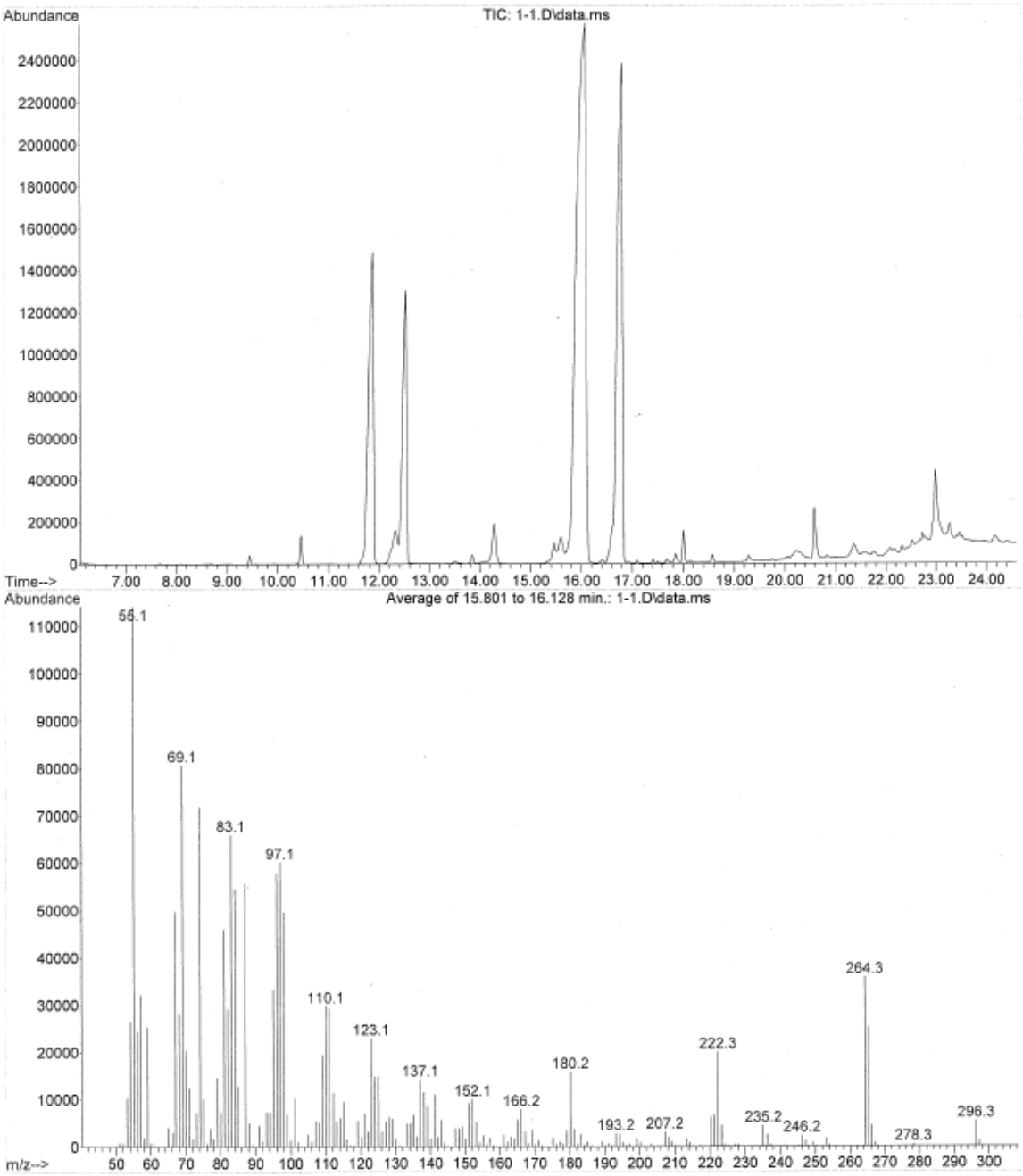

Figure 42: *Yarrowia* prototroph GC/MS total ion chromatogram with oleic acid MS.

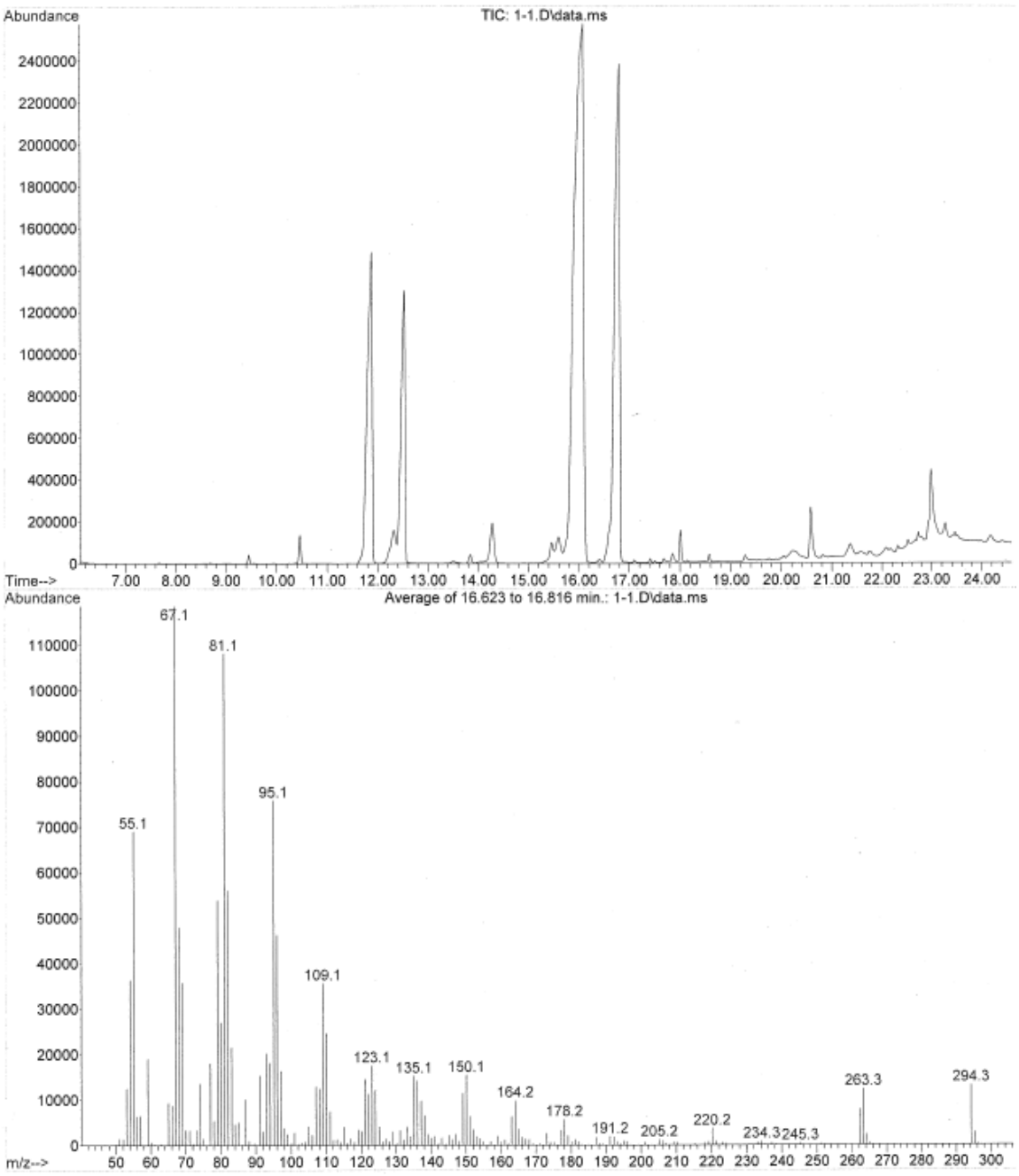

Figure 43: *Yarrowia* prototroph GC/MS total ion chromatogram with linoleic acid MS.

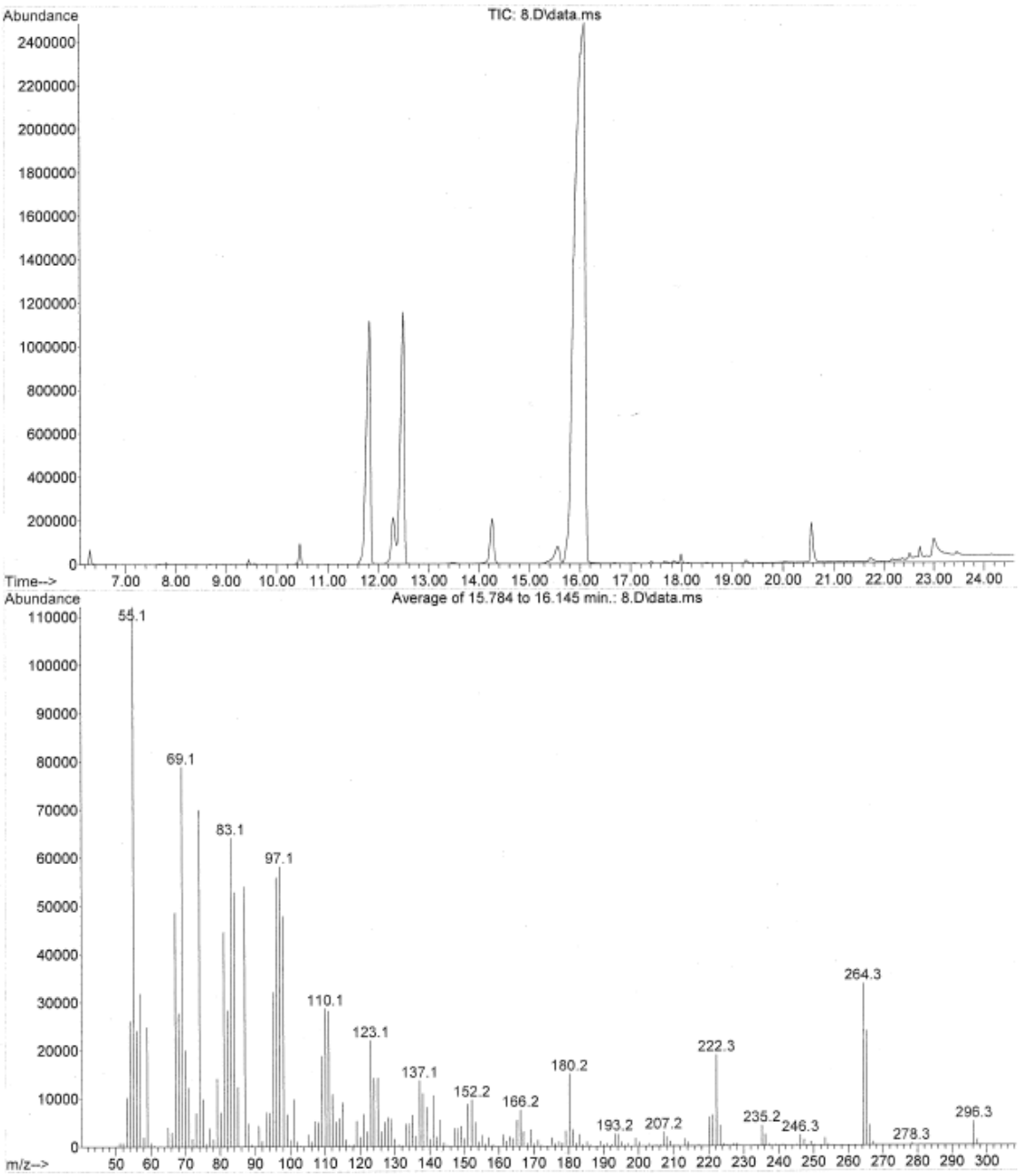

Figure 44: *Yarrowia* Δ*FAD2* #1 GC/MS total ion chromatogram with oleic acid MS.

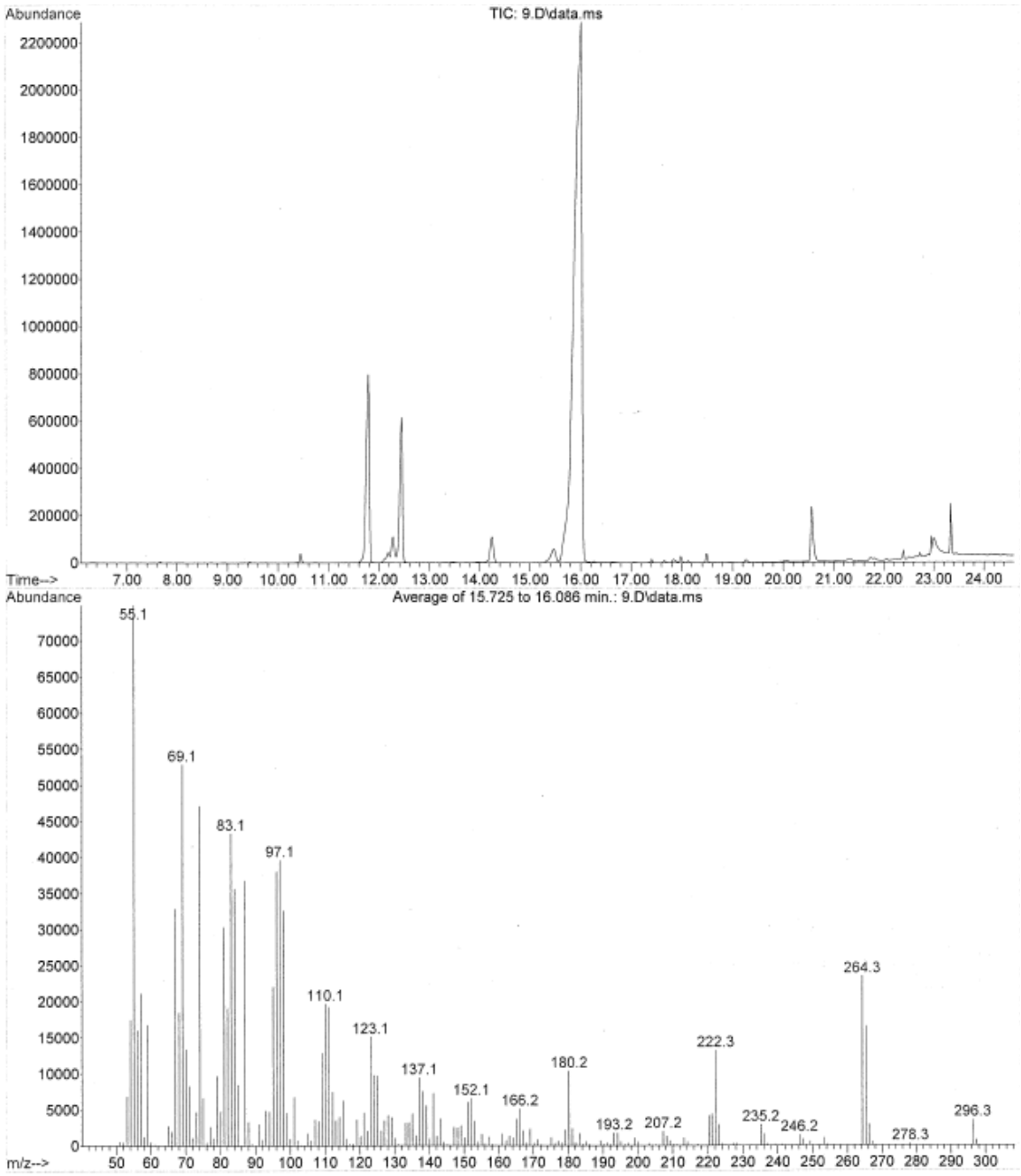

Figure 45: *Yarrowia* Δ*FAD2* #2 GC/MS total ion chromatogram with oleic acid MS

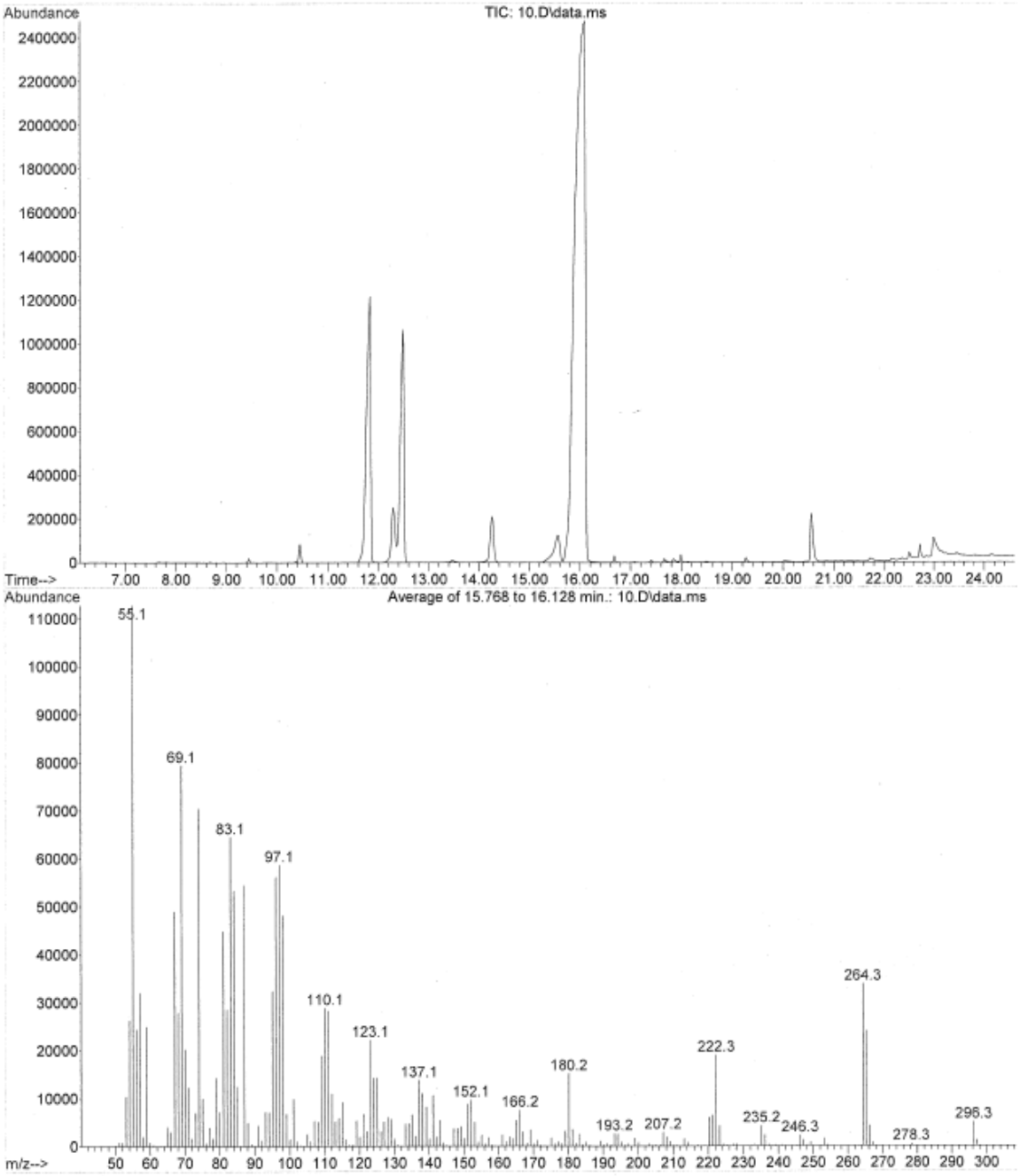

Figure 46: *Yarrowia* ΔFAD2 #3 GC/MS total ion chromatogram with oleic acid MS

Appendix B *Yarrowia* Knockout Construct Primers

Table 20: *POX2* Knockout primer list

Primer Name	Amplification Use	Sequence (From 5' to 3')
Pox2-A2-IScel	Amplification from gDNA	CTA TAT TAC CCT GTT ATC CCT AGC GTA ACT GGC GTC GTT GCT TGT GTG ATT TTT GA
Pox2-B1-IScel	Amplification from gDNA	AGT TAC GCT AGG GAT AAC AGG GTA ATA TAG TAG ACA AGC GGG TAT TTA TTG TAT GA
Pox2-A3	PCR amplification	GAT TCC GCC AAG TGA GAC TGG CGA TC
Pox2-A5	Verification of construct position	CCC TGG CTT GGA GAT GGT CGG TCC AT
Pox2-B4	PCR amplification	TCG ACA AGT ATT TGC GGT AAT TTG GG
Pox2-B6	Verification of construct position	TCG GTT GTT CAG AAG AGC ATA TGG CA
Pox2-C	Verification of construct position	CCG GTT CGA TTC CGG TGT CGT CCA AT
Pox2-E	Verification of construct position	CCG CCT CTT TGT TTG GTT TTT TTT CT
Pox2-F	Verification of construct position	TAA CAG TAC ACG ATT CAA CCA TAG CA
Pox2-F2	Verification of construct position	TAT AAT ACA TAC ATA TAT TAA CAG TA
HPH3	Verification of construct position	GAC CTG CCT GAA ACC GAA CTG C
HPH4	Verification of construct	ATG CCT CCG CTC GAA GTA GCG C
HPH3.1	PCR amplification	GTA CAC AAA TCG CCC GCA GAA GCG CG
HPH4.1	PCR amplification	GAA GCT GAA AGC ACG AGA TTC TTC GC

Table 21: Pox3 Knockout primer list

Primer Name	Amplification Use	Sequence (From 5’ to 3’)
Pox3-A2-IScel	Amplification from gDNA	CTA TAT TAC CCT GTT ATC CCT AGC GTA ACT TGT GTG TAT CGT AGA GGT AGT GAC GT
Pox3-B1-IScel	Amplification from gDNA	AGT TAC GCT AGG GAT AAC AGG GTA ATA TAG TAG ATG GAG CGT GTG TTC TGA GTC GA
Pox3-A3	PCR amplification	TAG TGT TTT TGT TGG TTT TTA TTT GA
Pox3-A5	Verification of construct position	CGG AAA AAT AGG GGG AAA AGA CGC AA
Pox3-B4	PCR amplification	GCT CAT TTT CGG TCT CCA AAC TGA TT
Pox3-B6	Verification of construct position	ATT TCT TGA CCT CAT CAA TGA CTT CT
Pox3-C	Verification of construct position	GGG CTC TTT ATC TCG AAT CAT GGT GG
Pox3-E	Verification of construct position	GCT GTT CGG TCG ATA GTC GGA GCT GT
Pox3-F	Verification of construct position	GAC AAC TTC TAA GAC ATG TCC TGG TT
HPH3	Verification of construct position	GAC CTG CCT GAA ACC GAA CTG C
HPH4	Verification of construct position	ATG CCT CCG CTC GAA GTA GCG C

Appendix C Other Relevant Plasmid Maps and Information

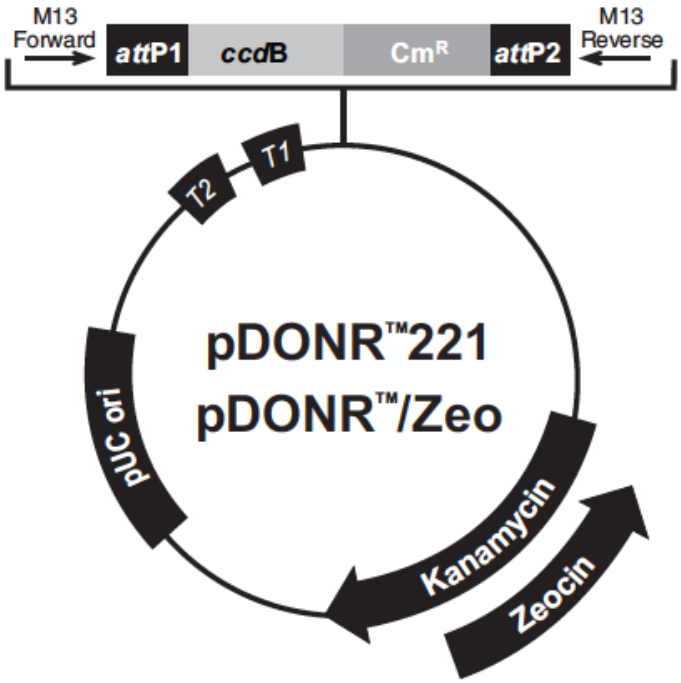

Comments for:	pDONR™221 4762 nucleotides	pDONR™/Zeo 4291 nucleotides
*rrn*B T2 transcription termination sequence (c):	268-295	268-295
rrnB T1 transcription termination sequence (c):	427-470	427-470
M13 Forward (-20) priming site:	537-552	537-552
*att*P1:	570-801	570-801
*ccd*B gene (c):	1197-1502	1197-1502
Chloramphenicol resistance gene (c):	1847-2506	1847-2506
*att*P2 (c):	2754-2985	2754-2985
M13 Reverse priming site:	3027-3043	3027-3043
Kanamycin resistance gene:	3156-3965	---
EM7 promoter (c):	---	3486-3552
Zeocin resistance gene (c):	---	3111-3485
pUC origin:	4086-4759	3615-4288

(c) = complementary strand

Figure 47: Map of the pDONR221 donor vector used for the BP Clonase reaction. Map courtesy of Life Technologies (70)

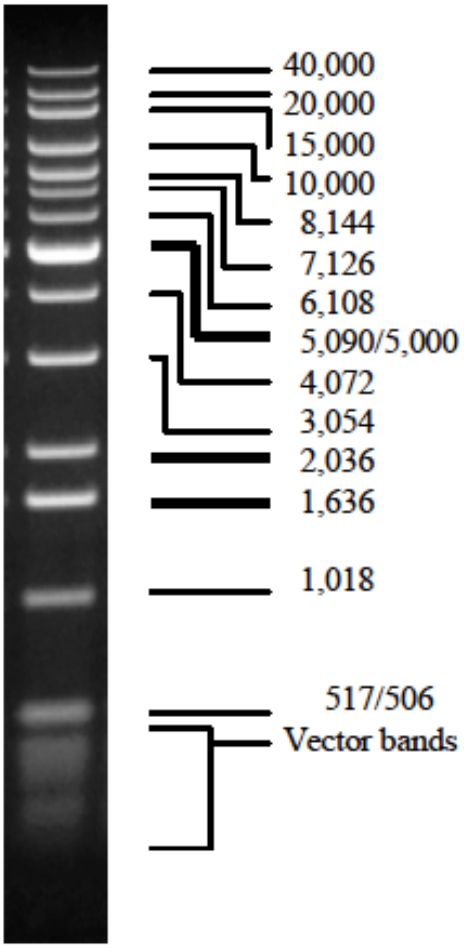

Figure
0.5 µg of 1 Kb DNA Extension Ladder, 0.7% gel, TAE buffer, 0.5 µg/ml ethidium bromide in gel and buffer, a horizontal gel apparatus, 8-tooth 0.8-mm comb, 22 volts (1.3 V/cm), 4 hours.

Quality Control
Agarose gel analysis shows that all bands larger than 500 bp are distinguishable.

Note: If the ionic strength of the sample is too low, blurring of the bands can occur.

Figure 48: Invitrogen 1kb DNA Extension Ladder documentation